

# **Fluctuations, correlations and non-extensivity in high-energy collisions\***

Oleg V. Utyuzh

The Andrzej Sołtan Institute for Nuclear Studies,  
Nuclear Theory Department,  
Hoża 69; 00-681 Warsaw, Poland

## **Abstract**

We investigate numerically the possible interrelations existing between fluctuations, correlations and non-extensivity in high energy collisions arising during hadronization process. In particular, using specially adopted for this purpose cascade hadronization model, we investigate the influence of space-time fluctuations of hadronizing source on the expected Bose-Einstein correlations pattern between produced secondaries. We investigate also traces of non-extensivity arising from the internal dynamical fluctuations present in hadronizing systems with special emphasis put on the problem of observability of the intrinsic fluctuations of temperature of hadronizing system. Finally, we propose a novel way of numerical modeling of Bose-Einstein correlations based on statistical approach known already in literature. It allows at the same time to describe both Bose-Einstein correlations and fluctuations present in hadronization process as given by intermittency pattern.

---

\*PhD Thesis presented to the Scientific Council of The Andrzej Soltan Institute for Nuclear Studies (SINS). Performed under supervision of Doc.dr.hab. Grzegorz Wilk in the Nuclear Theory Department of SINS. Defended on 26 February 2002.

## Contents

I. Introduction .....	1
II. Cascade Hadronization Model (CAS) .....	4
1. Introduction .....	4
2. Phase space characteristics of CAS .....	7
3. Configuration space characteristics of CAS .....	18
4. Intermittency in CAS .....	22
5. CAS and simple implementation of Bose-Einstein correlations (BEC) by means of the "afterburner" method .....	24
6. Summary .....	29
III. Examples of Tsallis statistics in multiparticle production .....	31
1. Introduction .....	31
2. MaxEnt for $q$ -statistics in multiparticle production processes (on the example of violation of Feynmann scaling law ) .....	32
3. $\Phi_n$ measure of "chemical fluctuations" in $q$ -statistics .....	38
4. Broadening of $p_T$ distributions as possible signature of intrinsic fluctuations of temperature .....	42
5. Summary .....	45
IV. Example of modeling of Bose-Einstein correlations (BEC) using CAS model. ....	47
1. Introduction .....	47
2. Momenta shifting method in CAS .....	48
3. Weighting of events - generalities .....	54
4. Summary .....	56
V. Proposition of new method of numerical modeling of BEC .....	57
1. Introduction .....	57
2. Algorithm .....	60
3. Numerical simulations of BEC .....	71
Single source .....	71
Multiple sources .....	74
4. BEC and intermittency .....	76
5. Example of confrontation with data for $e^+e^-$ annihilation into hadrons .....	79
6. Summary .....	82
VI. Summary and conclusions .....	84
Appendices .....	i
A. Hadronization based on application of information theory approach (MaxEnt) .....	i
B. Some basic notions on non-extensive statistics .....	vi
C. Some basic notions on Bose-Einstein correlations .....	xv
References .....	xix
Acknowledgments .....	xxviii

# I. Introduction

High-energy collisions were always at the frontier line of elementary particle physics. The reasons for this are diverse, the one we shall concentrate on here is the fact that such collisions result usually in large number of secondaries being produced<sup>1</sup>. It means that in overwhelming majority of high-energy collisions a substantial part of initial kinetic energy of the two impinging objects is transformed into a huge number of secondaries, each of them of relatively low energy. The simple initial state of low entropy is then transformed, because of collision, into an extremely complicated state characterized by large entropy  $S \sim \langle n \rangle$ . What one usually investigates here is the nature of such processes, especially when they take place in collisions between heavy nuclei. The reason for this special interest is that the Quantum Chromodynamics (QCD), which is believed to be the theory of strong interactions (responsible, among other things, for the multiparticle production processes) predicts formation, at some circumstances, a new state of matter: the Quark Gluon Plasma (QGP) [1,2]. It would consist of quarks and gluons only, liberated in such violent collisions in the volumes of nuclear size. The energy densities encountered in heavy ion collisions seem to be high enough for the QGP to be formed [3]. In such a case the produced secondaries would mostly come from the cooling and hadronization of the QGP fireballs (except of some photonic and leptonic observables which are coupled directly to the quarks and gluons at the early stage of QGP formation).

Although QCD can predict (in its lattice version [4]) the existence of QGP, its applicability to high-energy multiparticle processes is limited to hard collisions only, i.e., to scatterings proceeding with large momentum transfers. Majority of secondaries are, however, produced in soft processes in which only very limited amount of momentum (or transverse momentum) is transferred. All such processes, which we shall be interested in here, must therefore be modeled in some way. Because it is required that any such model reproduces as many as possible features of high-energy collisions describing a huge amount of degrees of freedom (like produced secondaries) the only possible approach is to present them in the form of Monte Carlo event generators following, in the closest possible

---

<sup>1</sup>They are mostly mesons, predominantly pions, therefore in our discussion, if not stated otherwise, we shall always understand that produced secondaries are pions with transverse masses  $\mu_T = \sqrt{\mu^2 + \langle p_T \rangle^2}$ . Their mean multiplicity is large,  $\langle n \rangle \gg 1$ , and grows with energy of reaction  $\sqrt{s}$  faster than longitudinal phase space,  $Y = \frac{1}{2} \ln \frac{E+p_L}{E-p_L} \sim \ln s$ :  $\langle n \rangle \sim \ln^2 s$  (some estimates indicate even faster, power-like, growth like, for example,  $\langle n \rangle \sim s^{1/4}$ ).  $E$  is energy and  $p_L$  is longitudinal momentum.

way, the multiparticle production process<sup>2</sup>. The large number of such generators existing at present means that, so far, no single code can satisfactorily reproduce all aspects of multiparticle processes and there are still not entirely clarified points. One of them is the role played by fluctuations, correlations and non-extensivity in hadronization processes, which will be the subject of this dissertation.

We shall concentrate here on the following topics:

- Numerical investigation of the apparent interrelation existing between the space-time fluctuations of the hadronic source and the expected Bose-Einstein correlations (BEC) pattern between identical secondaries [17]. The existence of such interrelation has been proposed some time ago in [18,19]. This will be presented in Chapter II using for this purpose suitable adaptation [20] of the cascade hadronization model (CAS) (in which the energy-momentum and, especially, the spatio-temporal structure of the production process is under full control) together with the "afterburner" method of implementation of BEC [21,22]. Material presented in this Chapter extends significantly what was already partially presented in [20]. We have found that one is not fully reproducing the simple analytical expectations of [18,19], at least not in the class of hadronization models represented by CAS.
- Investigation of some traces of the so-called non-extensivity caused by the apparent intrinsic dynamical fluctuations present in the hadronic system<sup>3</sup>. This will be done in Chapter III. The material presented there covers essentially the results of our works on Feynmann scaling violation in rapidity distributions [25], on the expected "chemical fluctuations" [26] in heavy ion collisions and on the possible temperature fluctuations [27] in hadronizing systems formed in heavy ion collisions.
- Proposition of new method of numerical modeling of BEC, which can be performed already on a single event level and which leads automatically to intermittency [28]. In this way fluctuations (as represented by intermittency) and correlations (as represented by BEC) are connected (at least to a some extent, as anticipated in [29] and [18]). This will be done in Chapter V. Short version of results concerning this subject has been presented in [23].

<sup>2</sup>There exist at present quite a number of such codes, for example, DPM [5], VENUS [6], String Fusion Model (SFM) [7] PCM [8], PYTHIA-LUND [9], RQMD [10], JETSET [11]) and new are still under construction (NEXUS [12], LUCIFER [13], ROC [14], Color Mutation Model (CMM) [15]. The up-to-date list of these codes is presented in [16].

<sup>3</sup>This subject is new in high energy physics, although the notion of non-extensivity is already highly recognized in other branches of physics. It is understood as possible deviation from the Boltzmann-Gibbs-Shannon statistics which is caused by some correlations and/or fluctuations of different sorts presented in the system under consideration. It is usually expressed, and we shall follow this line here, in terms of the so-called Tsallis statistics [24] characterized by one new parameter  $q$ , deviation of which from unity measures the amount of non-extensivity. For more details, see Appendix B.

As was already mentioned, our investigations will be limited in scope. We shall provide only a model study of fluctuation and correlation phenomena expected to occur in this part of high-energy process that is directly connected with the production of multiparticle state, i.e., in the hadronization process. More specifically, we shall mostly concentrate on a single hadronic source of mass  $M$  producing secondaries (assumed to be pions), leaving aside the problem how such mass is produced and how it is distributed in phase-space. In most cases only one-dimensional hadronization (i.e., limited to longitudinal phase space, with truncated transverse momenta) will be considered.

Because of this limited aim in our investigations we shall use rather simple dynamical picture of hadronization as presented by spatio-temporal and energy-momentum cascade model CAS [20], which is, however, (as we shall demonstrate) able to provide a variety of hadronization patterns. Whenever possible and desirable the results of this model will be confronted with the corresponding results provided by simple statistical hadronization model based on information theory approach (MaxEnt) [30], which has no spatio-temporal structure whatsoever (it is presented in Appendix A). In particular, MaxEnt model will allow us to study the influence of non-extensivity on multiparticle rapidity spectra discussed in Chapter III.

Because CAS model provides full control over the spatio-temporal and energy-momentum developments of the hadronization process, we have also used it to demonstrate how momenta shifting method of numerical modeling of BEC proposed previously in the literature can be applied in a novel way. The corresponding results are presented in Chapter IV and represent a kind of introduction to Chapter V. The last Chapter VI summarizes material presented in this dissertation. Some basic notions of the application of information theory approach to multiparticle production processes, non-extensive statistics, and Bose-Einstein correlations used throughout the paper are provided in Appendices A, B and C, respectively<sup>4</sup>.

---

<sup>4</sup>Throughout the whole dissertation (if not stated otherwise) the following convention has been adopted:  $\hbar = c = 1$ , time is in [ $fm$ ], length is in [ $fm$ ] and energy and momentum is in [ $GeV$ ].

## II. Cascade Hadronization Model (CAS)

### 1. Introduction

The multiparticle spectra of secondaries produced in high-energy collision processes are the most abundant sources of our knowledge of the dynamics of such processes. Among others, two features emerging from analysis of these spectra are of particular interest from the point of view of QGP searches:

- the so-called intermittent behavior observed in many experiments by analyzing factorial moments of spectra of produced secondaries,
- the Bose-Einstein correlations observed between identical particles.

Whereas the former is believed to indicate the existence of some (multi)fractal structure of the production process [28] and can serve as a probe of dynamics of hadronization process, the latter are established as the most important source of our knowledge on the space-time aspects of the multiparticle production processes [17] (see also Appendix C) and they can give us information about size of the system.

In this Chapter, we shall concentrate on the following problem. Some time ago it was argued [18] that, in order to make both phenomena compatible with each other, the emitting source should fluctuate in a scale-invariant (i.e., power-like) way. This can be achieved in two ways:

- (i) the shape of the interaction region is regular but its size fluctuates from event to event according to some power-like scaling law,
- (ii) the interaction region itself is a self-similar fractal extending over a very large volume.

In both cases the index describing power-like behaviour of some characteristic spatial dimension  $R$  of the system finds its way to similar index describing similar power-like, but now in momentum variable  $Q$ , behavior of factorial moments, which is a signal for intermittency. In what concern point (i) it was illustrated in [18,19] on the following simple analytical example. Namely, whereas the simple static gaussian source

$$\rho(r) = \frac{\pi^{3/2}}{R^3} \exp\left(-\frac{r^2}{R^2}\right), \quad (\text{II.1})$$

leads to the correlation function between identical particles of the form (cf. Appendix C and references therein)

$$C_2(p_1, p_2; R) = 1 + \exp\left(-\frac{1}{2}Q^2 \cdot R^2\right); \quad Q = |p_1 - p_2|, \quad (\text{II.2})$$

the same source with radius  $R$  fluctuating according to the probability distribution:

$$f(R) = \frac{\gamma}{L^\gamma \cdot R^{1-\gamma}} \cdot \Theta(R - L) \quad (\text{II.3})$$

( $\gamma \in [0, 1]$  is constant and  $L$  the necessary cut-off parameter) results in the correlation function of the form:

$$\begin{aligned} C_2(p_1, p_2) &= \int_0^L C_2(p_1, p_2; R) \cdot f(R) dR \\ &= 1 + \frac{\gamma}{(L \cdot Q)^\gamma} \int_0^{LQ} dx x^{\gamma-1} \exp\left(-\frac{x^2}{2}\right), \end{aligned} \quad (\text{II.4})$$

i.e., in its power-like dependence on  $Q$ . Similarly, as was indicated in [19], point (ii) is equivalent to the power-like behaviour of the source function itself:

$$\rho(r) = A \cdot |r|^{1-\frac{\gamma}{2}}, \quad \gamma \in (0, 1), \quad (\text{II.5})$$

because in this case

$$C_2(Q) = 1 + \frac{16A^2}{Q^\gamma} \left| \int_0^{LQ} \frac{dx}{|x|^{1-\frac{\gamma}{2}}} \cos x \right|^2, \quad (\text{II.6})$$

i.e., one finds approximate scaling of  $C_2(Q)$  for  $Q > 1/L$ , similarly as in (II.4)<sup>5</sup>.

In both cases the cut-off parameter  $L$  is somehow connected with the unknown spatial characteristic of the source and in reality the actual scaling can be influenced by the presence of the integral factor depending on  $Q$  in the integration limit. Only for  $LQ \gg 1$  this factor is just a numerical constant and real scaling follows. Notice that point (i) reflects the properties of the production process rather than properties of hadronization, which are summarized in point (ii). Because we shall not discuss here the production of the hadronizing source, therefore the question on which we would like to concentrate in this Chapter is whether (or to what extent) the conjecture (II.5) is valid in a more realistic scenario, in which one accounts for both the conservation laws and for the necessary spatial limitation of the production process. In a sense, it amounts to the replacing parameters  $L$  and  $\gamma$  above by some plausible physical picture of the hadronization process. The only

<sup>5</sup>Similar attempt to connect origin of intermittency with a possible power-law distribution of space-time region of hadronic emission, as given by eq.(II.5), has been also done in the framework of current ensemble model [31].

way to check this is to model both the spatio-temporal and energy-momentum developments of hadronization process using some plausible Monte Carlo method over which one has full control and which can be expected to show the above desired features. Because the natural models for fragmentation are cascades, we shall use to this end simple self-similar cascade process of the type discussed in [32], in which secondaries are produced at final stage of the sequential two-body decays of some original mass  $M$ . As already mentioned, for the purpose of this work we shall not address neither the origin of  $M$  nor its possible distribution, but assume it to be given and fixed. No resonance production and no final state interactions of any sort will be considered here and all produced particles will be assumed to be pions. This cascade will be then generalized by adding to it a simple (classical) space-time development. The hadronization model formed in this way will be called Cascade Hadronization Model (CAS for short). As we shall see, this model, although simple, can cover (almost) all types of behavior expected in hadronization processes, except of true BEC. In this chapter BEC will be therefore added in the form of "afterburner" advocated recently in [21]<sup>6</sup>.

Before proceeding to details of CAS let us stress that, although there exist a vast literature concerning the possible (multi)fractality in momentum space [28,34], its space-time properties are not yet fully recognized with [18,19,31] remaining so far the only representative investigations in this field. In this respect, CAS represents a new approach to this problem<sup>7</sup>. One should also keep in mind that the expected (multi)fractal picture (both in momentum and configuration spaces) of the production process is, strictly speaking, true only in the pure mathematical sense, i.e., for cascades proceeding *ad infinitum*, which is obviously not our case. This fact will have, as we shall see below, visible consequences in what concerns our results. Finally, it must be stressed that CAS is based on random multiplicative process taking place in the invariant mass  $M$  variable that is not directly measurable but seems otherwise most natural when modeling a real hadronic cascade process. Therefore the results obtained below will not necessarily be identical with the results of random multiplicative processes in some chosen, directly measurable variables (like energy, rapidity or azimuthal angle, each of which depends on  $M$  in an involved way dictated by the details of hadronization model used) [37].

We shall now discuss in turn the phase space and configuration space characteristics of CAS, the intermittency pattern it leads to, and the BEC it provides when endowed with simple "afterburner" approach.

<sup>6</sup>Cf. also [33]. Part of the material presented in this chapter has been already presented in [20]. The examples of more detail investigations of how CAS can be used for some other methods of modeling BEC presented in the literature are provided in Chapter IV.

<sup>7</sup>It should be noted that possible (multi)fractality in space-time alluded to in [18,19], which CAS is trying to realize is complementary to fractality pattern claimed to exist already on the level of hadronic structure [34–36].

## 2. Phase space characteristics of CAS

Let us start with phase space (i.e., energy-momentum) aspects of CAS. As in [32], it is assumed that the emitting source of mass  $M$  undertakes a series of two-body decays (branchings),  $M \rightarrow M_1 + M_2$ , in which the initial mass  $M$  decays into two masses  $M = k_{1,2} \cdot M$  in such way that  $k_1 + k_2 < 1$ . A part of  $M$  equal to  $(1 - k_1 - k_2)M$  is then transformed into kinetic energies of decay products  $M_{1,2}$ . The decay parameters  $k_{1,2}$  are responsible for most of the dynamics of CAS and will be taken as random numbers drawn from some assumed distribution  $P(k_{1,2})$ .

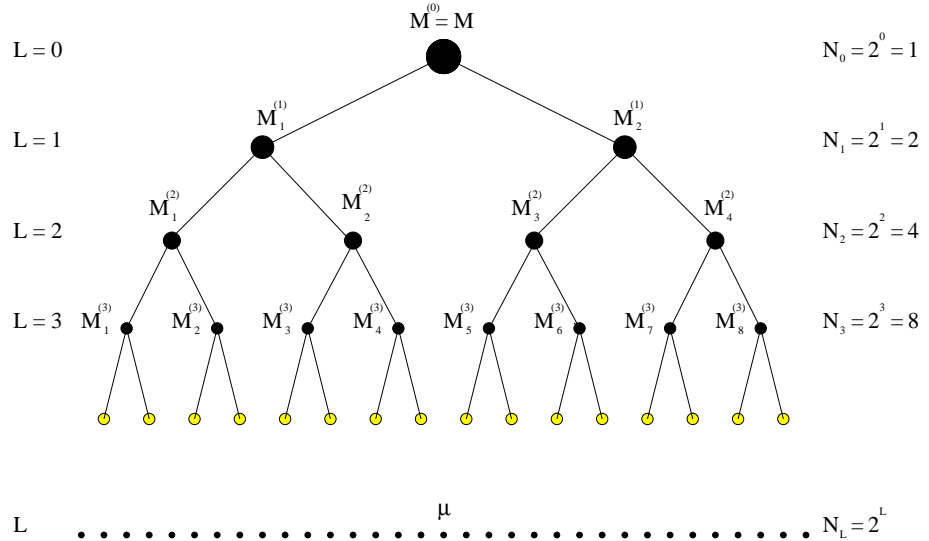


**Fig. II.1.** The scheme of our cascade process. Only  $1 \rightarrow 2$  processes in each vertex are allowed with exact energy-momentum and charge conservation imposed. The self-similarity observed here is believed to result in a (multi)fractal structure of the multiparticle production process, which such cascade models [32,38].

The process repeats itself in self-similar manner (see Fig.II.1) until  $M \geq \mu$  ( $\mu$  being the mass or transverse mass of the produced particles) with successive branchings occurring sequentially and independently from each other, and with different values of  $k_{1,2}$  at each branching, but with the energy-momentum conservation imposed at each step<sup>8</sup>.

---

<sup>8</sup>It should be stressed that in general case of the cascade process it is rather difficult to get final particles with the predefined mass  $\mu$  (unless imposing additional assumptions). That is why in our cascade we usually get particles with some distribution of transverse mass in the range  $(\mu, 2\mu)$ . This differs from the procedure employed in [20] where the residual excess of mass of final particles was transferred into the longitudinal momenta instead. This makes our results slightly different than those presented in [20] as mentioned in Section II.5 below. The conclusions reached in both cases remain, however, identical.

It can be therefore visualized as a kind of formation of Cantor-like set of points (representing masses), cf. Fig.II.2. However, because of the finiteness of  $\mu$ , contrary to the normal Cantor set, this one is limited. This is probably the best example of limitations encountered in all attempt of implementation of (multi)fractal ideas to the real world of physical multiparticle production processes (discussed in detail in [38]).

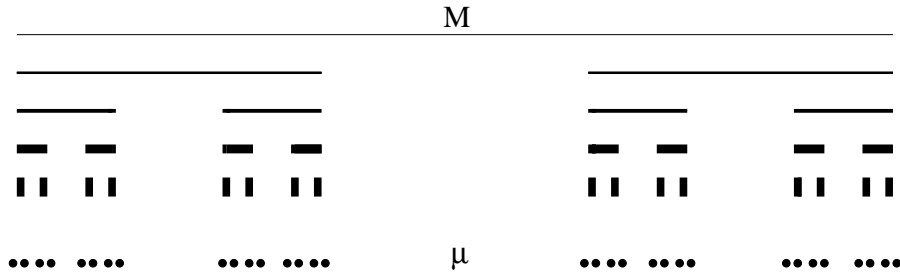


**Fig. II.2.** The Cantor set corresponding to our cascade process ( $k_1 = k_2 = \frac{1}{3}$  case is shown to make picture more transparent). In ideal case its fractal dimension (calculable in the limit  $\mu \rightarrow 0$  or  $M \rightarrow \infty$  only) would be  $d_F = \ln 2 / \ln 3$  [32,38].

Changing the dimensionality  $D$  of our cascade process (which is provided by restricting the possible directions of flights of the decay products in each vertex in a suitable way) from  $D = 1$  to  $D = 3$  and applying different distribution functions of decay parameters  $k_{1,2}$ ,  $P(k_{1,2})$ , one covers an enormously vast variety of different possible production schemes ranging from one-dimensional strings to thermal-like isotropic fireballs. This fact makes the CAS model a very promising tool for the investigations of some special features of hadronization processes, which is the subject of this study.

Of special interest is the one-dimensional cascade case,  $D = 1$ , which we shall discuss in more detail now. It is because one can provide in this case analytic formulas for rapidities  $Y_{1,2}$  of masses  $M_{1,2}$ , which are produced in each vertex from mass  $M$ . In the rest frame of the parent mass  $M$  located in this vertex

$$M \implies M_1 + M_2 = k_1 M + k_2 M,$$

energy conservation

$$M_1 \cosh Y_1 + M_2 \cosh Y_2 = M \quad (\text{II.7})$$

and momentum conservation

$$M_1 \sinh Y_1 + M_2 \sinh Y_2 = 0 \quad (\text{II.8})$$

lead to the following expression for rapidities  $Y_{1,2}$ , which turn out to depend only on the values of the respective decay parameters at this vertex,  $k_{1,2}$ :

$$\begin{aligned} Y_1 &= \pm \ln \left[ \frac{1}{2k_1} (1 + k_1^2 - k_2^2) + \frac{1}{2k_1} \cdot \sqrt{\Delta} \right], \\ Y_2 &= \mp \ln \left[ \frac{1}{2k_2} (1 - k_1^2 + k_2^2) + \frac{1}{2k_2} \cdot \sqrt{\Delta} \right], \end{aligned} \quad (\text{II.9})$$

where  $\Delta \equiv (1 - k_1^2 + k_2^2)^2 - 4k_2^2$ . Two extreme cases of particular interest can be distinguished here:

- totally symmetric cascade,
- maximally asymmetric cascade.

In the case of totally symmetric cascade decay parameters for a given vertex are equal and remain the same for all vertices,  $k_{1,2} = k$ . In this case the finally produced particles occur only at the very end of the cascade and the amount of total energy allocated to the production is maximal. Because the number of possible branchings characterizing the length of the cascade is equal to

$$l \leq L_{max} = \frac{1}{\ln \frac{1}{k}} \ln \frac{M}{\mu}, \quad (\text{II-10})$$

(where  $\mu \rightarrow \mu_T = \sqrt{\mu^2 + \langle p_T \rangle^2}$ ), the multiplicity of produced secondaries is given in this case by the following formula:

$$N_s = 2^{L_{max}} = \left( \frac{M}{\mu} \right)^{d_F}, \quad d_F = \frac{\ln 2}{\ln \frac{1}{k}}. \quad (\text{II-11})$$

It is interesting to notice that according to [32] (cf. also [39]) the exponent  $d_F$  is formally identical with generalized (fractal) dimension of the fractal structure of phase space formed by such cascade. The utility of such notion is greatly reduced, however, due to the necessary limited length of our cascade process as already mentioned before<sup>9</sup>. It is worth to note a kind of scaling present in eq.(II-11) where  $N_s$  depends on energy  $M$  solely through the ratio  $M/\mu$  and decay parameter  $k$ . Notice that the characteristic power-like behaviour of  $N_s(M)$  seen in eq.(II-11) is normally attributed to thermal models of multiparticle production [1,40]. For example, for hadronic gas with equation of state characterized by the velocity of sound  $c_0 = \frac{1}{\sqrt{3}}$  one gets  $N_s \sim M^{1/2}$ . The same behavior (on average) is obtained in our case for  $k_{1,2}$  chosen randomly from a triangle distribution  $P(k) = (1 - k)^a$  with  $a \simeq 1$ , which will be therefore used in all our numerical calculations (if not explicitly stated otherwise)<sup>10</sup>. The fact that multiplicity of produced particles is limited to the finite range of  $N_s \in (2, M/\mu)$  means that decay parameters are limited

<sup>9</sup>In fact, this observation is of general validity, in particular it applies to all other applications of the cascade mechanism to hadronization processes. The fact that maximal multiplicities  $N_{max} = \frac{M}{\mu}$  is always finite will distort the results naively expected from the mathematical model of such cascade processes. It is best visualized by the fact that the Cantor-like set in Fig.II.2 is limited in number of generations with its final points being of finite size given by the mass  $\mu$  of produced secondaries.

<sup>10</sup>We have dropped here, and in what follows, the normalization constant present in  $P(k)$ , which is not important in numerical simulations. It is equal to  $c = (1 + a)/[(1 - \mu/M)^{a+1} - (1/2)^{a+1}]$ .

to the interval  $k \in (\mu/M, 1/2)^{11}$ . For totally symmetric cascade ( $k_1 = k_2 = k_s$ ) in one dimension eqs.(II·9) reduce to

$$Y_1 = -Y_2 = Y(k_s) = \pm \ln \left[ \frac{1}{2k_s} + \sqrt{\left( \frac{1}{2k_s} \right)^2 - 1} \right]. \quad (\text{II}\cdot12)$$

In this case the corresponding rapidity distribution of  $N$  produced secondaries has a particularly simple form (cf. spikes in Fig.II.3 for  $Y_s = Y(k_s = \frac{1}{4})$ ):

$$f_s(y) = \frac{1}{2^{L_{max}}} \sum_{j=0}^{L_{max}} \binom{L_{max}}{j} \delta \{y - [2(j-1) - L_{max}] \cdot Y_s\}. \quad (\text{II}\cdot13)$$

It is given by finite number of points, equal to  $L_{max} + 1$ , in rapidity space at which one can find particles with their numbers given by the consecutive coefficients of binomial distribution.

For maximally asymmetric cascades  $k_1 = \mu/M$  and  $k_2 = k$ , i.e., at each vertex one has always a single final particle of transverse mass  $\mu$  being produced against some recoil random mass  $M_1 = k \cdot M: M \rightarrow \mu + M_1$ . In this case the amount of kinetic energy allocated to the produced secondaries is maximal. The corresponding rapidities  $Y_1$  and  $Y_2$  are now given by eqs.(II·9) with, respectively,  $k_1 = \mu/M$  and  $k_2 = k$  and are equal to

$$\begin{aligned} Y_1 &= \ln \left\{ \frac{M}{2\mu} \left[ 1 - k^2 + \left( \frac{\mu}{M} \right)^2 \right] \pm \frac{M}{2\mu} \sqrt{\Delta} \right\}, \\ Y_2 &= \ln \left\{ \frac{1}{2k} \left[ 1 + k^2 - \left( \frac{\mu}{M} \right)^2 \right] \mp \frac{1}{2k} \sqrt{\Delta} \right\}, \end{aligned} \quad (\text{II}\cdot14)$$

where  $\Delta = \left[ 1 - k^2 + \left( \frac{\mu}{M} \right)^2 \right]^2 - 4 \left( \frac{\mu}{M} \right)^2$ . Also here the resultant multiplicity  $N_a$  is given by the length  $L_{max}$  of the cascade, which is limited by the condition  $M_l = k^l \cdot M \geq \mu$ . It means therefore that the corresponding multiplicity is given by the following formula:

$$N_a = 1 + L_{max} = 1 + \frac{1}{\ln \frac{1}{k}} \cdot \ln \frac{M}{\mu}, \quad (\text{II}\cdot15)$$

where  $L_{max}$  is the same as before and given by eq.(II·10). Notice that energy dependence of multiplicity  $N_a$  is now logarithmic one<sup>12</sup> but the same kind of scaling in  $M/\mu$  as observed in eq.(II·11) is present also here.

<sup>11</sup>In real cascade calculations, i.e., with values of  $k_{1,2}$  taken from distribution  $P(k_{1,2})$ , this is not true because it would restrict formation of objects with large masses. Instead one should take  $k_{1,2}$  from a whole interval,  $(\mu/M, 1)$  and account for energy-momentum conservation constraint imposed at each vertex, i.e., for the fact that  $k_1 + k_2 \leq 1$ .

<sup>12</sup>In thermal models formalism such behaviour corresponds to a one-dimensional fireball with the equation of state characterized by the velocity of sound  $c_0 \rightarrow 1$  [41].

The above extreme examples clearly show that multiplicities obtained in CAS cover, in principle, all possible energy dependencies of the multiplicities of produced particles ranging from logarithmic to power-like dependence on the original mass  $M$ . They depend solely on decay parameters  $k_{1,2}$  of the cascade, i.e., on the form of  $P(k_{1,2})$  assumed, and scale in the ratio  $M/\mu$ . The dynamics is therefore hidden in the form of  $P_{k_{1,2}}$  one uses, which, if necessary, could be a subject of further investigations. This problem will not be pursued here. These observations remain true for both one and three dimensional cascades.

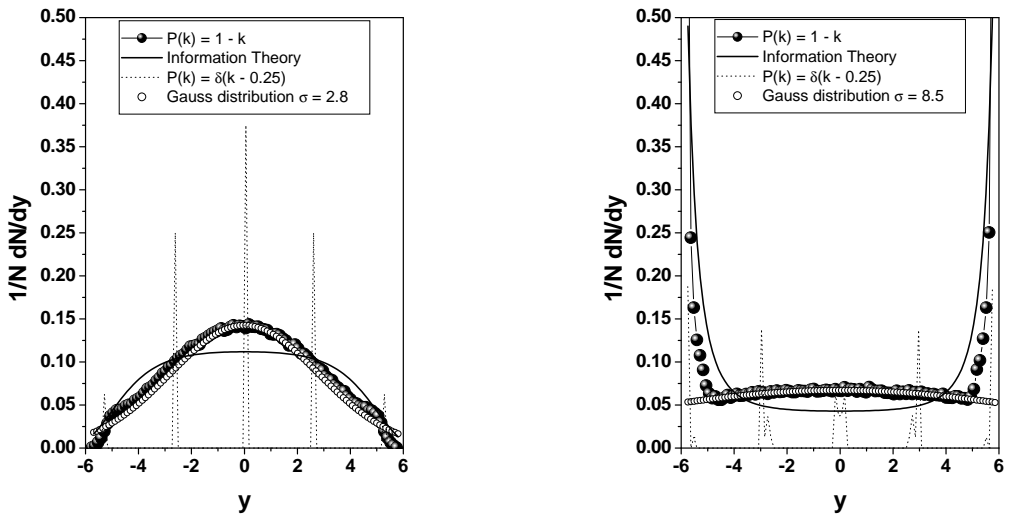


**Fig. II.3.** Examples of rapidity distributions of secondaries for normal one-dimensional cascade (with  $k_{1,2}$  distributed randomly according to  $P(k_{1,2}) = (1 - k_{1,2})^a$  with  $a = 1$ , left panel, black points) and asymmetric one-dimensional cascade (with  $k_1 = \mu_T/M$  and  $k_2$  distributed randomly according to  $P(k_2) = (1 - k_2)^a$  with  $a = 1$ , right panel, black points) calculated for  $M = 100$  GeV and  $\mu_T = 0.3$  GeV. Histograms are for fixed  $k_1 = k_2 = \frac{1}{4}$ , left panel and for  $k_1 = \mu_T/M$  and  $k_2 = \frac{1}{4}$ , right panel. Open circles show the best gaussian fits (cf. eq.(II-18)). Full lines present the most probable (one-dimensional) thermal-like distributions, provided by MaxEnt model (cf. eq.(II-19) below) with  $\beta = 0.043$  GeV $^{-1}$  for symmetric cascade and  $\beta = -0.052$  GeV $^{-1}$  for asymmetric one.

In Fig.II.3 one can see examples of rapidity distributions calculated for symmetric and asymmetric one dimensional ( $D = 1$ ) cascades originating from mass  $M = 100$  GeV and resulting in  $\langle N_s \rangle = 22$  or  $\langle N_a \rangle = 5$  particles, respectively. Notice that whereas CAS, being a self-similar cascade in invariant masses, leads, according to [32,38], to a fractal structure in masses as expressed by eq.(II-11), it does not seem to result in fractal structure in rapidity space  $Y$ . As seen in eq.(II-12) and in Fig.II.3, produced particles are always located in a limited number of points,  $n_{loc} = 1 + L_{max}$ , which for  $M \rightarrow \infty$  or  $\mu \rightarrow 0$  are proportional to  $n_{loc} \sim \ln \frac{M}{\mu} / \ln \frac{1}{k}$ . They always cover distance of measure zero, to be compared to the corresponding available rapidity range equal to  $L_{max} \cdot Y(k_s)$  (for  $k_1 = k_2 = k_s$  cascade). This will have profound consequences in what concerns intermittency provided by CAS, see Chapter II.4 below.

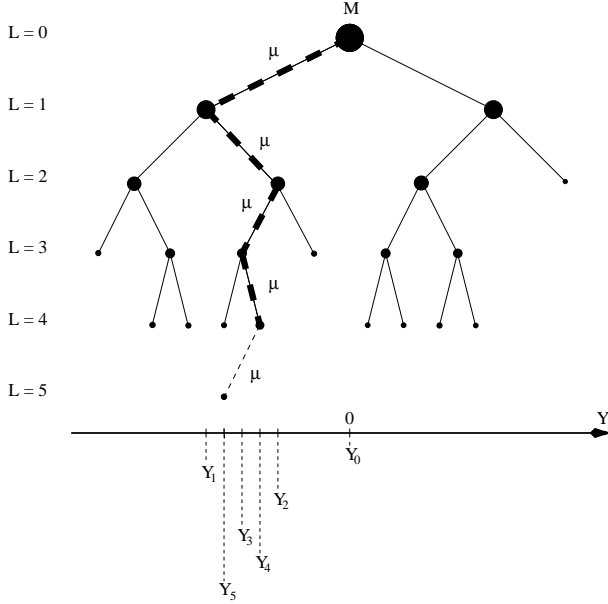


**Fig. II.4.** The production of final particle of mass  $\mu$  in the case of general symmetric cascade visualized as a random walk in rapidity space. The rapidity of original mass  $M$  is set to be equal zero. The trace of finally observed particle  $\mu$  through the cascade process is clearly shown through the sequence of rapidities of all intermediate masses:  $Y_0 \rightarrow Y_1 \rightarrow Y_2 \rightarrow Y_3 \rightarrow Y_4 \rightarrow Y_5$ .

It is interesting to observe that distributions of particles obtained from both cascades are, at least in the central part of the plot, very well approximated by Gaussian distributions. To understand this fact let us notice that rapidity of given final particle can be regarded as final position in a kind of random walk performed in rapidity space, which starts from  $Y = 0$  and which steps are given by the actual value of decay parameter  $k$ , cf. eq.(II·9). Fig.II.4 shows example of such process for the general symmetric cascade with  $k$  drawn from distribution  $P(k_{1,2})$ . In this case the step  $Y(k)$  is given by eq.(II·12) and depends on the value of  $k$ . Because  $k$  is random variable therefore  $Y(k)$  is also random and we have random walk (to the left or right in a given step) with a fluctuating step size. The situation is more involved for asymmetric cascades where, in addition, dependence on the recoiled mass occurs as well, cf. eq.(II·14). For the totally symmetric cascades with fixed value of decay parameter  $k$  the only randomness left will be therefore the choice "right/left" made for each consecutive step with its value equal to constant  $Y(k)$  as given by eq.(II·12). Let us consider now cascade of length  $L_{max}$ . The probability  $\mathcal{P}_l$  of having  $l$  steps to the right (left) out of the total number of  $L_{max}$  steps is given by

$$\mathcal{P}_l = \binom{L_{max}}{l} \left(\frac{1}{2}\right)^l \left(\frac{1}{2}\right)^{L_{max}-l}, \quad (\text{II·16})$$

where combinatorial term in parentheses counts the possible number of different ways of arranging  $l$  ( $m = L_{max} - l$ ) indistinguishable steps to the right (left) and the factor  $(1/2)^l(1/2)^{L_{max}-l}$  gives the probability for this event to occur. Therefore, the probability  $P(y, L_{max})$  to reach some distance  $y = (l - m) Y_s$  after performing  $L_{max}$  steps, starting

from the origin,  $Y = 0$ , is given by

$$P(y, L_{max}) = \frac{L_{max}!}{[\frac{1}{2}(L_{max} + y/Y_s)]! [\frac{1}{2}(L_{max} - y/Y_s)]!} \left(\frac{1}{2}\right)^{\frac{1}{2}(L_{max} + y/Y_s)} \left(\frac{1}{2}\right)^{\frac{1}{2}(L_{max} - y/Y_s)}. \quad (\text{II-17})$$

Taking now the large  $L_{max}$  limit of this expression, with the length of the step  $Y_s$  smaller than any (macroscopic) length of interest in the problem,  $\Omega$ , i.e., situation when  $Y_s \ll \Omega$ , one can approximate the expression for  $P(y, L_{max})$  by the following Gaussian formula

$$P(y) \simeq \exp\left(-\frac{y^2}{2\sigma^2}\right), \quad \sigma = Y(k = \frac{1}{4}) \cdot \sqrt{\langle L_{max} \rangle}. \quad (\text{II-18})$$

It is obtained by taking logarithm of eq.(II-17), applying Sterling's formula:

$$\ln L_{max}! = \left(L_{max} + \frac{1}{2}\right) \ln L_{max} - L_{max} + \frac{1}{2} \ln 2\pi + O(L_{max}^{-1}),$$

and reexponentiating again the obtained result. It is interesting to notice at this point that almost identical behaviour of rapidity distributions emerges from hydrodynamical models of multiparticle production [40,41] for which  $\sigma$  would be given by details of the assumed equation of state characterized by the velocity of sound  $c_0$ . It means therefore, that CAS can mimic not only thermal models (as mentioned before) but also hydrodynamical ones, especially those with the continuous emission of particles, as proposed in [42].

For asymmetric cascade,  $M \rightarrow \mu + (k \cdot M)$ , the existence of two different rapidity steps (one for particle  $\mu$  and another for the recoil mass  $k \cdot M$ ) prevents in practice such simple exercise. Nevertheless, as can be seen in Fig.II.3, also in this case the central region is well fitted by very broad Gaussian (corresponding to  $c_0^2 \rightarrow 1$  in [40,41]).

Before leaving this subject one should mention that Gaussian formula above do not apply at the ends of rapidity region, cf. Fig.II.3, which are dominated by very small  $L_{max}$ . This is especially true for the case of asymmetric cascade.

In Fig.II.3 we have also plotted the rapidity distributions expected by using the so called MaxEnt hadronization model, details of which are given in Appendix A. For mass  $M$  and some limited transverse mass  $\mu$  (the same as that in the case of CAS above), and for the mean multiplicities  $N = \langle N_s \rangle$  or  $N = \langle N_a \rangle$  as above, it provides the least biased and most probable distribution in one dimension (here in rapidity) obtained by means of the information theory [30]. This distribution contains no additional information but only that given mass  $M$  is hadronizing instantaneously into exactly  $N$  particles of transverse mass  $\mu_T$  and it is obtained by maximizing suitably defined information entropy (cf. Appendix A). As a result we obtain the following single particle distribution (cf. eq.(A-14))

$$f_I(y) = \frac{1}{Z} \exp[-\beta \cdot \mu_T \cosh y], \quad (\text{II-19})$$

where

$$Z = \int dy f_I(y), \quad (\text{II.20})$$

and  $\beta = \beta(M, N)$  is the corresponding Lagrange multiplier ensuring proper conservation of energy in the case when  $N$  particles with transverse mass  $\mu_T$  are produced from the source of mass  $M$  (the antisymmetric form of momentum,  $p = \mu_T \sinh y$ , with respect to transformation  $y \rightarrow -y$ , together with symmetric form of  $f_I(y)$  makes the corresponding Lagrange multiplier for momentum conservation equal zero).

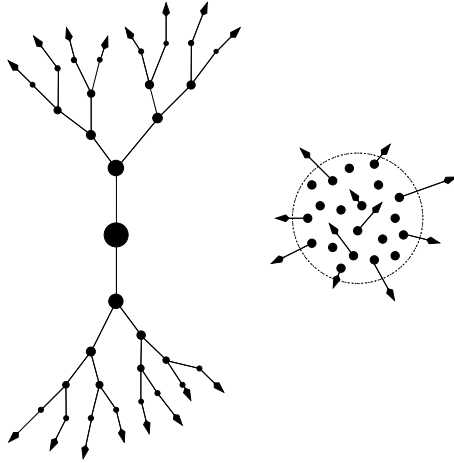


**Fig. II.5.** Schematic views of the cascade process (CAS - on the left) and hadronization based on information theory (MaxEnt - on the right). The former is sequential with strong momentum-position correlations, the later is understood as occurring instantaneously in the whole phase space available.

As we see in Fig.II.3, cascade distributions contain more information as they differ substantially from the *a priori* least informative MaxEnt distributions<sup>13</sup>. It should be stressed here that although (II.19) resembles the formula used in thermodynamical models, no thermal equilibrium has been assumed here, so its validity is of greater range (in particular the "temperature"  $\beta$  can assume not only positive but also negative values depending on the number of particles produced, cf. the maximally asymmetric cascade example in Fig.II.3 and further discussion of this point in Chapter III, especially eqs.(III.6) and (B.29).). Actually, also here one observes a kind of scaling, this time in the variable  $\frac{M}{N}$  (in the mean energy per particle cf. eq.(A.18) in Appendix A).

<sup>13</sup>This additional information is the sequential decay scheme allowing to calculate the multiplicity distributions of produced particles,  $P(N)$ , which are assumed as given from somewhere else in MaxEnt, see Fig.II.5. One should stress here also that, whereas in CAS the energy-momenta are conserved locally, i.e., in each decay vertex, in MaxEnt the conservation is global, i.e., for the whole event. The actual differences in the corresponding informational entropies calculated for both distributions shown in Fig.II.3 are not big:  $S_{\text{CAS}} = 2.3$  and  $S_{\text{MaxEnt}} = 2.4$  (to be compared with flat distribution for which  $S$  is maximal, i.e.,  $S_{\text{MAX}} = 2.5$ ).

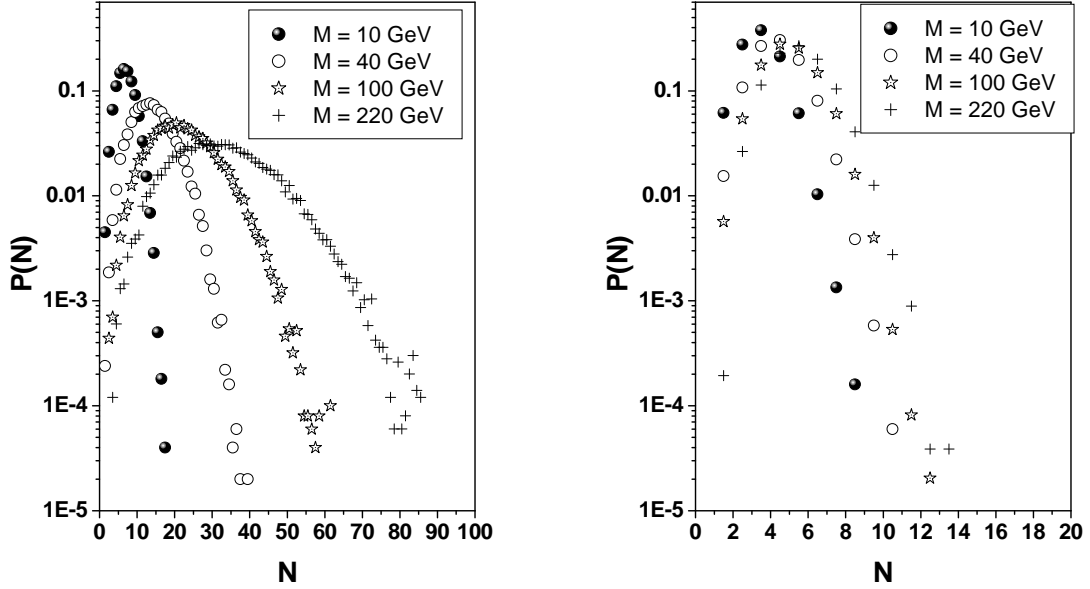


**Fig. II.6.** Multiplicity distributions  $P(N)$  for (one-dimensional) normal (left) and asymmetric (right) cascades of masses  $M = 10, 40, 100$  GeV (for  $\mu = 0.3$  GeV and  $k_{1,2}$  given by the same triangle distributions  $P(k)$  as in Fig.II.3).

The scaling feature of CAS model mentioned previously means in particular that the shape of the multiplicity distribution,  $P(N)$ , of secondaries produced by the source  $M$  is in our case entirely given by distribution  $P(k_{1,2})$  of decay parameters  $k_{1,2}$ . We shall calculate it now using, as already mentioned above, the simple triangle form of  $P(k) = (1-k)^a$ , motivated by the fact that for  $a \simeq 1$  it provides the commonly accepted energy behavior of the mean multiplicities  $N(M) \sim M^{0.4-0.5}$ . The example of  $P(N)$  for  $D = 1$  cascades are shown in Fig.II.6 (multiplicity distributions for  $D = 3$  cascade are the same) with their main characteristics listed in **Tables I**.

$M$ [GeV]	Normal cascade			Asymmetric cascade			Normal cascade		
	$\langle N \rangle$	$\sigma$	$\sigma/\langle N \rangle$	$\langle N \rangle$	$\sigma$	$\sigma/\langle N \rangle$	$\langle N_{ch} \rangle$	$\sigma$	$\sigma/\langle N_{ch} \rangle$
10	7.04	2.40	0.34	3.47	1.05	0.30	5.11	2.05	0.40
40	14.22	5.23	0.37	4.41	1.28	0.29	9.92	3.80	0.38
100	22.42	8.40	0.37	5.02	1.40	0.28	15.36	5.89	0.38
220	33.01	12.63	0.38	5.57	1.49	0.27	22.43	8.74	0.39

**Table I.** The mean multiplicity  $\langle N \rangle$  and dispersion  $\sigma = \sqrt{\langle N^2 \rangle - \langle N \rangle^2}$  for multiplicity distributions  $P(N)$  shown in Fig.II.6. Mean multiplicities and dispersions for charged particles produced by normal cascade are also shown.

The above results for charged multiplicity distributions resemble to some extent those for  $e^+e^-$  annihilations (cf. [43]). This is natural because only there one has situation with the original energy  $M$  being fixed. On the other hand with  $P(k_{1,2})$  used here our  $P(N)$

distributions are systematically broader (the values listed in **Table I** should be confronted with the experimental values of  $\sigma/\langle N \rangle$  equal to 0.33, 0.29 and 0.29 for energies 14.0, 34.5 and 91.2 GeV, respectively [44]). However, they are apparently not broad enough to be comparable with hadronic data (our  $\sigma/\langle N \rangle$  as listed in **Table I** deviate substantially from the value  $\sim 0.58$  as given by the so called Wróblewski formula [45]:  $\sigma = 0.58(\langle N \rangle - 1)$ ). It must be remember, however, that experimental results are, so far, obtained only in inclusive type of experiments and there is still possibility that results obtained on event-by-event basis (i.e., with  $M$  being fixed) will resemble those presented here.

One of the characteristic features searched for in multiproduction processes is the so-called KNO scaling [46]. According to it the probability distributions  $P_s(N)$  to produce  $N$  particles in a certain collision process should exhibit the following scaling (homogeneity) property:

$$P_s(N) = \frac{1}{\langle N(s) \rangle} \cdot \Psi \left( \frac{N}{\langle N(s) \rangle} \right), \quad (\text{II.21})$$

where  $\langle N(s) \rangle$  denotes average multiplicity of secondaries at collision energy  $\sqrt{s}$ . This scaling law, asserts that if we rescale  $P_s(N)$  measured at different energies via stretching (shrinking) the vertical (horizontal) axes by  $\langle N(s) \rangle$ , these rescaled curves will coincide with each other. It means that the multiplicity distributions become simple rescaled copies of some universal function  $\Psi(z)$  depending only on the scaled multiplicity  $z = n/\langle N(s) \rangle$ . As can be seen in Figs.II.7, this is, indeed, the case for our cascade model as well except perhaps the lowest energy  $M = 10$  GeV for which one observes deviation for large  $z$  (however, one should remember that for such low  $M$  the higher multiplicities are strongly depleted). The asymmetric cascade does not show such property, cf. Fig.II.8, at least not as exactly as in Fig.II.7. In Fig.II.7 we show fit to the KNO curve performed by using Polyakov type formula [47]

$$\Psi(z) = Nz^{\mu k-1} \exp(-[Dz]^\mu), \quad N = \frac{\mu D^{\mu k}}{\Gamma(k)}. \quad (\text{II.22})$$

As one can see the parameters used changed from (curve "1")  $k = 0.99$ ,  $\mu = 3.0$ ,  $D = 0.89$  to (curve "2")  $k = 1.01$ ,  $\mu = 2.8$  and  $D = 0.88$  (to be compared with those obtained for LEP  $e^+e^-$  data:  $k = 1.5$ ,  $\mu = 1.7$  and  $D = 0.85$  [47]). We shall not pursue this problem further.

The scaling exhibited by CAS should be contrasted, however, with the observed strong violation of KNO scaling at very high energies for  $p\bar{p}$  collisions (and also expected to occur, albeit to a lesser degree, in  $e^+e^-$  annihilation processes) [43]. It would suggest again that, from the point of view of our CAS model, violation of scaling is coming from the composite character of the hadronizing source (with a number of elementary subsources of the type discussed here with masses  $M_i$  violation of scaling would have to originate in dynamics leading to the peculiar distribution of  $M_i$ 's). It must be noted, however, that although CAS is a real cascade model, we do not find it necessary to resort to a more involved scaling prescriptions, as, for example, the one proposed recently in [47] and claimed to be

especially appropriate to the cascade processes of all kinds. The original application of the KNO prescription seems to be enough for our limited purpose here.

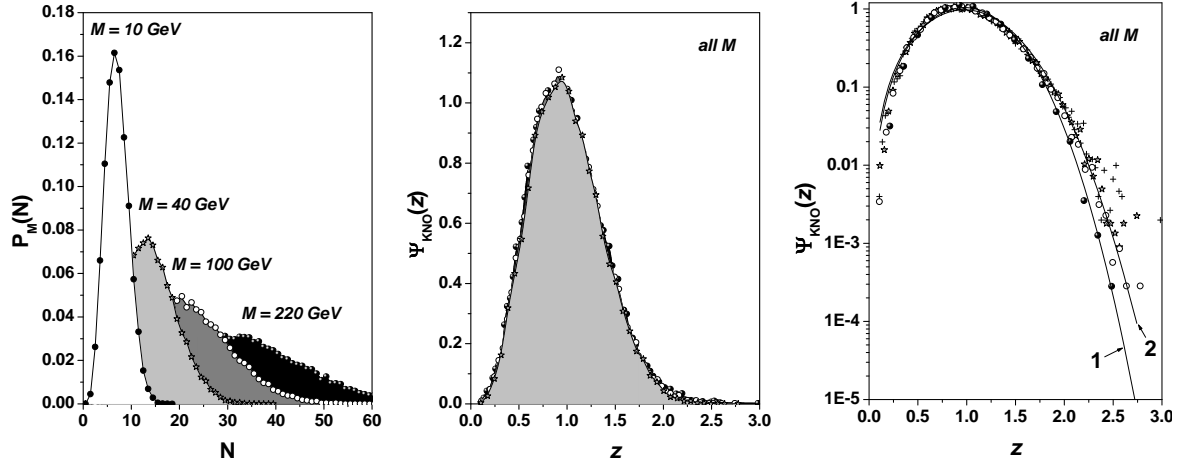


**Fig. II.7.** KNO-scaling for cascade processes, cf. left panel of Fig.II.6 ( $\sqrt{s} = M$  in our case). Curves "1" and "2" are obtained using formula (II.22) with parameters given in text.

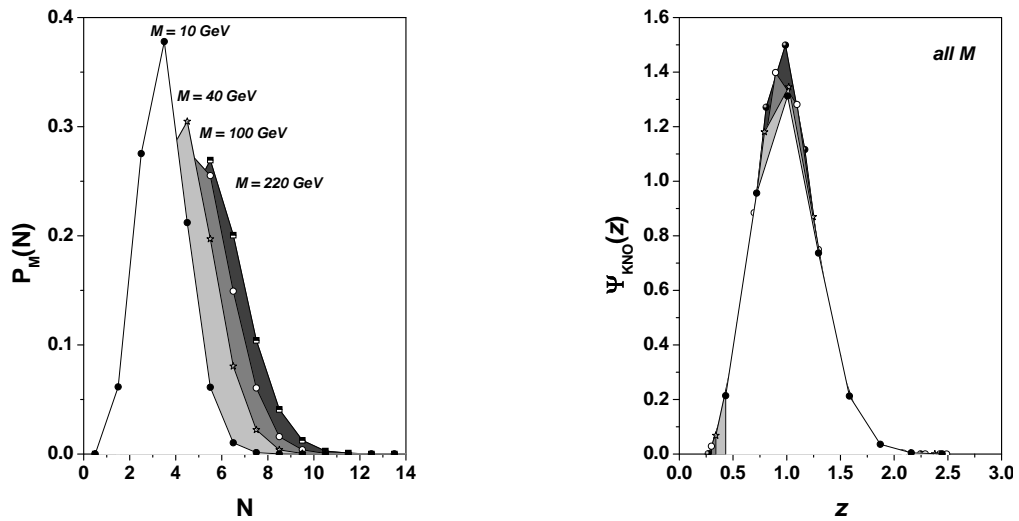


**Fig. II.8.** KNO-scaling for asymmetric cascade processes, cf. right panel of Fig.II.6 ( $\sqrt{s} = M$  in our case).

### 3. Configuration space characteristics of CAS

In order to be able to investigate the cascade development in configuration space we shall now add some space-time elements to our cascade. To this aim we introduce some fictitious finite "lifetime"  $t$  for each vertex mass  $M_l$  (defined in its rest frame), and, in order to make it more realistic, to allow it to fluctuate according to some prescribed distribution law  $\Gamma(t)$ . This procedure is a purely classical one, i.e., we are not treating  $M_l$  as resonances as in [48]. Instead, they are regarded to be real objects (clusters) with masses given by the corresponding values of decay parameters  $k_{1,2}$  and with the respective velocities equal to  $\vec{\beta} = \vec{P}_{1,2}/E_{1,2}$ , with  $(E_{1,2}; \vec{P}_{1,2})$  being the energy momenta of the corresponding decay product given in the rest frame of the parent mass in each vertex. The energy momentum and charges are strictly conserved in each vertex separately. For decay/branching law we shall assume the following simple form:

$$\Gamma(t) = \frac{2-q}{\tau} \cdot \left[ 1 - (1-q) \frac{t}{\tau} \right]^{1/(1-q)} \xrightarrow{q \rightarrow 1} \Gamma(t) = \frac{1}{\tau} \cdot \exp \left[ -\frac{t}{\tau} \right]. \quad (\text{II-23})$$

This form allows, by means of additional parameter  $q$ , to account for a variety of possible influences caused by, for example, long-range correlations, memory effects, possible additional fractal structure present in the production process [24] or by some intrinsic, internal fluctuations of parameter  $\frac{1}{\tau}$  not accounted for [49–51]. They all result in non-extensivity of some thermodynamical variables (like entropy) with  $|1-q|$  being the measure of this non-extensivity (cf., Appendix B). For  $q=1$  we recover simple exponential decay law. In the case of cascade the  $q$  can be regarded as describing different type of its spatio-temporal diffuseness:  $q > 1$  corresponds to a more dilute distribution of particle production points (elongating therefore spatial dimension of cascade) whereas  $q < 1$  has opposite effect, i.e., it makes spatial cascade more dense and shorter (cf. Appendix B).

With both phase-space and spatio-temporal evolution settled, it is straightforward to get our cascade in the form of the Monte-Carlo code with two (or three, including  $q$ ) parameters: decay vertices  $k_{1,2}$  and "lifetime"  $\tau$ . The main features of one-dimensional case have been already demonstrated above. The only difference between one and three-dimensional cascades is in the fact that whereas in the former decay products can flow only along one, chosen direction, in the later the flow direction in each vertex is chosen randomly from the isotropic angular distribution. To allow for some non-zero transverse momentum in the one-dimensional case we are using there the transverse mass  $\mu_T = 0.3$  GeV. For the three-dimensional cascade  $\mu_T$  is instead set simply to pion mass,  $\mu = 0.14$  GeV. In every case all decays are described in the rest frame of the corresponding parent mass in a given vertex. To get final distributions one has therefore to perform a number of Lorentz transformations to the rest frame of the initial mass  $M$ . As output we are getting in each event a number  $N_j$  of secondaries of mass  $\mu$  with both well defined energy-momenta and space-time coordinates of the branchings in which at least one final particle has been created,

$$\left\{ E_i = \sqrt{\mu^2 + \vec{P}_i^2}; \vec{P}_i \right\}_{i=1,\dots,N_j} \quad \text{and} \quad \{t_i, \vec{r}_i\}_{i=1,\dots,N_j}.$$

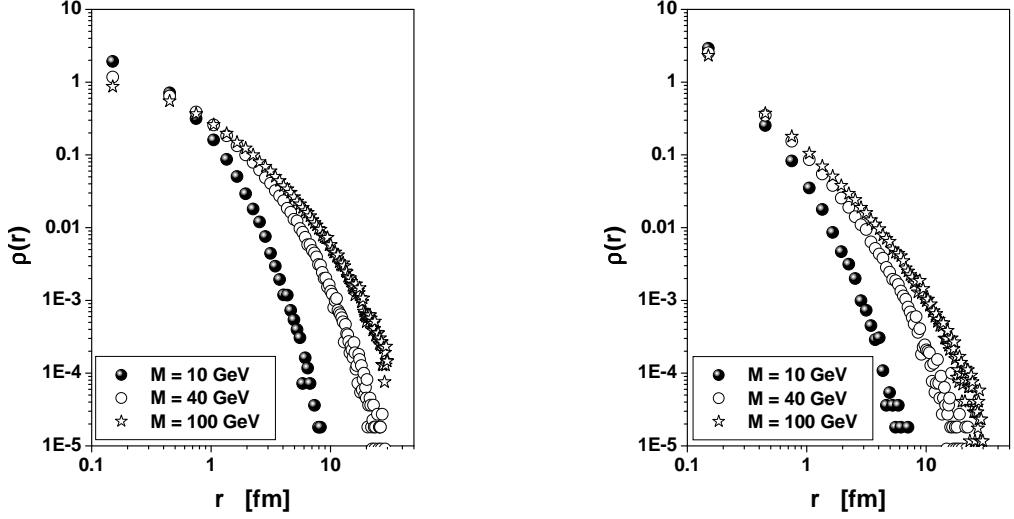


**Fig. II.9.** Normalized density distribution of the production points  $\rho(r)$  for one-dimensional cascades,  $r = |x|$ . Two different choices of the evolution parameter  $\tau$  are considered:  $\tau = 0.2$  fm, left panel, and  $\tau = 0.2/M$  (in fm, the mass  $M$  is the parent mass in a given vertex), right panel. Both panels show results for three different masses  $M$  of the source:  $M = 10, 40$  and  $100$  GeV. In all cases  $k$  is chosen from the same triangle distribution as in Fig.II.3.

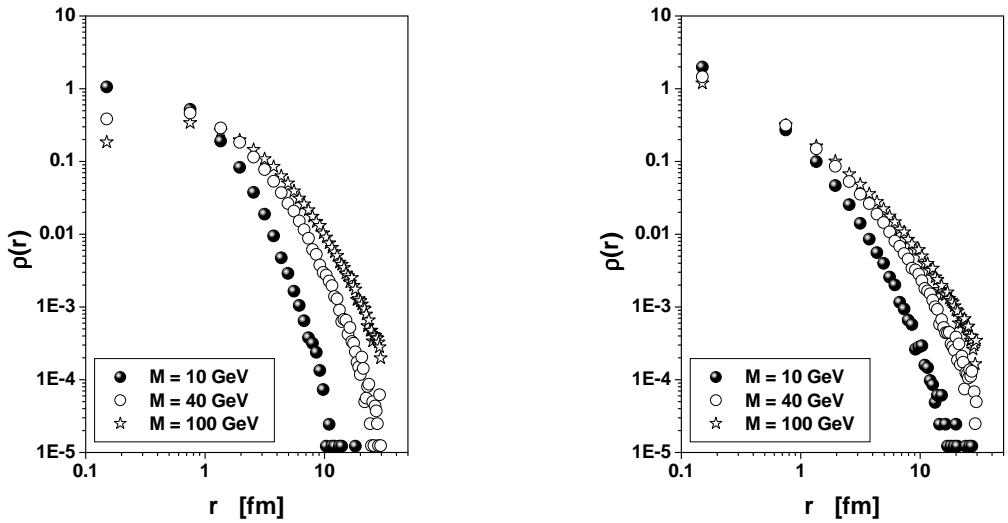


**Fig. II.10.** Normalized density distribution of the production points  $\rho(r)$  for three-dimensional cascades with the same parameters as in Fig.II.9,  $r = \sqrt{x^2 + y^2 + z^2}$ .

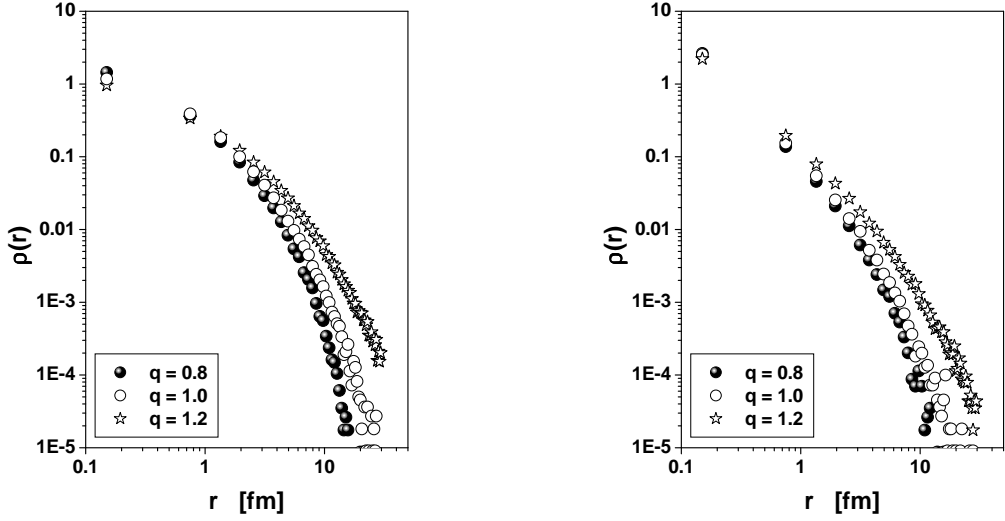


**Fig. II.11.** Normalized density distribution of the production points  $\rho(r)$  for one-dimensional cascades of different diffusiveness. Two different choices of the evolution parameter  $\tau$  are considered:  $\tau = 0.2$  fm, left panel, and  $\tau = 0.2/M$  (in fm, the mass  $M$  is the parent mass in a given vertex), right panel. Both panels show results for mass  $M = 40$  GeV and the three values of the non-extensivity parameter  $q$ :  $q = 0.8, 1.0$  and  $1.2$ . In all cases  $k$  is chosen from the same triangle distribution as in Fig.II.3.

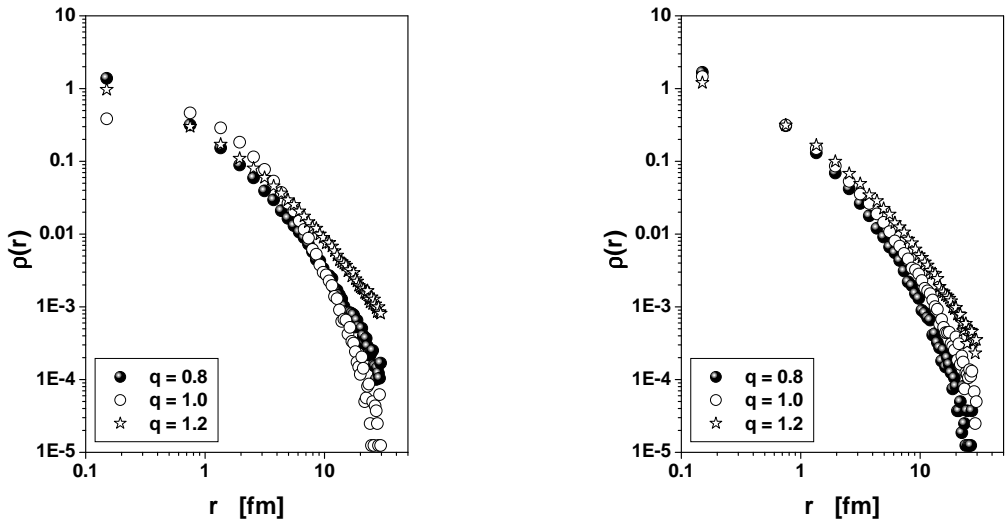


**Fig. II.12.** Normalized density distribution of the production points  $\rho(r)$  for three-dimensional cascades with the same parameters as in Fig.II.11.

We shall now discuss the shape of spatial distributions of the production points, one obtains in this way. Our special interest will be to check to what extent  $\rho(r)$  exhibits the

expected [18,19,31] power-like (or Lévy) behavior of the type (cf. eq.(II·5))

$$\rho(r) \sim r^{-\alpha} \quad (\text{II}\cdot24)$$

in spatial variable ( $r = |x|$  for  $D = 1$  or  $r = \sqrt{x^2 + y^2 + z^2}$  for  $D = 3$ ).

As one can see in Figs.II.9 and II.10 where typical behavior of the density  $\rho(r)$  of points of particle production for different choices of parameter  $\tau$  for one- and three-dimensional cascades are exhibited, the expected behaviour as given by eq.(II·24) with  $\alpha = \text{const}$  is not seen at all, i.e., one can only select different ranges in  $r = x$  with different  $\alpha$ , or just say that  $\alpha = \alpha(r)$ . Actually the resultant picture depends on how rapidly our cascade develops in space-time. Changing  $\tau$  from  $\text{const } \tau = 0.2 \text{ fm}$  to, for example, mass dependent  $\tau = \frac{0.2}{M}$ <sup>14</sup> (i.e., proceeding from a "slow" to "fast" cascades), one gets picture resembling scaling, although even here no single  $\alpha$  for all range of  $r$  can be found. This fact is caused by the finiteness of our cascade process, which has its origin in the finiteness of the ratio  $M/\mu$ .

The same is true also for  $q \neq 1$  (i.e., for more diluted or more dense cascades), cf. Figs.II.11 and II.12. The previously mentioned fact that different  $q$  should in practice lead to cascades of different spatial lengths is now clearly visible:  $q < 1$  case looks similar to  $M < 40 \text{ GeV}$  case, whereas  $q > 1$  is similar to  $M > 40 \text{ GeV}$  case.

The finiteness of our cascades allow us to calculate their mean sizes ("radii") defined as ("Size A" in Table II):

$$r_A = \langle r \rangle = \int d^3r r \cdot \rho(r). \quad (\text{II}\cdot25)$$

They differ from the mean-square radii ("Size B" in Table II) defined as

$$r_B = \langle r \rangle_{ms} = \frac{1}{N_{\text{event}}} \sum_j^{N_{\text{event}}} \sqrt{\frac{1}{N_{\text{particle}}} \sum_i^{N_{\text{particle}}} (r_{ij} - \bar{r}_{ij})^2}, \quad (\text{II}\cdot26)$$

with  $r = |x|$  for  $D = 1$  and  $r = \sqrt{x^2 + y^2 + z^2}$  for  $D = 3$ . The persistent feature of  $\rho(x)$  obtained here from CAS is the fact that they are definitely neither Gaussian (or exponential) nor power-like for any reasonable choice of parameters. The corresponding values of these sizes (in [fm]) are listed in the **Table II**. **Table II** contains also values of exponents in (II·24) for  $r \rightarrow 0$ ,  $\alpha_0$ , and for large distances,  $\alpha_\infty$ . For "slow" cascades ( $\tau = 0.2 \text{ fm}$ ) there is general tendency to get for small  $r$ , smaller  $\alpha_0$ , i.e., flatter (sources even exhibiting a depletion of production points for  $D = 3$  case and for larger masses).

---

<sup>14</sup>For a possible dynamical origin of such behavior of  $\tau$  see [52]. Here it is used mainly to speed out the spatio-temporal development of cascade in comparison with  $\tau = \text{const}$  case. For  $\tau \propto 1/M$  one gets visible congestion of production points near the initial mass  $M$  (i.e., near  $r = 0$ ).

This is not the case for "fast" cascades with  $\tau \approx 1/M$ .

We have demonstrated, therefore, that in practice it is very difficult (if not impossible, at least in the framework of CAS model) to get hadronic source exhibiting power-law spatial structure of the type (II.24) (or II.3). It means that there is no simple fractal source (of the type investigated in [18,19,31]) in CAS<sup>15</sup>. It is difficult to imagine any other model of hadronization, which would contain more intrinsic sources of fluctuations than CAS, therefore our results clearly indicate that simple analytical estimation of the type presented in [18,19,31] do not find its numerical realization in realistic models (at least, not to the naively expected level). This should be kept in mind when discussing results for intermittency and BEC presented below and in Section 5 of this Chapter.

#### 4. Intermittency in CAS

Intermittency in high-energy collisions was defined [54,28] as a specific property of the spectra of the produced particles. The spectrum is called intermittent if the scaled factorial moments

$$F_q \left( \delta = \frac{\Delta}{M_{bin}} \right) = \frac{M_{bin}^{q-1}}{\langle N \rangle^q} \left\langle \sum_{m=1}^{M_{bin}} n_m (n_m - 1) \dots (n_m - q + 1) \right\rangle \quad (\text{II.27})$$

obey the power law

$$F_q(\delta) = \left( \frac{\Delta}{\delta} \right)^{f_q} F_q(\Delta) \quad (\text{II.28})$$

for  $\delta \rightarrow 0$ . Here  $\delta$  and  $\Delta$  are phase-space volumes in which  $F_q$  is calculated, and  $n_m$  is the multiplicity of particles in the given volume.  $\langle \dots \rangle$  denotes averaging over events and  $q$  is an integer,  $q \geq 2$ . The positive constants  $f_q$  are called intermittency exponents.

It is interesting to note that our results presented in Fig.II.13 (left panel), although obtained for essentially the same type of cascade as discussed in [32], substantially differ from the intermittency pattern obtained there, i.e., our cascade shows much weaker (if at all) intermittency. After closer inspection of formulas derived in [32] the reason becomes obvious. Namely, at some point (eqs.(9) of [32]) one identifies there the original mass  $m_0$  (equal to  $M$  in our case) with the maximal rapidity (modulo proportionality constant) and the final mass  $m_T$  (our  $\mu$ ) with the size of the rapidity bin  $\delta y$  (using the same proportionality constant). In this way the intermittency in masses (natural for this kind of model) is *assumed* to transfer itself in the same form to the rapidity space. This is, however, not correct, cf. eqs.(II.12). It means that numerical results of [32] concerning intermittency and presented in rapidity space correspond to the same type of cascades as discussed in [28,37] (i.e., formulated directly in rapidity) and have nothing to do with

<sup>15</sup>The best one can get is something similar to a multifractal structure, for example as defined in [53].

the initial cascade proceeding (as in CAS model) in masses and described by fractal dimension  $d_F = \ln 2 / \ln \frac{1}{k}$ , as in eq.(II.11). Therefore fractal dimension  $d_F$  deduced in [32] from the experimental data has nothing to do with fractal dimension of mass cascade discussed there. In fact, its value corresponds to a very large number from the point of view of CAS model, resulting in unrealistic mass dependence of multiplicity, leading to  $\langle N_s(M) \rangle \simeq M^{0.8-0.9}$  instead of the expected  $\langle N_s(M) \rangle \simeq M^{0.4-0.5}$  used by us.

In Fig.II.13 (right panel), we present results of calculation for another kind of the distribution of the decay parameters  $k_{1,2}$ , which is now taken in the form  $P(k) = (1 - k)^{-0.98}$ . In this case, one has much longer cascade, with two times bigger mean multiplicity than before,  $\langle N \rangle = 43.4$  instead of  $\langle N \rangle = 22.4$ . Therefore this changes significantly the observed intermittency pattern, as seen in Fig.II.13. Notice also that such choice of  $P(k)$  results in the energy dependence of mean multiplicity equal to  $\langle N_s(M) \rangle \simeq M^{0.63}$  which is still far away from that used in [32]<sup>16</sup>.

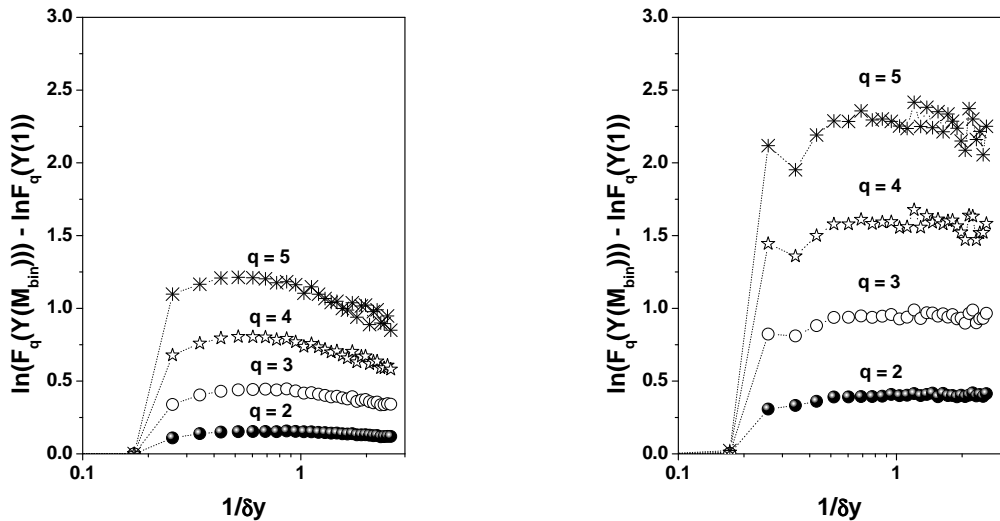


**Fig. II.13.** Example of the scaled "horizontal" moments  $F_q$  as function of the reverse width of the bin in rapidity space,  $1/\delta y$ , for the one-dimensional cascades calculated for negative pions. Left panel shows the first five moments for the cascade of mass  $M = 100$  GeV and  $\mu_T = 0.3$  GeV with  $k_{1,2}$  chosen randomly from the triangle distribution,  $P(k) = 1 - k$ , whereas the right panel presents the same results for the cascade governed by decay parameters  $k_{1,2}$  drawn from the distribution  $P(k) = (1 - k)^a$  with  $a = -0.98$ . Notice that  $Y(1)$  corresponds to maximal range of rapidity  $|y| < 5.82$  in this case. The vertical scale is in the same variable as in [32].

To summarize: we observe only weak intermittency (in rapidity variable, in which most of the intermittency results are presented) in CAS. This can be contrasted with results

---

<sup>16</sup>The results on intermittency in CAS presented in [20] are, unfortunately, based on mistaken formula used for numerical calculations and are not correct.

of the other intermittency models (like [28,37]). The reason for what is seen in Fig.II.13 has been already mentioned in Chapter II.2 above and illustrated by Fig.II.3. Namely, the multiplicative process in invariant masses does not mean the same type behaviour in any other variable, for example in rapidity. In a given event (i.e., for a given set  $\{k_{1,2}\}$ ) particles are located only in a finite number of points in rapidity. Once the number of bins exceeds this number, the factorial moments  $F_q \sim M^{q-1}$ . The averaging over events smoothes this behaviour to what is seen in Fig.II.13. Only when one forces to have more than one particle in a bin, notwithstanding the bin number, as it will be the case discussed in Chapter V.5 (after imposing Bose statistics on produced particles), the true intermittent signal will start to be visible.

## 5. CAS and simple implementation of Bose-Einstein correlations (BEC) by means of the "afterburner" method

Let us proceed now to our main point, namely, to the question of whether one can see in BEC some special features which could be attributed solely to the branchings and to their space-time and momentum space structure. At first glance, the answer seems to be negative as it is easy to check that correlation function (cf. Appendix C) for the like-sign pairs of particles provided by CAS,

$$C_2(Q = |p_i - p_j|) = \frac{dN(p_i, p_j)}{dN(p_i) \cdot dN(p_j)} \quad (\text{II.29})$$

does not show any evidence of BEC. It is also true if we endow our cascade process with the production of charges by assuming that only such vertices can occur:

$$\{0\} \rightarrow \{-\} + \{+\}, \quad \{+\} \rightarrow \{+\} + \{0\} \quad \text{and} \quad \{-\} \rightarrow \{-\} + \{0\}$$

. In this case  $C_2$  calculated for like charge pairs also does not show any correlations<sup>17</sup>. We shall proceed therefore as in many other investigations discussed in literature. Namely, because our aim is not data fitting but checking if, and to what extent, the BEC via its  $C_2$  observable is sensitive to different choices of the cascade processes provided by different sets of parameters, we have decided to use the ideas of the BEC "afterburners" advocated in [21]. And because we are not so much interested in particular values of the "radius" and "coherence" parameters,  $R$  and  $\lambda$  (cf. eqs.(II.31) and (II.32) below), but in the systematics emerging from our study, we shall use for this exploratory research the most primitive, classical version of such "afterburner". The procedure we employ is therefore very simple. After generating a set of  $i = 1, \dots, N_l$  particles for the  $l$ th event we choose all pairs of the same sign and endow them with the weight factors of the form

$$C = 1 + \cos [(r_i - r_j) \cdot (p_i - p_j)], \quad (\text{II.30})$$

<sup>17</sup>This is, however, to be expected, because the only way to have eq.(II.29) showing "primordial" BEC (i.e., already at a given event) is to introduce them from the very beginning, for example in the way done in [55]. Such possibility will be explored in Chapter V where we shall propose our way of introducing such "primordial" BEC into events provided by event generator.

where  $r_i = (t_i, \vec{r}_i)$  and  $p_i = (E_i, \vec{p}_i)$  for a given particle.

The results obtained from  $N_{event} = 50000^{18}$  events are presented in Figs.II.14 and II.15<sup>19</sup>. They are displayed for the same sequence of parameters  $M$  (mass of the source),  $D$  (its dimensionality) and  $\tau$  (the evolution parameter) as in Figs.II.9 and II.10. The characteristic feature to be noted is a substantial difference between  $D = 1$  and  $D = 3$  dimensional cascades both in the width of the  $C_2(Q)$  and in their shapes. Whereas the former are more exponential-like (especially, for  $\tau = 0.2$  fm) the latter are more gaussian-like with a noticeably tendency to flattening out at very small values of  $Q$ . There is also difference between "slow" (constant  $\tau$ ) and "fast" ( $\tau \sim \frac{1}{M}$ ) cascades, especially for  $D = 1$  case.

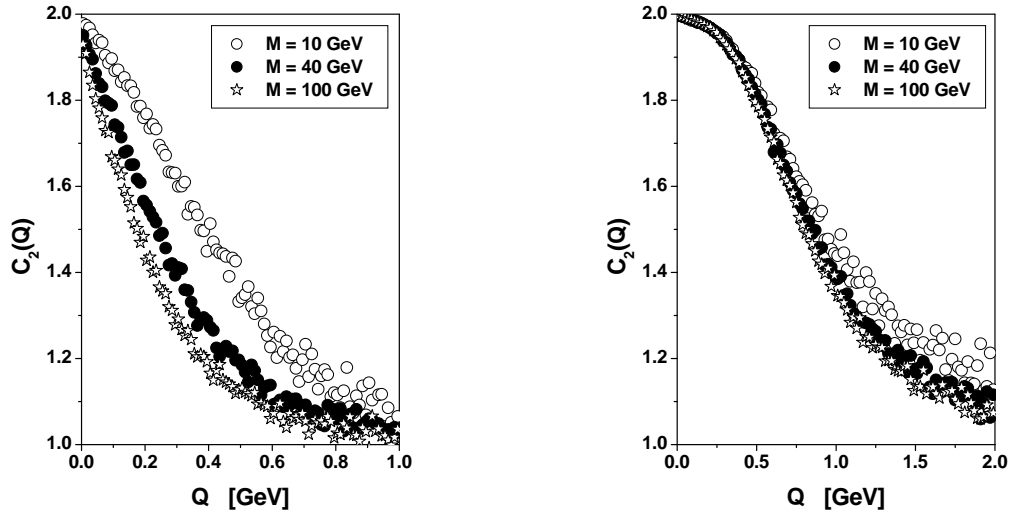


**Fig. II.14.** The correlation functions  $C_2(Q = |p_i - p_j|)$  for one-dimensional cascades with the evolution parameter  $\tau$  taken as  $\tau = 0.2$  fm - left panel, and as  $\tau = 0.2/M$  (in fm, the mass  $M$  is the parent mass in a given vertex) - right panel. Both panels show results for three different masses  $M$  of the source:  $M = 10, 40$  and  $100$  GeV.

The former lead to substantially different shapes in this case. In  $D = 3$  this effect is not so visible, although it is also present (for  $\tau \sim \frac{1}{M}$  case the correlation function  $C_2$  is broader for both cases). For  $D = 1$  case the length of the "slow" cascade (i.e., the radius of the production region) dictates the width of  $C_2(Q)$ . There is practically no such effect for the remaining cases. The  $M/\mu$  scaling observed before in multiplicities is not present here. This is because  $C_2$  depends on the differences of momenta,  $p = \mu_T \sinh y$ , which do not scale in  $M/\mu$  and on sources  $\rho(r)$ , which do not scale either. The flattening mentioned

<sup>18</sup>This is the standard number of events used throughout this work to calculate all results shown here.

<sup>19</sup>As mentioned already in II.2 (footnote 8) these results are slightly different from those presented already in [20] because of different procedure of ending the cascade. The conclusions reached remains, however, unchanged.

above for  $D = 3$  cascades can be probably regarded as being the most distinctive signature of the possible fractal structure combined with  $D = 3$  dimensionality of the cascade.

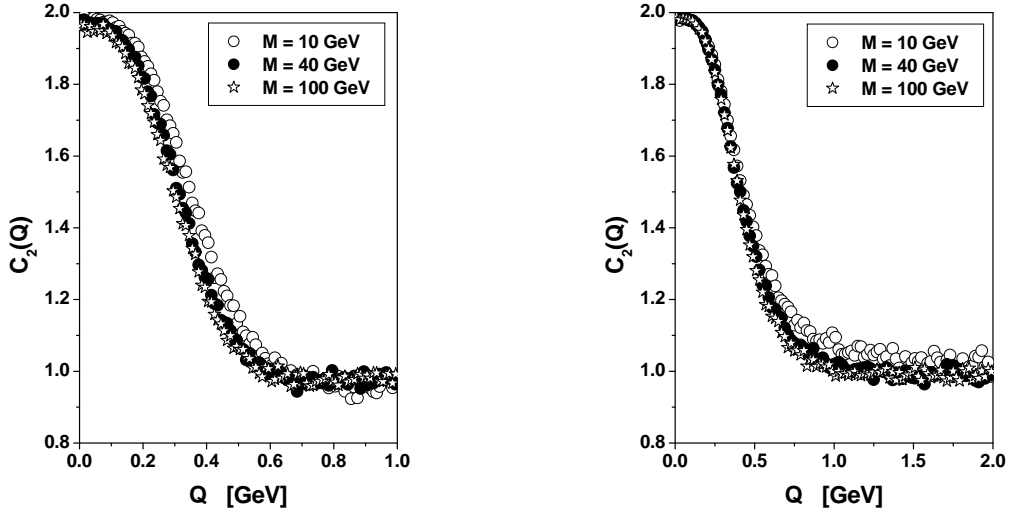


**Fig. II.15.** The same as Fig. II.14 except that each panel shows results for 3-dimensional cascades.

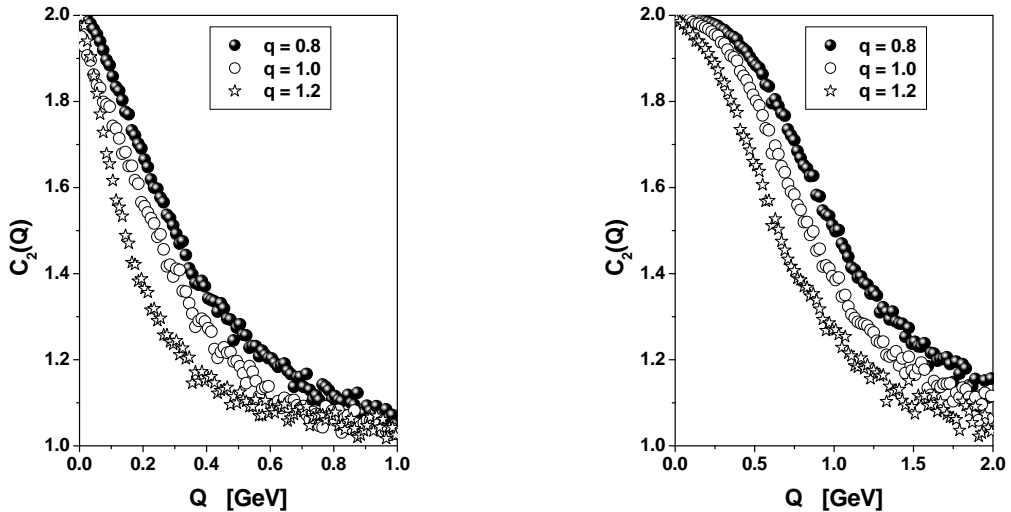


**Fig. II.16.** The correlation functions  $C_2(Q = |p_i - p_j|)$  for one-dimensional cascades with the evolution parameter  $\tau$  taken as  $\tau = 0.2$  fm - left panel, and as  $\tau = 0.2/M$  (in fm, the mass  $M$  is the parent mass in a given vertex) - right panel. Both panels show results for mass  $M = 40$  GeV and three values of the non-extensivity parameter  $q$ :  $q = 0.8, 1.0$  and  $1.2$ .

Namely, the correlations of the position-momentum type existing here, as in all flow phenomena, are in the case of  $D = 3$  cascades not necessarily vanishing for very small differences in positions or momenta between particles under consideration. The reason is that our space-time structure of the process can have in  $D = 3$  a "patchy" pattern, i.e., it can have a kind of "holes" or regions in which the number of produced particles is very small or which are simply not populated at all. Such pattern is characteristic feature of

any cascade process. This is perhaps the most characteristic feature for multifractal (i.e., cascade) process of the type considered here.

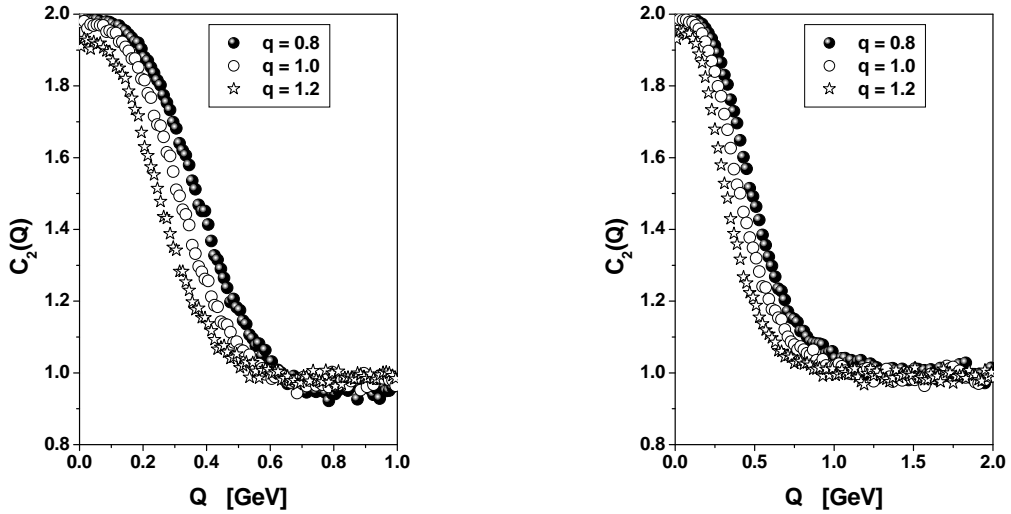


**Fig. II.17.** The same as Fig. II.16 except that each panel shows results for 3-dimensional cascades.

Figs. II.16 and II.17 display the same quantities as Figs. II.14 and II.15, respectively, but this time calculated for  $M = 40$  GeV and for different values of the parameter of non-extensivity  $q$  in decay distribution  $\Gamma(t)$  defined in (II.23), which leads to different diffusiveness of the cascade. As can be seen from Figs. II.16 and II.17 it mimics (to some extent) the changes attributed in Figs. II.14 and II.15, respectively, to different energies (making cascade effectively shorter for  $q = 0.8$  and longer for  $q = 1.2$ ). The results of Figs. II.16 and II.17 (taken for  $M = 40$  GeV) should be then compared with those of Figs. II.14 and II.15 for  $M = 10$  and  $M = 100$  GeV. They demonstrate that effects of longer or shorter cascades in momentum space (as given by different  $M$  in Figs. II.14 and II.15) is similar, from the point of view of the correlation function, to effects of the more or less condensed cascades in the position space as given by  $q$  here (we remind again that for  $q > 1$  cascade is larger and more dilute and for  $q < 1$  it is shorter and more dense). In order to see whether there is any connection between the size of cascade defined in eqs. (II.25) and (II.26) and width of the correlation function  $C_2(Q)$  we have fitted results of Figs. II.14 - II.17 either by exponential,

$$C_2(Q) = \gamma [1 + \lambda_e \exp(-R_e \cdot Q)], \quad (\text{II.31})$$

or by gaussian formula (whichever provided better results in a given case),

$$C_2(Q) = \gamma \left[ 1 + \lambda_g \exp\left(-\frac{1}{2} R_g^2 \cdot Q^2\right) \right], \quad (\text{II.32})$$

which are usually used in literature [17]. We have found that whereas for exponential formula fits are usually quite good there are some problems with gaussian form. This is connected with the visible flattening of  $C_2(Q)$  for small  $Q$  mentioned above. Therefore formula (II.32) is used in a restricted range of  $Q$  only, i.e., for  $Q > Q_{cut}$  where  $Q_{cut}$  varies

between  $Q_{cut} = 0.04$  GeV for Fig.II.14 (right panel) to  $Q_{cut} = 0.14$  GeV for Fig.II.17 (right panel). Coming back to exponential fits one should mention that also here one feels effect of flattening, which is reflected by the unusual values of  $\lambda$  (exceeding unity) in some cases. The general impression is, however, that sizes of the cascades as given by source distribution functions  $\rho(r)$  are essentially not systematically connected with the size parameter  $R$  obtained from fits to the corresponding correlation functions  $C_2$  (it seems to be a general problem of BEC generators, see remarks following eq.(IV.22) in Chapter IV below).

Figure		Type of cascade				spatial source				$C_2(Q)$			Type of fit
$\rho(x)$	$C_2(Q)$	$D$	$M$ [GeV]	$q$	$\tau$ [fm]	$\alpha_0$	$\alpha_\infty$	Size A [fm]	Size B [fm]	$R$ [fm]	$\lambda$	$\gamma$	
<b>II.9</b>	<b>II.14</b>	1	10	1.0	0.2	0.91	5.26	0.43	0.43	0.26	2.23	0.63	exp
left	left	40	40			0.56	4.96	1.06	1.42	0.59	1.10	0.96	
left	left	100	100			0.41	3.42	1.82	2.93	0.79	1.00	0.99	
<b>II.9</b>	<b>II.14</b>	1	10	1.0	$\frac{1}{M}$	2.30	4.30	0.22	0.21	0.29	0.72	1.16	gau
right	right	40	40			1.74	3.82	0.39	0.55	0.31	0.81	1.10	
right	right	100	100			1.59	3.28	0.59	1.10	0.33	0.83	1.09	
<b>II.11</b>	<b>II.16</b>	1	10	0.8	0.2	0.84	5.62	0.81	1.09	0.50	1.19	0.96	exp
left	left	40	40			0.68	4.97	1.06	1.42	0.59	1.10	0.96	
left	left	100	100			0.64	3.36	1.79	2.65	1.13	0.97	1.05	
<b>II.11</b>	<b>II.16</b>	1	10	0.8	$\frac{1}{M}$	1.83	5.62	0.33	0.45	0.29	0.79	1.12	gau
right	right	40	40			1.91	1.74	4.43	0.55	0.31	0.81	1.10	
right	right	100	100			1.50	3.36	0.65	1.07	0.32	0.90	1.07	
<b>II.10</b>	<b>II.15</b>	3	10	1.0	0.2	0.20	5.28	0.74	0.82	0.88	1.09	0.95	gau
left	left	40	40			-0.30	4.72	1.75	2.34	0.98	1.04	0.97	
left	left	100	100			-0.53	3.50	2.91	4.36	1.00	1.02	0.97	
<b>II.10</b>	<b>II.16</b>	3	10	1.0	$\frac{1}{M}$	1.34	4.23	0.54	0.69	0.61	0.92	1.04	gau
right	right	40	40			1.02	3.36	1.11	1.90	0.67	0.98	1.00	
right	right	100	100			0.89	2.72	1.68	3.47	0.72	1.01	0.99	
<b>II.12</b>	<b>II.17</b>	3	10	0.8	0.2	0.91	3.23	1.27	2.47	0.85	1.13	0.94	gau
left	left	40	40			-0.30	4.72	1.75	2.34	0.98	1.04	0.97	
left	left	100	100			0.72	2.32	2.39	5.71	1.11	0.95	0.99	
<b>II.12</b>	<b>II.17</b>	3	10	0.8	$\frac{1}{M}$	1.14	4.14	0.81	1.33	0.60	0.99	1.01	gau
right	right	40	40			1.02	3.40	1.11	1.90	0.67	0.98	1.00	
right	right	100	100			0.89	2.66	1.68	3.20	0.78	0.96	1.00	

**Table II.** The summary of information on the source function  $\rho(r)$  as provided in Fig.II.9 - II.12 and on the correlation functions  $C_2(Q)$  in Figs.II.14 - II.17. Dimensionality  $D$ , mass  $M$ , extensity type  $q$  and life-time  $\tau$  of the source fully identify cascade in question. The  $R$  and  $\lambda$  are "radius" and "chaoticity" parameters obtained from the (exponential - "exp" or gaussian - "gau") fits to  $C_2(Q)$ . using eqs.(II.31) or (II.32). The "size A" and "size B" are defined by eqs.(II.25) and (II.26), respectively, and  $\alpha_{0,\infty}$  denotes powers in  $\rho(r)$  (cf. eq.II.24) for  $r \rightarrow 0, \infty$ , respectively.

This probably indicates that neither of two form used to fit  $C_2(Q)$  are adequate in the case of BEC obtained from CAS model by "afterburner" method. All these should be kept in mind when inspecting the respective  $R$ 's presented in **Table.II**<sup>20</sup>.

## 6. Summary

To summarize:

- Our results show that such apparently "realistic" model of hadronization, as that provided by CAS, never leads to the simple power-like structure in space as expected in [18], therefore, one is not fully reproducing analytical expectations of [18,19] in what concern the expected power-like shape of  $C_2$  function. The influence of what is represented in eq.(II-6) by the integral factor occurs to be more important than naively expected and is not vanishing for any choice of parameters considered here. Such structure of the source can be easily understood by taking into account some features of the model used to obtain it. The most important is the fact that cascade process proceeds in invariant mass  $M$  of hadronizing system and can not proceed *ad infinitum* because of the finiteness of the mass of the produced secondaries. As result, the subset of points in the phase space representing the finally produced particles is possessing only approximate fractal structure and can be described only by *the truncated Lévy distribution* instead of the ordinary Lévy distribution corresponding to the power-law behaviour (and true fractal structure).
- Another thing that is worth to stress here is the fact, that contrary to other cascade models, our cascade process does show only weak (if at all) intermittency pattern. This has the same origin as above, namely that fractality in mass distribution does not transmit itself (at least not directly and in full strength because of finiteness of our cascade) to rapidity space in which we look for intermittency. One must also keep in mind strong influence of conservation laws that our cascade process is forced to obey and the stochastic nature of the process itself. One of the evidences of such strong dependence on the conservation laws is a sub-Poissonian character

<sup>20</sup>One should mention at this point that, as shown in [56], the power-like (Lorentzian type) shape of source function:

$$\rho(\xi) = \frac{3}{4} \pi^2 R^4 \frac{1}{(1 + \xi^2/R^2)^{5/2}}, \quad (\text{II-33})$$

which is similar but not identical to our sources, leads to purely exponential form of

$$C_2(Q) = 1 + \exp(-2RQ) \quad (\text{II-34})$$

(with  $\xi^2 = r^2 + (ct)^2$ ). According to [56] it gives the best fit (in terms of  $\chi^2$  values) to data considered there. However, differences between this fit and other more conventional ones (i.e., based on Gaussian or exponential shapes of the source) are not dramatic. This means that in reality it will be very difficult to establish by means of BEC the possible existence of fractal structure of the emitting source.

of the multiplicity distribution observed for small values of initial energy  $M$  and for this part of the cascade, which corresponds to asymmetric case, cf. Fig.II.6 and **Table I**. This is because by imposing constraints caused by demand to fulfill the conservation laws one introduces into system a kind of anti-correlations. This in turn introduces the antibunching effect [57], which results in a more predictable final distributions [57].

- In what concerns Bose-Einstein correlations, it should be mentioned that due to the classical character of our cascade process the final two-particle distributions do not obey the Bose-Einstein statistics. For calculations of the two-particle correlation function, the simplified version of the afterburner procedure has been therefore used. It was shown that there is disagreement between sizes of the sources provided by CAS and the radius parameter obtained from the fit to the correlation function (as observed also in other approaches, see Chapter IV.3). On the other hand the observed shapes of  $C_2(Q)$  function are sensitive to details of the cascade.

## III. Examples of Tsallis statistics in multiparticle production

### 1. Introduction

Although the notion of non-extensivity and Tsallis statistics has already occurred in the previous Chapter, its real presentation will be given here. This Chapter is therefore devoted to three examples of Tsallis statistics occurring in multiparticle production processes, which we have worked out in [25–27]. Two of these examples [25,27] illustrate the role of intrinsic fluctuations existing in the system under consideration in making it a non-extensive one (in the way presented in [49–51]), one provides example of application of Tsallis statistics to event-by-event analysis of some specific multiparticle data [26]<sup>21</sup>.

A few introductory remarks are in order here. Let us start with observation that to describe high-energy collisions with a huge number of degrees of freedom one usually uses thermodynamical methods and concepts that follow the classical Boltzmann-Gibbs (BG) approach [1,40,58]. In some cases, however, either some deviations from the expected behavior are observed experimentally or it is known that the conditions necessary for BG to apply are satisfied (if at all) only approximately. This includes all situations characterized by the presence in the system long-range interactions, long-range microscopic memories, intrinsic fluctuations and by the space-time (and phase space as well) (multi)fractal structure of the process. One of the most probable candidate for this kind of phenomena can be Quark Gluon Plasma, formation of which is expected in ultra-relativistic heavy ion collisions. It is rather common opinion that because of the extreme conditions of density and temperature encountered in high energy nuclear collisions, memory effects and long-range color interactions give rise to the presence of non-Markovian processes in the kinetic equation [59] affecting the thermalization process toward equilibrium as well as the standard equilibrium distribution [60]. Such kind of physical phenomena can be described

---

<sup>21</sup>This, of course, does not yet exclude any of the other explanations of phenomena discussed here present in the literature. For a time being, the approach based on notions of non-extensive statistics is, however, the most economical one, compressing many effects mentioned here into the appropriate change of statistics, which is provided by the simple parameter  $q \neq 1$ . For  $q \rightarrow 1$  the usual BG statistics is recovered and one comes back to the usual statistical model.

most economically (by introducing only one new parameter  $q$ ) and adequately by the so-called non-extensive statistics introduced some time ago by Tsallis [24] (cf. Appendix B for more details on basic notion of non-extensivity).

In what concerns intrinsic fluctuations, it all comes down to the observation (cf. Appendix B, eqs.(B·35)-(B·42)) that whenever one has exponential formula describing some physical quantity,  $\exp\left(-\frac{x}{x_0}\right)$ , in which parameter  $1/x_0$  is a fluctuating quantity (with fluctuations distributed according to gamma function), then the resultant distribution (i.e., averaged over these fluctuations) is of the power-like type

$$\left\langle \exp\left(-\frac{x}{x_0}\right) \right\rangle_{x_0} \rightarrow \exp_q\left(-\frac{x}{\bar{x}_0}\right) = \left[1 - (1-q)\frac{x}{\bar{x}_0}\right]^{\frac{1}{1-q}}. \quad (\text{III}\cdot1)$$

The parameter  $q$  is connected in this case with the relative variance of distribution describing fluctuations  $\frac{1}{x_0}$ :

$$q = 1 \pm \omega, \quad (\text{III}\cdot2)$$

where  $\omega$  is relative variance of such fluctuations:

$$\omega = \frac{\left\langle \left(\frac{1}{x_0}\right)^2 \right\rangle - \left\langle \frac{1}{x_0} \right\rangle^2}{\left\langle \frac{1}{x_0} \right\rangle^2}. \quad (\text{III}\cdot3)$$

## 2. MaxEnt for $q$ -statistics in multiparticle production processes (on the example of violation of Feynmann scaling law )

Let us start with our first example, which deals with problem of the apparent violation of Feynmann scaling in multiparticle production [61]. It is especially important in cosmic ray physics [62] and we shall discuss it from this perspective. The shape of the  $x = E/E_0$  spectra of secondaries measured there ( $E$  is the actual energy of particle and  $E_0$  its maximal possible energy) is of great importance in all investigations concerning developments of cosmic ray cascades [62] (cf. also [63]). The crucial problem of practical importance is the *existence* or *nonexistence* of the Feynmann scaling [61], which says that  $x$ -spectra of secondaries are energy independent. However, whereas in cosmic ray applications we are interested mainly in the  $x > 0.1$  region, the available experimental information is coming from accelerator data [64–66], which are limited to rather small values of  $x$ <sup>22</sup>. In this region of phase space Feynmann scaling is violated. The status of the Feynmann scaling

<sup>22</sup>Actually in accelerator experiment  $x = 2p_L/\sqrt{s}$  with invariant energy  $\sqrt{s}$  replacing the initial energy  $E_0$  and with longitudinal momentum  $p_L$  replacing the energy  $E$  of the secondary under investigation.

in the large  $x$  region is still an open question with strong suggestion that in this region the  $x$  spectra behave as proposed in [62]:

$$\frac{dN}{dx} = Da \frac{(1 - a' x)^4}{x}, \quad (\text{III}\cdot 4)$$

(with  $D$ ,  $a$ ,  $a'$  being parameters obtained from fits to data). This problem has been already addressed in many places but either in a model dependent way [67] or by using some parameterizations [62,63]. We would like to investigate this problem proceeding in a maximally model independent way by using framework of the generalized Tsallis statistics. We shall do this by applying the non-extensive version of the information theory model (based on Tsallis  $q$ -entropy) outlined in Appendix A to describe the hadronization process part of the high energy multiparticle production [25].

Let us start with the model independent part of our investigation. According to the procedure described in Appendix A *the least biased and most plausible* single particle rapidity distribution,  $f(y) = \frac{1}{N} \frac{dN}{dy}$ , for hadronization process in which a mass  $M$  hadronizes into  $N$  secondaries of mean transverse mass  $\mu_T = \sqrt{m^2 + \langle p_T \rangle^2}$  each, can be written in the framework of BG statistics as (cf. eq.(A\cdot14) and eq.(II\cdot19) above)<sup>23</sup>

$$f(y) = \frac{1}{Z(M, N, \mu_T)} \exp [-\beta(M, N) \cdot \mu_T \cosh y]. \quad (\text{III}\cdot 5)$$

Here  $Z(M, N, \mu_T)$  comes from the normalization of  $f(y)$  whereas the Lagrange multiplier  $\beta(M, N)$  is to be calculated from the energy conservation constraint. Notice that *there is no free parameter here*. This should be contrasted with the popular use of eq. (III\cdot5) as a "thermodynamical parameterizations" with inverse "temperature"  $1/\beta = T$  being a free, positively defined parameter. According to [30]  $\beta(M, N)$  is positive defined, i.e.,  $\beta(M, N) \geq 0$ , only when

$$N \geq N_0 \simeq 2 \ln \left( \frac{M}{\mu_T} \right) = 2 \ln (N_{max}). \quad (\text{III}\cdot 6)$$

In the case of  $N = N_0$  we have  $\beta = 0$  and, respectively,  $f(y) = \text{const}$ , i.e., one has *exact* Feynmann scaling in this case.

The actual situation is, however, much more complicated. The comparison with data cannot be done in such model independent way because of the fluctuations in  $M$  and  $N$  caused by different initial conditions encountered in different events. The initial mass  $M$  is only a part of the initial available energy  $\sqrt{s}$ , i.e.,  $M = K\sqrt{s}$ , where  $K$  is so called inelasticity of reaction and is varying from event to event according to inelasticity distribution  $\chi(K)$  [68]. Similarly, the number of particles  $N = N(M)$  produced from

<sup>23</sup>This is just the MaxEnt model of hadronization used already in the previous Chapter (cf. Fig.II.3) and which will be used again in Chapter V.

mass  $M$  fluctuates according to multiparticle distribution  $P(N; M)$  [69]. Both  $\chi(K)$  and  $P(N; K\sqrt{s})$  have to be provided from elsewhere. This external source of  $M$  and  $N$  forms therefore a kind of *external reservoir* (or kind of *heat bath*) characterized by  $\chi(K)$  and  $P(N; M)$ <sup>24</sup>. One expects therefore that

$$\frac{dN}{dy} = \int_0^1 dK \chi(K) \sum_N N P(N; K\sqrt{s}) \frac{1}{Z(K\sqrt{s}, N)} \exp [-\beta(K\sqrt{s}; N) \mu_T \cosh y], \quad (\text{III.7})$$

where  $\beta(K\sqrt{s}, N)$  is still calculated from the energy conservation constraint but where inelasticity distribution  $\chi(K)$  and multiplicity distribution  $P(N; K\sqrt{s})$ , which are the main source of fluctuations, are two new functions providing, for a given event, the values of  $M$  and  $N$ , respectively.

The question which we shall address here is the following: is the full knowledge of  $\chi(k)$  and  $P(N; M)$  (out of which only form of multiplicity distribution can be regarded as known from other considerations) really necessary to describe experimental multiparticle data or can it be done in a more economical way? This brings us to one of the possible sources of occurrence of non-extensivity, namely to fluctuations present in the system [49,50]. In [30] it was shown that, in a wide range of energies and multiplicities, (cf. eq.(A.18))

$$\beta \sim \frac{N}{M} = \frac{1}{\sqrt{s}} \frac{N}{K},$$

i.e., it is given by the ratio of the two fluctuating quantities mentioned above:  $N$  and  $K$ . It can be shown that, in the case of  $\chi(K) = \text{const}$  and  $P(N; M)$  being Poissonian one gets for distribution of the ratio  $\frac{N}{K}$  the form of gamma distribution, for which one can expect eq.(III.1) to be fully applicable (with  $x = \frac{2\mu_T}{\sqrt{s}} \cosh y$  and  $\bar{x}_0$  being a mean value of the fraction  $\frac{N}{M}$  discussed above, the average is over parameter  $\frac{1}{x_0}$  representing here this fraction).

We make therefore conjecture that convolution (III.7) can be replaced by the following simple formula

$$\frac{dN}{dy} = \langle N(s) \rangle \cdot \frac{1}{Z_q} \left[ 1 - (1-q)\beta(\sqrt{s}; \frac{3}{2}\langle N(s) \rangle) \cdot \mu_T \cosh y \right]^{\frac{1}{1-q}}, \quad (\text{III.8})$$

which should then be used to describe (or fit, in terms of the parameter  $q$ ) the existing experimental data [64–66]. The only free parameter (characterizing the strength of fluctuations existing in the system, according to eqs.(III.3) and (B.42), is now the non-

<sup>24</sup>This is, of course, still a simplification as we do not consider here the possible multisource effect assuming that it is, to some extend, accounted for by the shape of  $P(N; M)$ .

extensivity parameter  $q^{25}$ . Here

$$Z_q = \int dy \exp_q(-\beta_q \mu_T \cosh y) \quad (\text{III.9})$$

and  $\langle N(s) \rangle$  is the mean (single non-diffractive) charged multiplicity at given energy  $\sqrt{s}$ .

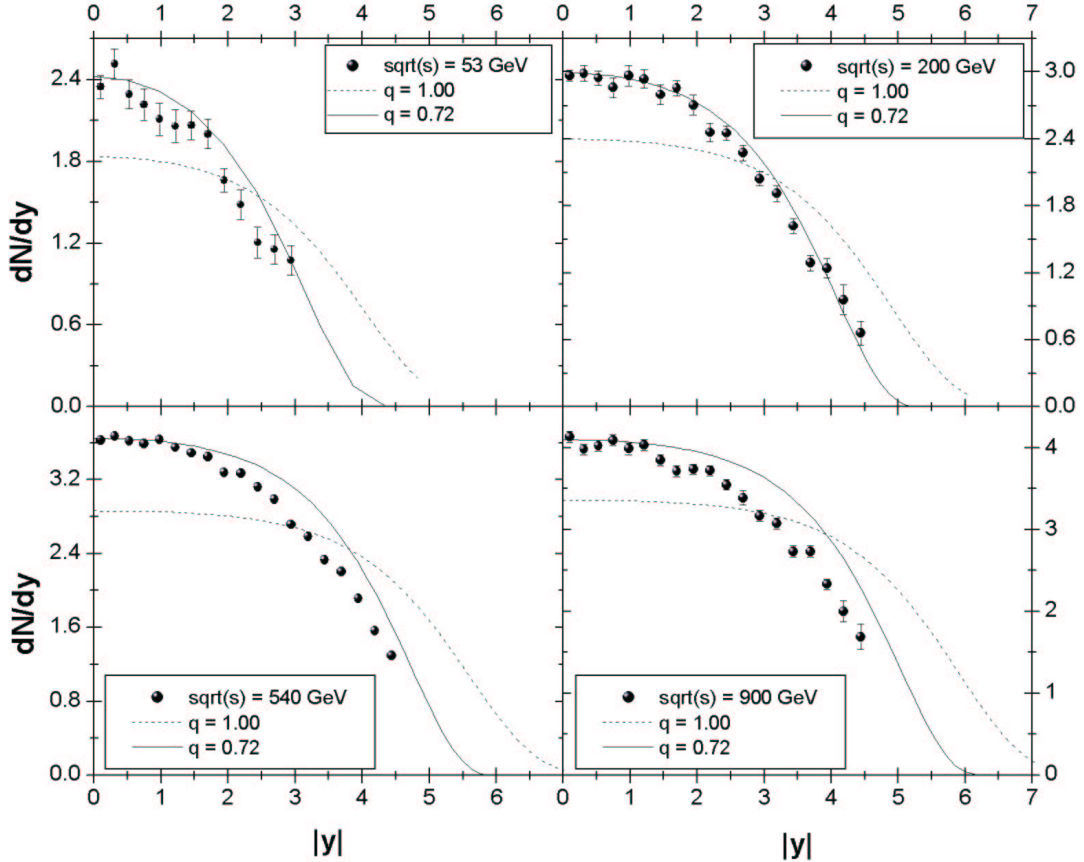


**Fig. III.1.** Comparison of eq.(III.8) with UA5 [64] rapidity distribution data for  $q = 1$  and  $q = 0.72$ .

Notice that  $\beta_q$  is calculated from the energy conservation constraint (B.27), which involves all produced particles, i.e., it is calculated for  $\frac{3}{2}\langle N(s) \rangle = \langle N_{total}(s) \rangle$  particles. For the same reason care must be taken when one addresses data at  $\sqrt{s} = 630$  GeV because part of them is obtained for charged and part for neutral particles. In both cases the  $\beta_q$  must be the same (i.e., calculated for total multiplicity at given energy) whereas multiplicity in front of the formula has to be chosen accordingly to the actual situation.

---

<sup>25</sup>Although such simple connection between  $q$  and  $\omega$  is not necessarily valid for a general choices of  $\chi(k)$  and  $P(N; M)$ , we assume here that the single parameter  $q$  and the specific power dependence as given by eq.(III.1) can still summarize to a high accuracy the action of all fluctuations resulting from both  $\chi(K)$  and  $P(N; M)$  distributions.

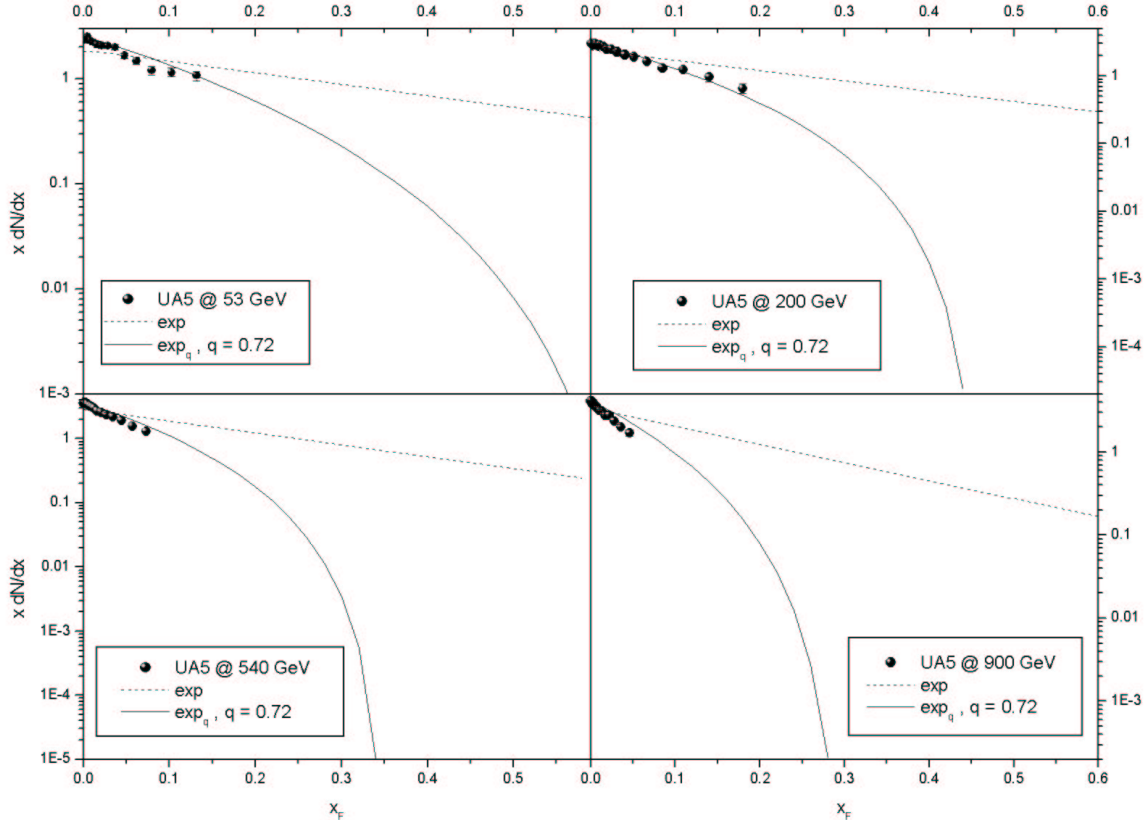


**Fig. III.2.** The same as in Fig.III.1 but this time for  $x_F = \frac{2p_L}{\sqrt{s}}$  variable, the same as in eq.(III.4).

In Fig.III.1 we show our results both for  $q = 1$  and for our best fit to UA5 data [64] with  $q = 0.72$ . In all calculations the experimentally observed variation of  $\mu_T$  with energy has also been accounted for by using the following simple interpolation formula:  $\mu_T = 0.3 + 0.044 \ln(\sqrt{s}/20)$  GeV. The results are reasonable, especially for 53 and 200 GeV. For higher energies our distributions start to be broader than data and this cannot be improved by changing  $q$  because diminishing its value (in order to make distributions narrower) will spoil the agreement with data for small rapidities. In Fig.III.2 the same results are shown but this time for the  $x_F = \frac{2p_L}{\sqrt{s}}$  variable used in eq.(III.4). Fig.III.3 shows that P238 [65] and UA7 [66] data cannot be fitted together with UA5 [64] data, as they demand a slightly bigger value of  $q = 0.85$ , cf. Fig.III.3. Notice that P238 data are for charged and UA7 data for neutral particles, therefore they must be described with, respectively,  $\frac{2}{3}\langle N_{total} \rangle$  and  $\frac{1}{3}\langle N_{total} \rangle$  in eq.(III.8). This leads to differences clearly seen in Fig.III.3<sup>26</sup>.

---

<sup>26</sup>When presenting data in the variable  $x_F = \frac{2\mu_T}{\sqrt{s}} \sinh y$  introduced before care must be taken when using (III.8) as now:

$$\frac{dN}{dy} = \sqrt{\frac{4\mu_T^2}{s} + x_F^2} \cdot \frac{dN}{dx_F}.$$

It is interesting to notice that we can reproduce eq.(III·4) proposed in [62] using our eq.(III·8) with  $q = 0.75$ , i.e., with value of  $q$  which is not very far from the value obtained in our fits, i.e.  $q = 0.72$ . We conclude therefore that in this way the phenomenological equation eq.(III·4) describing observed Feynman scaling violation gets its theoretical justification in terms of the intrinsic fluctuations present in the system under consideration and coming from the fluctuations of inelasticity and multiplicity combined together. However, the fact that at higher energies one is not getting perfect agreement with data indicates that there are also some other factors besides fluctuations mentioned here influencing such distributions. Such possibility must be kept in mind when searching for a perfect fit, which is, however, not our goal here.

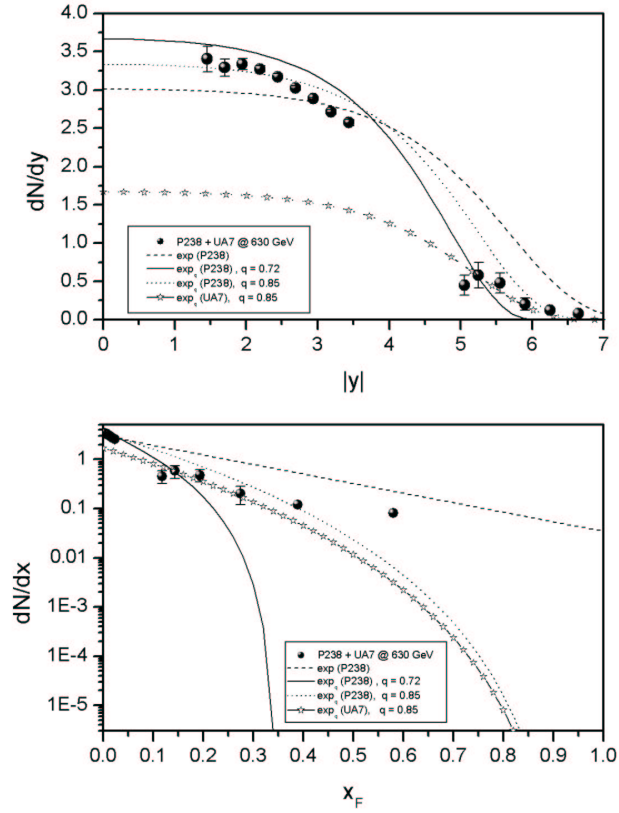


**Fig. III.3.** Comparison of eq.(III·8) with P238 [65] and UA7 [66] data for rapidity distributions (upper panel) and  $x_F = \frac{2p_T}{\sqrt{s}}$  distribution (lower panel).

Before closing this section let us stress the fact that in the case discussed above  $q < 1$ , i.e., the possible fluctuations causing this effect must be of completely different type than those discussed below, in Section 4, where  $q > 1$ . Actually at this moment we cannot provide any convincing explanation of this fact (similar to the fluctuations of the intrinsic

---

Whereas the  $s$ -dependent terms are negligible at higher energies they are still substantial at, say,  $\sqrt{s} = 53$  GeV.

temperature used to explain  $q > 1$  case). From the purely technical point of view, the values of  $q < 1$  are desired because in this case the (longitudinal) phase space used for particle production is limited to rapidities satisfying inequality (cf. eq.(B·28)):

$$1 - (1 - q)\beta_q\mu_T \cosh y > 0, \quad (\text{III}\cdot10)$$

i.e., to  $|y| < \text{Arcosh} \frac{1}{(1-q)\beta_q\mu_T}$ , which in our case is within the normal kinematical limit for rapidity (cf. eq.(B·5) and relevant discussion on this point in Appendix B).

### 3. $\Phi_n$ measure of "chemical fluctuations" in $q$ -statistics

Our second example will be devoted to description in terms of  $q$ -statistics the, so called, "chemical fluctuations" expected in event-by-event analysis of heavy ion collisions. The point is that in central ultrarelativistic collisions at RHIC and LHC one expects to produce at least  $\sim 10^4$  particles, and this presents the remarkable opportunity to analyze, on event-by-event (EbyE) basis, fluctuations in physical observables such as particle multiplicities, transverse momenta, correlations and ratios of particle multiplicities of different species. Analysis of single events with large statistics can reveal very different physics than studying averages performed over large statistical sample of events. A central issue for EbyE analysis is the question whether or not collisions with similar initial conditions experience the same dynamical history (modulo effects caused by the fluctuations originated because of the finite-number of produced secondaries). From very general arguments and from the observed behavior of normal matter near the phase boundaries we expect to observe significant changes in fluctuations near the QCD phase boundary [70,71]. The amplitude and character of these changes and their observability for given finite collision systems are major questions for the EbyE physics.

Some time ago a novel method of investigation of fluctuations in EbyE analysis of high-energy multiparticle production data has been proposed [72]. It consists in defining a suitable measure  $\Phi$  of a given observable  $x$  being exactly the same for nucleon-nucleon and nucleus-nucleus collisions if the later are simple superposition of the former.

$$\Phi_x = \sqrt{\frac{\langle Z^2 \rangle}{\langle N \rangle}} - \sqrt{\bar{z}^2} \quad \text{where} \quad Z = \sum_{i=1}^N z_i. \quad (\text{III}\cdot11)$$

Here  $z_i = x_i - \bar{x}$  where  $\bar{x}$  denotes the mean value of the observable  $x$  calculated for all particles from all events (the so called inclusive mean) and  $N$  is the number of particles analyzed in the event. In (III·11)  $\langle N \rangle$  and  $\langle Z^2 \rangle$  are averages of EbyE observables over all events whereas the last term is the square root of the second moment of the inclusive  $z$  distribution. By construction, if particles are produced independently  $\Phi_x = 0$  [72]<sup>27</sup>.

---

<sup>27</sup>For some other recent discussions of event-by-event fluctuations see [73]. Our contribution to this discussion, not discussed here, is presented in [74].

There exists already a vast literature concerning application of  $\Phi_x$  to  $x = p_T$  case (cf. [26,74] for more details and references). In the mean time the use of this variable has been extended, so far only theoretically, to the possible study (planned already by NA49) of the EbyE fluctuations of the "chemical" (particle type) composition of the final stage of high-energy collisions [75]<sup>28</sup>.

The following natural question arises at this point: is the  $\Phi$  measure, and in what way, sensitive to the possible non-extensivity present in the system? As was suggested recently in [59], the extreme conditions of density and temperature occurring in ultrarelativistic heavy ion collisions can lead to memory effects and long-range color interactions and to the presence of non-Markovian processes in the corresponding kinetic equations (cf., for example [60]). The generalization of  $\Phi$  measure for this case applied to  $p_T$  variable,  $\Phi_{p_T}$ , was proposed and discussed there (cf. also [78]).

Here we would like to present possible generalization of the analysis of the chemical fluctuations discussed in [77] to the case of non-extensive statistics in a manner identical to that presented in [59] for the case of transverse momenta. We shall follow here our analysis published in [26]. As in [77] we have computed the  $\Phi$  measure for the system of particles of two sorts,  $\pi^-$  and  $K^-$ , i.e., nonstrange and strange hadrons with multiplicities  $\langle n_\pi \rangle$  and  $\langle n_K \rangle$ , respectively. Since

$$\langle N \rangle = \langle n_\pi \rangle + \langle n_K \rangle \quad (\text{III}\cdot12)$$

one immediately finds that in definition (III\cdot11)

$$\langle z^2 \rangle = \frac{\langle n_\pi \rangle \langle n_K \rangle}{\langle N \rangle} \quad (\text{III}\cdot13)$$

and

$$\langle Z^2 \rangle = \frac{\langle n_\pi \rangle^2 \langle n_K^2 \rangle + \langle n_\pi^2 \rangle \langle n_K \rangle^2 - 2 \langle n_\pi \rangle \langle n_K \rangle \langle n_\pi n_K \rangle}{\langle N \rangle^2}. \quad (\text{III}\cdot14)$$

Assuming, as in [77], factorization, i.e., that

$$\langle n_i n_j \rangle = \langle n_i \rangle \langle n_j \rangle. \quad (\text{III}\cdot15)$$

one gets (III\cdot14) in the form

$$\langle Z^2 \rangle = \frac{\langle n_K \rangle^2}{\langle N \rangle} \langle \Delta n_\pi^2 \rangle - \frac{\langle n_\pi \rangle^2}{\langle N \rangle} \langle \Delta n_K^2 \rangle, \quad (\text{III}\cdot16)$$

where  $\langle \Delta n^2 \rangle = \langle n^2 \rangle - \langle n \rangle^2$ . We shall now consistently replace the mean occupation numbers by their  $q$ -equivalents (cf. eq.(B\cdot32)), which under some approximations, valid

<sup>28</sup>The first data from NA49 on such fluctuations have been already published very recently in [76] but they were not analyzed using  $\Phi$  measure approach.

for small values of non-extensivity  $|1 - q|$ , can be expressed in the following analytical form [79]:

$$\langle n \rangle_q = g_i V \int \frac{d^3 p}{(2\pi)^3} \langle n \rangle_q(E) \quad (\text{III.17})$$

with

$$\langle n \rangle_q(E) = \left\{ [1 + (q-1)\beta(E-\mu)]^{1/(q-1)} \pm 1 \right\}^{-1}, \quad (\text{III.18})$$

where  $\beta = 1/kT$ ,  $\mu$  is chemical potential and the  $+/-$  sign applies to fermions/bosons. Notice that in the limit  $q \rightarrow 1$  (extensive statistics) one recovers the conventional Fermi-Dirac and Bose-Einstein distributions. Following the same procedure as in [59] one gets

$$\langle \Delta n^2 \rangle_q = g_i V \int \frac{d^3 p}{(2\pi)^3} \langle \Delta n^2 \rangle_q(E) \quad (\text{III.19})$$

with

$$\langle \Delta n^2 \rangle_q(E) = \frac{\langle n \rangle_q(E) [1 \mp \langle n \rangle_q(E)]}{1 + (q-1)\beta(E-\mu)} \quad (\text{III.20})$$

for fermions (-) and bosons (+). eqs.(III.15) and (III.20) allow us to calculate  $\langle Z^2 \rangle_q$  and  $\Phi_q$  for chemical fluctuations.

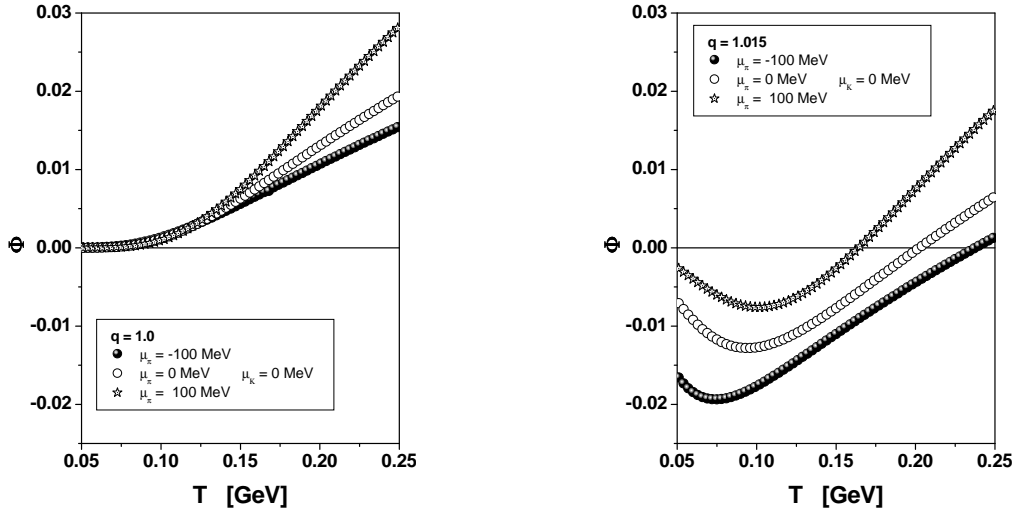


**Fig. III.4.**  $\Phi$ : measure of the kaon multiplicity fluctuations (in the  $\pi^- K^-$  system of particles) as a function of temperature for three values of the pion chemical potential. The kaon chemical potential vanishes. The resonances are neglected. Left panel: results of [77] (in linear scale); right panel: our results for  $q = 1.015$

Our results are presented in Figs.III.4 and III.5 where modifications caused by the non-extensivity  $q = 1.015$  (chosen in such a way as to fit the  $p_T$  spectra in Fig.III.6,

see discussion below) to the results of [77] for directly produced particles are shown. For simplicity we have restricted ourselves here only to comparison with results of [77] without resonances. Actually, one can argue that resonance production belongs, according to our philosophy, already to the non-extensive case because it introduces correlations. It means that resonances should be responsible for (at least a part of) the effect leading to a nonzero  $|1 - q|$ . This is best seen inspecting results of [77] with resonances included, which show that  $\Phi$  in this case also changes sign. The use of parameter  $q$  is, however, more general as it includes all other possible effects as well. As in [59] (where  $\Phi$  for transverse momenta  $p_T$  has been considered), a rather large sensitivity of predictions presented in [77] to the parameter  $q$  has been observed. According to the non-extensive statistics philosophy this fact indicates a large sensitivity to the (initial and boundary) conditions present in the ultrarelativistic heavy ion collisions and existence of some kind of memory effects in such systems, as mentioned in references [60].

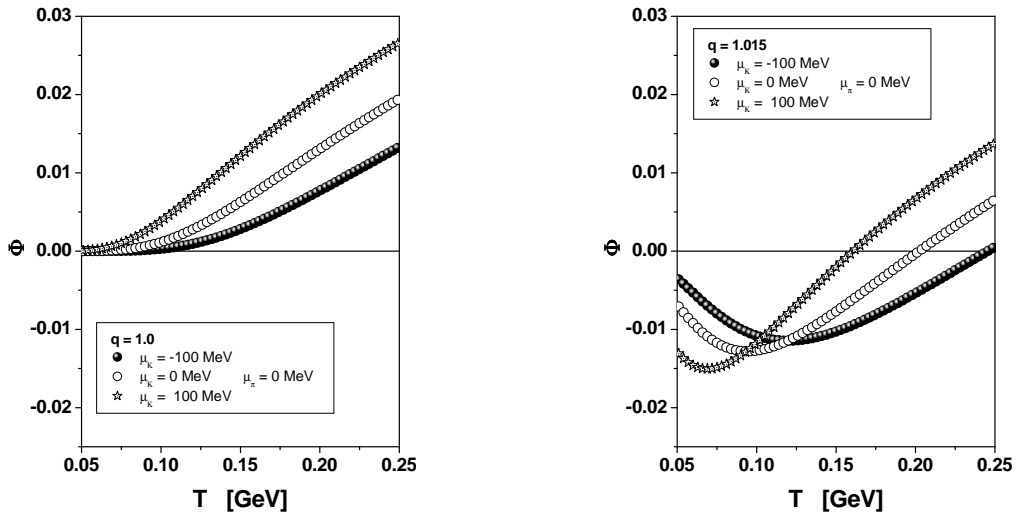


**Fig. III.5.**  $\Phi$ : measure of the kaon multiplicity fluctuations (in the  $\pi^-K^-$  system of particles) as a function of temperature for three values of the kaon chemical potential. The pion chemical potential vanishes. The resonances are neglected. Left panel: results of [77] (in linear scale); right panel: our results for  $q = 1.015$

Notice (cf. also [59]) that, as is clearly seen in Fig. III.6, the same pattern of fluctuations is already present in the transverse momentum spectra of produced secondaries, i.e., the same value of  $q$  brings new "q-thermal" curve in agreement with experiment in the whole range of  $p_T$  presented. If it would emerge also in the future data on the fluctuations of chemical composition discussed here, i.e., if parameter  $q$  would turn out to be similar (modulo experimental errors), it would signal that both observables, fluctuations of which is investigated, are similarly affected by the external conditions mentioned before and that they can be easily parameterized phenomenologically by a single parameter  $q$ , i.e., by the measure of the non-extensivity of the nuclear collision process.

#### 4. Broadening of $p_T$ distributions as possible signature of intrinsic fluctuations of temperature

In our last example we shall concentrate on the result presented in Fig.III.6 (cf. [27]). It is potentially very important and interesting because, as indicated in [49–51], it can be interpreted as being caused by the fluctuations of temperature  $T$  taking place in the hadronic system<sup>29</sup>.

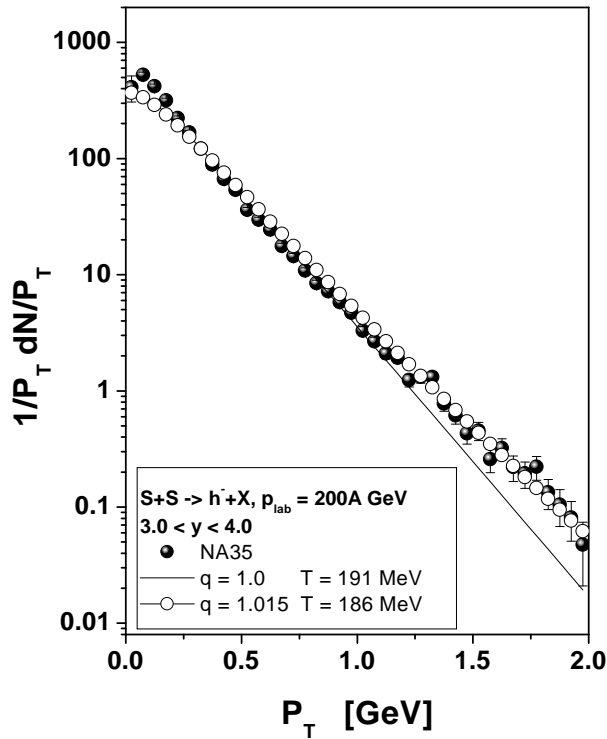


**Fig. III.6.** The results for  $p_T$  distribution: notice that  $q = 1.015$  results also describe the tail of distribution not fitted by the conventional exponent (i.e.,  $q = 1$  in our case, also cf. [59]). Data are taken from [80].

This observation can have profound consequences in high energy multiparticle production processes because of the following:

- ALICE detector at LHC will look (among other things) for the creation of Quark Gluon Plasma (QGP), i.e., the system with big number of degree of freedom (quark and gluons) and negligible interaction (asymptotic freedom);

---

<sup>29</sup>We are aware of other possible explanations of this effect, for example by the flow of hadronic matter [59], but in this example we shall explore only its possible connection with non-extensive statistics.

- this calls for a thermodynamical description of (at least some) relevant observables and this in turn calls for the temperature  $T$  of the system under investigation as one of the most important quantities;
- $T$  can be deduced most directly (at least this is believed to be the case) by looking at  $p_T$  spectra because ( $\mu_T = \sqrt{m^2 + p_T^2}$ )

$$\frac{dN}{dp_T} \propto \exp\left(-\frac{\mu_T}{T}\right). \quad (\text{III.21})$$

This is widely accepted approach, notwithstanding the fact that both details of what  $T$  really means and whether (III.21) is a proper form for  $\mu_T$ -dependence are still subject to hot debate and modeling. Taking therefore (III.21) as our starting point we want to concentrate on question: is it possible that  $T$  is fluctuating quantity [70,71,78,81] and if so, does it fluctuates only from event-to-event or also in a given event?

We are not going to discuss the problem of internal consistency (or inconsistency) of the notion of fluctuations of temperature in thermodynamics referring in this matter to [82]. What we want to do is to check whether event-by-event analysis allows us (at least *in principle*) to detect fluctuations of temperature taking place *in a given event*. This is more than indirect measure of fluctuations of  $T$  proposed some time ago in [83] or more direct fluctuations of  $T$  *from event to event* discussed in [78].

According to [49–51] such fluctuations of temperature  $T$  can be described by the power-like form given by eq.(III.1), which in our case results in

$$\frac{dN}{dp_T} \propto \left[1 - (1-q) \left(\frac{1}{T_0}\right) \cdot \mu_T\right]^{\frac{1}{1-q}}. \quad (\text{III.22})$$

The new parameter occurring here is identical to the Tsallis non-extensivity parameter [24] and it is tightly connected with the size of such fluctuations as given by eqs.(III.2) and (III.3).

After inclusive production processes discussed at the beginning of this Chapter (leading to  $q < 1$ ) this is another example (this time  $q > 1$ ) how the intrinsic fluctuations can influence the measured distribution making it the power-like (known also in the literature as the Lévy type) (III.22). However, inclusive processes are not able to provide unambiguous answer what is the source of such behavior. This can be done only in the careful analysis of event-by-event data, especially those for heavy ion collisions. Two scenarios are possible here and should be subjected to experimental verification [27]:

- (1)  $T$  is constant in each event but because of different initial conditions it fluctuates from event to event. In this case in each event one should find exponential dependence (III.21) with  $T = T_{\text{event}}$  and possible departure from it will occur only after averaging over all events. It will reflect fluctuations originating in different initial conditions for each collision from which given event originates. This situation is illustrated in left panel of Fig.III.7 where  $p_T$  distributions for  $T = 200$  MeV (black

symbols) and  $T = 250$  MeV (open symbols) are presented. All other details are the same as listed below for the right panel of Fig.III.7. Such values of  $T$  correspond to typical uncertainties in  $T$  expected at LHC due to different initial conditions. Notice that both curves presented here are straight lines of different slope.

- (2)  $T$  fluctuates in each event around some value  $T_0$ . In other words the system under consideration consists of a number of parts described with different temperature  $T_0 \pm \delta T$ . In this case one should observe departure from the exponential behavior already on the single event level, which should be fully given (III.22) with  $q > 1$ . It reflects situation when, due to some intrinsically dynamical reasons, different parts of a given event can have different temperatures [49,50]. The right panel of Fig.III.7 shows typical event of this type obtained in simulations performed for central  $Pb+Pb$  collisions taking place for beam energy equal  $E_{beam} = 3 A\cdot\text{TeV}$  in which density of particles in central region (defined by rapidity window  $-1.5 < y < 1.5$ ) is equal to  $\frac{dN}{dy} = 6000$  (this is the usual value given by event generators like VENUS, SHAKER, HIJING, cf. [16]). Black symbols represent exponential dependence obtained for  $T = 200$  MeV (the same as in the left panel of Fig.III.7), open symbols show the power-like dependence as given by (III.22) with the same  $T$  and with  $q = 1.05$  (notice that the corresponding curve bends slightly upward here). In this typical event we have  $\sim 18000$  secondaries, i.e., practically the maximal possible number. Notice that points with highest  $p_T$  correspond already to single particles.

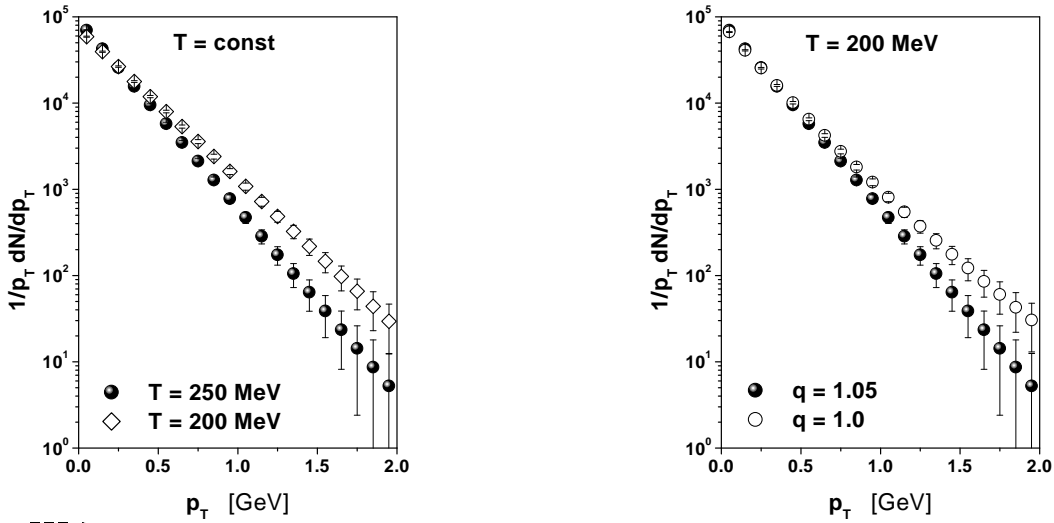


**Fig. III.7.** Left panel - normal exponential  $p_T$  distributions (i.e.,  $q = 1$ ) for  $T = 200$  MeV (black symbols) and  $T = 250$  MeV (open symbols). Right panel - typical event from central  $Pb + Pb$  at  $E_{beam} = 3 A\cdot\text{TeV}$  (cf. text for other details) for  $T = 200$  MeV for  $q = 1$  (black symbols) exponential dependence and  $q = 1.05$  (open symbols).

The results presented in Fig.III.7 clearly indicate that such differentiation will be very hard experimentally, although not totally impossible. If successful, it would, however, be very rewarding because of the following important fact: our  $\omega = q - 1$  has in

this case physical meaning of the total heat capacity  $C$ , because, according to a basic thermodynamic relation (cf. Landau and Lifschitz book in [82]),

$$\frac{\sigma^2(\beta)}{\langle \beta \rangle^2} = \frac{1}{C} = \omega = q - 1, \quad \beta = \frac{1}{T}. \quad (\text{III.23})$$

Therefore, measuring in addition to the temperature  $T$  also the non-extensivity  $q$  describing its fluctuation (and, because of this, the total heat capacity  $C$ ) could be of great practical importance for our understanding of dynamics of heavy ion collisions [70,71,78,81]. In particular it should not only facilitate checking the commonly made assumption that an approximate thermodynamics state is obtained in a single collision but also, by knowing the heat capacity, it could provide considerable information about its thermodynamics (especially in what concerns the existence and the type of the possible phase transitions [70,71,78,81])<sup>30</sup>.

## 5. Summary

To summarize:

- We have presented here examples of the non-extensivity caused by some intrinsic fluctuations leading both to  $q < 1$  (Section III.2) and to  $q > 1$  (Section III.4). The possible underlying physics connected with fluctuating temperature  $T$  and total heat capacity  $C$  was shortly discussed only for  $q > 1$  case. In the  $q < 1$  situation is not clear in what concerns its possible physical illustration [50]. In this case the parameter which is fluctuating does not reach a stationary state and the corresponding distributions are defined only in the limited region of phase space.
- We have also presented (in Section III.3) one particular application of "chemical" fluctuations as expected in event-by-event analysis performed in terms of  $q$ -statistics. Notwithstanding other possible explanations of this phenomenon, the use of  $q$ -statistics seems to be economical and promising one because by introducing a single additional parameter changing the underlying statistics one summarizes action of many (both known and yet unknown) factors. However, to be of practical importance it will have to be supplemented with similar analysis of much broader set of experimental data, which is so far not yet considered by experimentalists.

One should mention at this point very interesting result providing (as we believe) support to our conjectures above. Namely, recent analysis of high energy  $p+p$  interactions [84] shows that the mean multiplicity of neutral mesons produced in such reactions as a function of their mass (in the range from  $m_\eta = 0.55$  GeV to  $m_\gamma = 9.5$  GeV) and the transverse mass  $m_T$  spectra of pions (in the range of  $m_T \simeq 1 - 5$  GeV), both show a

<sup>30</sup>It is interesting to realize that for the Planckian gas at  $T = 186$  MeV, occupying volume of the order of the volume of sulfur nucleus, one gets  $C = 34.4$  per degree of freedom, which leads, using (III.23), to  $q = 1.015$  obtained for such system for the  $p_T$  dependence of produced secondaries.

remarkable universal behaviour following over 10 orders of magnitude the same *power law* function  $c \cdot x^{-P}$  (with  $x = m$  or  $x = m_T$ ) with  $P \simeq 10.1$  and  $P \simeq 9.6$ , respectively. In this work such a form was just *postulated*. Nevertheless it is straightforward to show that in non-extensive approach such behavior corresponds to  $q = 1 + 1/P$ , what results in  $q \sim 1.1$ , quite close to results obtained when analyzing  $e^+e^-$  annihilation data by means of  $q$ -statistics [85]. This can be regarded as a hint for non-extensivity being present in multiparticle production processes. Such interpretation is additionally supported by the fact that in both cases considered in [84] the constant  $c$  is the same. It turns also out that, apparently, there is no such phenomenon in  $AA$  collisions. If confirmed by future data, this finding would probably have simple and interesting explanation: in nuclear collisions volume of interaction is much bigger than in elementary collisions, therefore heat capacity  $C$  is also bigger and, according to eq.(III-23)  $q$  is smaller. One should then expect that  $q_{hadronic} \gg q_{nuclear}$ , as apparently observed, and what can be subjected to further experimental verification. In this way fluctuations could be behind many apparently non-standard behaviours observed in multiparticle physics.

# IV. Example of modeling of Bose-Einstein correlations (BEC) using CAS model.

## 1. Introduction

We shall return now to the problem of numerical modeling of BEC, mentioned already in the course of discussing CAS model in Chapter II. This time we shall demonstrate how CAS model can be used together with momenta shifting method of [86] (Section IV.2). This Chapter should be considered as a kind of introduction to Chapter V and therefore it also contains (in Section IV.3) short outline of the weighting method proposed in [87] and further investigated and developed in [88–91]. We shall mention there also special weighting procedure proposed for the LUND model [92].

Let us start with general remark that, whereas it is essentially straightforward to introduce BEC in the analytical calculations (see Appendix C), its implementation in the Monte Carlo event generators built to deal with multiparticle production is so far not totally satisfactory. In fact in most cases one cannot even say that these are real implementation of BEC effect, they are rather its imitations (better or worse). What one can only hope for is to *model* BEC, i.e., to reproduce on some stage the corresponding quantity of interest, like the corresponding two-particle correlation function

$$C_2(Q = | p_i - p_j |) = \frac{dN(p_i, p_j)}{dN(p_i) \cdot dN(p_j)}. \quad (\text{IV.1})$$

The main idea behind all such attempts is to bunch somehow particles of the same sign provided by given event generator. Models differ only in particular methods to obtain this effect. In [11,86] this is done locally by shifting slightly momenta of the finally produced like-charge mesons in an appropriate way (pulling them closer to each other in momentum space) and correcting afterwards the whole event for the possible energy-momentum imbalance introduced in this way. Similar effect can be obtained in the pseudo-potential approach [93] (this procedure is designed to model the collapse of a multiparticle wave function into a properly symmetrized state, as required by Bose-Einstein quantum statistics, cf. works [94]). Other method is to multiply each event by a weight factor calculated on the basis of the outcome of a particular event generator. In this case events, which already have (by chance) desired like-sign pair distribution are counted as many times as necessary to obtain the right result. To this category belongs also the “afterburner”

method [21] used in [20] and discussed in Chapter II. Such global weighting procedure preserves energy-momentum conservation for a given event but changes final single-particle distributions obtained from event generator and should be therefore corrected accordingly.

As was already mentioned previously, instead of using such local or global weighting procedures one can try to build generator, which would produce bunching observed in eq.(IV.1) automatically (i.e., which would posses Bose-Einstein statistics built in by definition). This has been done in [55] using information theory approach and will be discussed below in Chapter V where we propose extension of this approach to other generators (providing results of calculations performed using CAS and MaxEnt as working examples) enlarging therefore its practical applicability.

## 2. Momenta shifting method in CAS

Because of its cascade structure CAS model allows to implement shifting of momenta without destroying the energy-momentum balance. This is possible when such shifting is performed at the intermediate stages of cascade only. Before going into details, let us first recollect, for completeness, the main ideas of original shifting of momenta procedure as proposed in [11,86]. All major properties of event are in this case calculated without any reference to the BEC, which is then introduced as additional perturbation. It looks therefore as a kind of final-state interactions, although underlying physics is different. According to the procedure proposed in [11,86] one takes hadrons produced by some event generator (in case of [86] it is string fragmentation in JETSET), where no BEC effects are present, and shifts slightly the momenta of the finally produced mesons of the same charge in such a way that inclusive distribution of identical pairs with the relative momentum separation  $Q = |p_i - p_j|$  of identical pairs is enhanced by factor

$$f_{BE}(Q) = 1 + \lambda \cdot \exp(-Q^2 R^2), \quad (\text{IV.2})$$

where  $\lambda$  and  $R$  are free parameters. The choice of this factor is arbitrary and, as it was mentioned in [89], such implementation of the interference effects is only an imitation, i.e., it does not explain the origin of the enhancing factor, but it only demands that it reproduces correctly the shape of  $C_2$ . The  $\lambda$  and  $R$  are parameters to be chosen in such a way as to reproduce the finally observed shape of  $C_2(Q)$ .

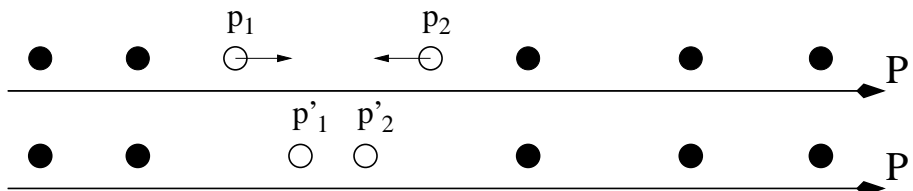


**Fig. IV.1.** Schematic presentation of momenta shifting procedure. The black dots in second line have to be also shifted in the opposite way if one wants to preserve over-all energy-momentum conservation.

Assuming that original distribution in  $Q$  is given just by the phase space, i.e., that the number of pairs  $dN(Q)$  with relative distance  $Q$  is proportional to the phase space they occupied,

$$dN(Q) \sim d^3p/E \propto Q^2 dQ^2 / \sqrt{Q^2 + 4m^2}, \quad (\text{IV.3})$$

an appropriate shift  $\delta Q$  for a given pair with separation  $Q$  can be calculated from the following equation (which is essentially a particle number conservation relation):

$$\int_0^Q \frac{q^2 dq}{\sqrt{q^2 + 4m^2}} = \int_0^{Q+\delta Q} f_{BE}(q) \frac{q^2 dq}{\sqrt{q^2 + 4m^2}}. \quad (\text{IV.4})$$

For an arbitrary  $f_{BE}(Q) \geq 1$ ,  $\delta Q$  is negative and the pairs are pulled closer together. Schematically, this can be viewed in Fig.IV.1. Applying this procedure one is able to generate  $C_2 > 1$  for small  $Q$ , dropping below unity at intermediate  $Q$  and approaching unity from below for large  $Q$ , i.e., the pattern which is usually observed in experimental data. The essential limitation of this procedure is the fact that invariant mass of pair of particles subjected to this procedure is changed (because it is not possible to simultaneously conserve both energy and momentum). Moreover, as it was shown in [89], the shape of the enhancement factor (IV.2) is distorted even more violently by the global effect of the momenta shifting performed to adjust to new values of  $Q$  (it means that initial values of parameters  $\lambda$  and  $R$  in eq.(IV.2) are changed). Authors of [86] argued that this method reproduces the assumed shape in the final distributions only for sources of size exceeding 2 fm. Therefore, they concluded that imitating BEC effect in JETSET by momenta shifting is reasonable only for large sources (e.g., for sources formed in heavy ion collisions).

Can one use our CAS introduced in Chapter II to perform similar shifting but without violations of energy-momentum conservation? As mentioned above, when applied to finally produced particles, such procedure violates energy-momentum balance and leads inevitably to changes in all single particle distributions and one must therefore correct them for these effects. It would just lead to repetition of [86] and brings nothing new. However, in case of our cascade process CAS we can apply this procedure to masses produced on intermediate levels of cascade, which posses the same type of charges (i.e., for example, positive charges) and which are not coming from the same intermediate common predecessor (cf. Fig.IV.2). This can be thought as a kind of not final, but intermediate state interactions.

To be more specific, we shall illustrate this on a simple example shown in Fig. IV.2. Let us select two such masses  $M_1$  and  $M_2$ , with four-momenta

$$P_1 = \left( E_1 = \sqrt{M_1^2 + p_1^2}, p_1 \right) \quad \text{and} \quad P_2 = \left( E_2 = \sqrt{M_2^2 + p_2^2}, p_2 \right),$$

respectively. As before, we are dealing, for simplicity, with  $D = 1$  cascade only. The

proposed procedure consists in the following replacement of momenta (here  $\Delta = P_2 - P_1$ ):

$$\begin{aligned} P_1 &\rightarrow P'_1 = P_1 + \frac{\gamma}{2} \cdot \Delta, \\ P_2 &\rightarrow P'_2 = P_2 - \frac{\gamma}{2} \cdot \Delta. \end{aligned} \quad (\text{IV.5})$$

Such replacement brings both objects (i.e., masses  $M_1$  and  $M_2$ , both possessing the same charge) closer in the phase space  $\{P_{1,2}\}$  by an extent given by parameter  $\gamma$ ,  $\gamma \in (0, 1)$ . For  $\gamma = 0$  there is no effect, for  $\gamma = 1$  the effect is maximal and

$$P'_{1,2} = \frac{1}{2}(P_1 + P_2). \quad (\text{IV.6})$$

At the same time energy-momentum of this system is conserved because

$$P_1 + P_2 = P'_1 + P'_2. \quad (\text{IV.7})$$

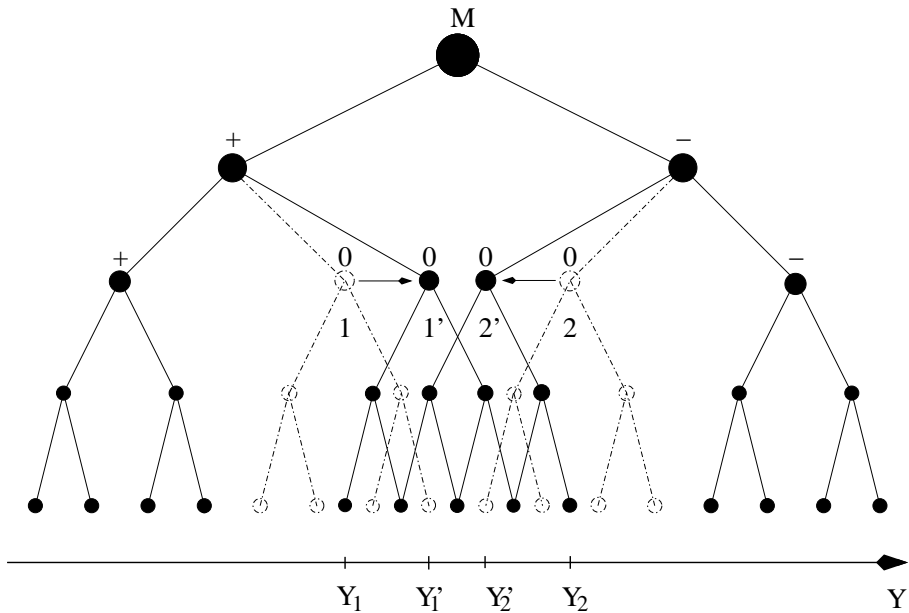


**Fig. IV.2.** Schematic presentation of momenta shifting procedure in the case of CAS (for  $D = 1$  case). The originally neutral mass  $M$  produces at the second level of cascade two neutral masses  $M_1$  and  $M_2$ , which are now subjected to shifting procedure described in text. The same procedure is repeated on every further step of cascade and involves masses of the same charge.

This is achieved by changing the original masses:

$$M_{1,2} \rightarrow M'_{1,2} = \sqrt{(P'_{1,2})^2}.$$

Such procedure is in our case fully acceptable because those are masses of intermediary objects on a given level of the cascade process and their values depend on the form of decay parameter distribution  $P(k_{1,2})$  in vertices, which can be changed according to our

demand (as long as the restrictions imposed by the general cascade process are satisfied). Taking  $\gamma = 1$  as an example one gets:

$$M_1'^2 = M_2'^2 = \frac{1}{4} (P_1 + P_2)^2 = \frac{1}{4} (M_1^2 + M_2^2) + \frac{1}{2} (P_1 \cdot P_2), \quad (\text{IV.8})$$

i.e., application of the proposed procedure results in two objects of masses bigger than the original ones sitting on top of each other in the momentum space. This leads to elongation of the cascade, i.e., changes its characteristics. However, contrary to the previous cases where momenta of final particles were shifted, all those changes are completely under control and energy-momentum conservation is always preserved. What changes is the multiplicity distribution, in the above example it will increase because length of the cascade increases.

To apply this method numerically one needs to have some additional control over the chances of such "intermediate state interaction" to happen. This can be achieved in many ways<sup>31</sup> but, since we are interested mostly in checking if (and how) this method works, we shall simply assume that these chances are maximal (i.e., we use  $G_{1,2} = 1$  in (IV.9)).

It is straightforward to generalize this procedure to any number of objects  $M_{1,\dots,N}$  with four-momenta  $P_{1,\dots,N}$ .

$$\underbrace{\dots + \mathcal{O}_i + \dots}_{\mathcal{N}} \quad \Rightarrow \quad \underbrace{\dots + \mathcal{O}_i^* + \dots}_{\mathcal{N}} \quad (\text{IV.10})$$

The momentum transformation (IV.5) in this case can be rewritten in more general form

$$\{P_i\} \rightarrow \left\{ P'_i \right\} \equiv P_i + \sum_{j \neq i}^N \Delta_{ij}^{(\mathcal{N})}(P_i, P_j), \quad (\text{IV.11})$$

with

$$\Delta_{ij}^{(\mathcal{N})} = \frac{\gamma}{\mathcal{N}} \cdot (P_i - P_j). \quad (\text{IV.12})$$

Finally, the four-momentum of  $i$ -th object is

$$P'_i = \left( 1 - \gamma \cdot \frac{\mathcal{N} - 1}{\mathcal{N}} \right) P_i + \frac{\gamma}{\mathcal{N}} \sum_{j \neq i}^N P_j \quad \xrightarrow{\gamma=1} \quad P'_i = \frac{1}{\mathcal{N}} \sum_{j=i}^N P_j. \quad (\text{IV.13})$$

<sup>31</sup>For example, one can assume that for a given pair of objects discussed above there is attached to it a probability function  $G_{1,2}$  given, for example, in a simple Gaussian form:

$$G_{1,2} = \text{const} \cdot \exp \left[ -\frac{(P_1 - P_2)^2}{4(\sigma_1^2 + \sigma_2^2)} \right], \quad (\text{IV.9})$$

with widths  $\sigma_{1,2}$  being new parameters.

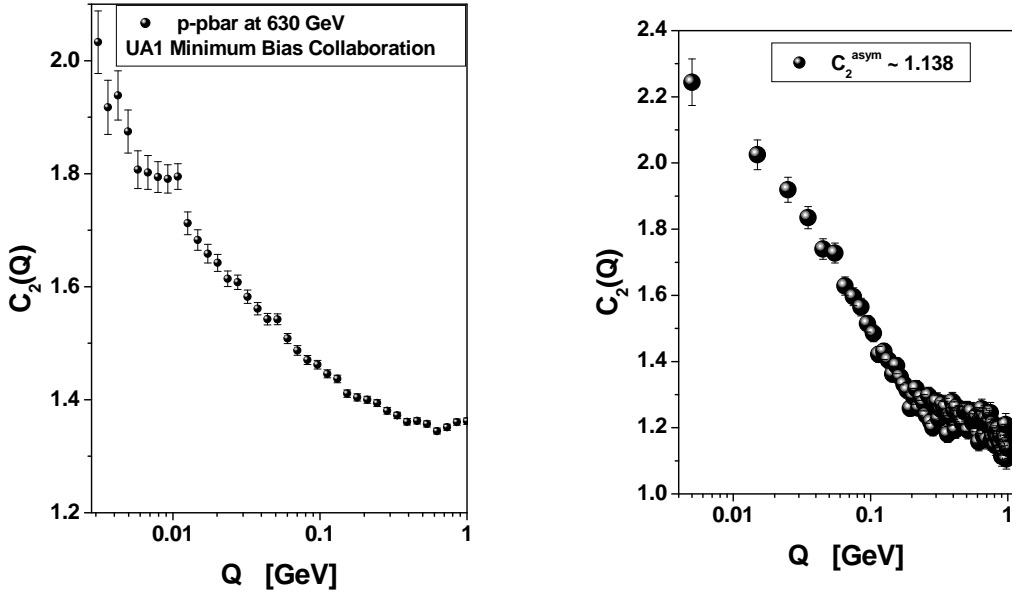


**Fig. IV.3.** Left panel shows data on  $C_2(Q)$  for negative particles at  $\sqrt{s} = 630$  GeV from UA1-Minimum-Bias-Collaboration [95]. Right panel presents example of  $C_2(Q)$  as given by the shifting procedure (with weights  $P = 1$  corresponding to maximal interaction) applied to the classical cascade CAS developed in Chapter II.

Results for  $C_2$  obtained using this prescription with  $\gamma = 1$  at all levels of the cascade in CAS model shown at right panel of Fig.IV.3. It is interesting to notice that they are similar to the experimental results obtained in UA1 experiment some time ago [95] and discussed in [96] (cf. Fig.IV.3 (left panel)). Namely, one gets  $C_2(Q) > 1$  for large  $Q$  and  $C_2(Q) > 2$  for  $Q \rightarrow 0$ . It means that physical picture underlying both results should be also similar. In [96] it was argued that such behaviour of  $C_2$  originates from the long-range correlations present in the hadronization process. As pointed there such correlations may be related to fluctuations of some quantities influencing the hadronizing system. Let us label them summarily by  $\xi$ . It is known [17] that  $m$ -particle Bose-Einstein correlation function calculated at a fixed value of the parameter  $\xi$  is given by:

$$C_m(p_1, \dots, p_m | \xi) = \frac{\rho_m(p_1, \dots, p_m | \xi)}{\rho_1(p_1 | \xi) \cdots \rho_1(p_m | \xi)}, \quad (\text{IV.14})$$

and for a purely chaotic source it is limited from above by

$$C_m(p_1, \dots, p_m | \xi) \xrightarrow{p_1 = \dots = p_m} m!. \quad (\text{IV.15})$$

However, as was shown in [96] eq.(IV.15) does not hold when  $\xi$  is fluctuating according to a probability distribution  $h(\xi)$  with

$$\int d\xi h(\xi) = 1. \quad (\text{IV.16})$$

In this case one has instead

$$C_m(p_1, \dots, p_m | \xi) \xrightarrow{p_1 = \dots = p_m} m! \cdot \frac{\langle \xi^m \rangle}{\langle \xi \rangle^m}, \quad (\text{IV.17})$$

and, for  $|p_i - p_j| \rightarrow \infty$  ( $i \neq j, i, j = 1, \dots, m$ ),

$$C_m(p_1, \dots, p_m | \xi) \rightarrow \frac{\langle \xi^m \rangle}{\langle \xi \rangle^m} = C_m^{\text{asympt.}} \approx F_m. \quad (\text{IV.18})$$

It means that the  $m$ -particle correlation function in such case can have intercepts above  $m!$  and saturates at the values above unity for large momentum differences. This is precisely the behaviour we observe here (albeit on different scale of  $Q$ , one should remember, however, the illustrative character of our numerical calculations). In **Table III** are listed correlation characteristics of our cascade leading to Fig.IV.3 with identification that in our case  $\xi = k_{1,2}$ .

$m$	$\langle k^m \rangle$	$\frac{\langle k^m \rangle}{\langle k \rangle^m}$	$C_m$
2	0.1516	1.2279	2.4557
3	0.0748	1.7242	10.3452
4	0.0407	2.6671	64.0095

**Table III.** Asymptotic values of the correlation function  $C_m$  and moments  $\langle k^m \rangle$  of the decay parameter distribution function  $P(k)$  used for cascade simulations presented at Fig.IV.3.

Although these results look very interesting and promising, nevertheless one cannot say, that we are modeling in this way the real BEC. The reason is that, as is obvious from Fig.IV.4, we observe also strong correlations for all charged pairs (albeit a bit weaker than for like charges only). This is because although we correlate only likely charged masses on a given cascade level, they decay further according to the normal decay rules used in CAS for charge conservation in vertices ( $\{0\} \rightarrow \{+-\}$ ,  $\{-\} \rightarrow \{0-\}$  and  $\{+\} \rightarrow \{0+\}$ ), which mixes charges again. In this way correlations imposed on the same level of cascading, say  $\{++\}$ , are getting diluted during the further cascading process and find their way to, say  $\{+-\}$  as well. Therefore, although such modeling preserves all kinematical constraints and provides reasonable  $C_2$ , it cannot be regarded as genuine modeling of BEC, at least not in the form discussed here. The knowledge of the hadronization process provided by CAS is therefore not helpful for better modeling of BEC using this method. On the other hand our example shows the possible way of introducing long range correlations in the system and how they reflect themselves in the final form of  $C_2$ . One should remark here, however, that, anticipating already results presented below in the next Chapter (cf. Fig.V.6 and V.7), there exist probably the possible remedy to this problem (not discussed

here). Namely, one could coalesce the nearby clusters of the same sign into one multiply charged object and allow it to decay further. This would enhance the like sign effect over the unlike sign also present here. One needs however, additional assumptions concerning the numerically extremely complicated problem of proper ending of such cascade with multicharged vertices (the same as mentioned in Chapter V.2 below).

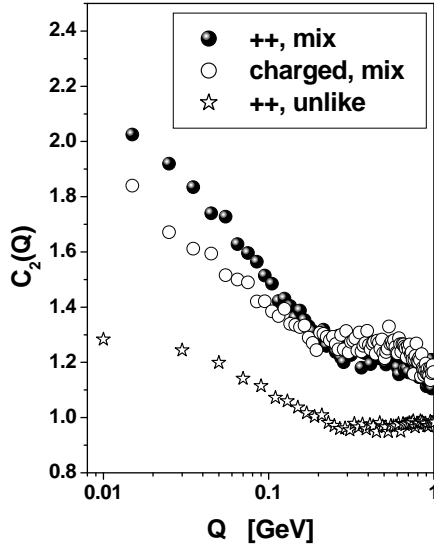


**Fig. IV.4.** Comparison of correlation functions as given by shifting procedure as in Fig.IV.3 for the three different subsets of the "data"-event and "reference"-event (cf. eq.(C.11) in Appendix C): full circles correspond to the case when  $C_2$  is calculated for positive pions with reference event taken as mix-event, open circles to positive and negative pions with mixing of events and open stars to positive pions with reference event constructed from unlike pairs.

### 3. Weighting of events - generalities

Let us proceed now to weighting of events procedures as proposed for general event generators in [87] and later developed in [88–91]. We shall mention also weighting method proposed specifically for the LUND model in [92]. According to this approach weight  $w_{ij}^{BEC}$  can be associated with each individual event given by event generator and used to convert results without BEC to those showing characteristic BEC pattern as given by  $C_2(Q)$ . In first example [87–91] global weighting factor for a final state with  $n$  identical bosons is usually constructed (under assumption on factorization in momentum space) as a sum over all permutations  $P(\{i\})$  of  $n$  elements [88]

$$W(p_1, \dots, p_n) = \sum_{\{P(i)\}} \prod_{i=1}^n w_2(p_i, p_{P(i)}), \quad (\text{IV.19})$$

where  $w_2(p_i, p_j)$  is a two-particle weight factor reflecting the effective source size. Unfortunately, the big number of pions of a given sign the necessary numerical calculations

become prohibitively long<sup>32</sup>. To resolve this problem one can apply a kind of clustering procedure [90]. According to it one separates the sum over all  $n!$  permutations into terms where only permutations which change positions of exactly  $K$  particles are taken into account:

$$W(n) = \sum_K W^{(K)}. \quad (\text{IV.20})$$

In principle, the form of weights should come from the symmetrization of wave function considerations or the Wigner function approach [21,22,87,88,91] and should reflect the Fourier transform of the expected spatio-temporal form of hadronizing source function. In practice, however, it all comes down to a suitable parameterization. For example, a reasonable description of the effect of BEC is obtained with a simple gaussian form of the weighting factor [88]:

$$w_2(p_i, p_j) = \exp \left[ -\frac{1}{2} (p_i - p_j)^2 \cdot R_{input}^2 \right], \quad (\text{IV.21})$$

or, with even simpler factor given by the step function form of  $w_2$  [89]:

$$w_2(p_i, p_j) = \begin{cases} 1 & \text{for } -(p_i - p_j)^2 = Q^2 < \frac{1}{R_{input}^2}, \\ 0 & \text{otherwise.} \end{cases} \quad (\text{IV.22})$$

The  $R_{input}$  is dimensional parameter which controls correlation of pairs of momenta (being therefore a kind of correlation length). It is important to realize this fact because when fitting data this parameter turns out to differ substantially from the final radius of the hadronizing source.

These weights should then be used to select from all events provided by given event generator only those, which already show desired bunching (i.e., for which  $C_2 > 1$  in (IV.1)) and count them as many times as necessary to get the observed  $C_2$ . Because this is practically impossible task one simply multiplies each event by the corresponding weight. Such procedure preserves energy-momentum balance provided by event generator but changes total multiplicity distribution. It needs therefore, when necessary, running again the event generator with a new initial parameters, in order to get right distributions. Notice that this procedure can be perceived as just a kind of filtering of only those events which, by sheer chance, are already showing desired pattern of BEC and enhancing them accordingly.

Second example is provided by weighting procedure used by Andersson and Hofmann [92] for the LUND string model of multiparticle production. The main quantity in this case is matrix element

$$\mathcal{M} = \exp [(i\kappa - b/2) \cdot \mathcal{A}]. \quad (\text{IV.23})$$

<sup>32</sup>See [97] for technical details concerning practical calculation of eq.(IV.19).

Here  $\kappa$  is the string tension,  $b$  is related to the breaking probability per unit area of the string (and hence to the form of the fragmentation function), and  $\mathcal{A}$  is the total space-time area spanned by string. The imaginary part of it is given by original model, the real part is added by assumption in order to allow for the interference effect leading to BEC when symmetrizing amplitudes. Using the fact that the same final state can be obtained for different areas  $\mathcal{A}$  in (IV.23) (the simplest example being the permutation of the momenta of two identical particles) one calculates an effective weight as [92]

$$W_{BEC} = 1 + \sum_{\mathcal{P}' \neq \mathcal{P}} \frac{\cos\left(\frac{\Delta\mathcal{A}}{2\kappa}\right)}{\cosh\left(\frac{b\Delta\mathcal{A}}{2} + \frac{\Delta(\sum p_{\perp q}^2)}{2\kappa}\right)}, \quad (\text{IV.24})$$

where  $\mathcal{P}' \neq \mathcal{P}$  means that the sum should run over all permutations of momenta of identical particles, except for the original configuration itself. The area difference  $\Delta\mathcal{A}$  and the sum of the particles transverse momenta can be rewritten in a dimensionless way as

$$\frac{\Delta\mathcal{A}}{2\kappa} = \delta p \cdot \delta x, \quad \frac{\Delta(\sum p_{\perp q}^2)}{2\kappa} = \delta p_{\perp} \cdot \delta x_{\perp}, \quad (\text{IV.25})$$

where  $\delta p = p_i - p_j$  with  $\delta x_L = (\delta t; 0, 0, \delta z)$  and  $\delta p_{\perp} = p_{\perp i} - p_{\perp j}$  with  $\delta x_{\perp} = x_{\perp i} - x_{\perp j}$ . This weight is then applied in the same manner as before [92]. The role of  $R_{input}^2$  before is now played by the area difference, i.e., it emerges from the generator itself.

#### 4. Summary

To summarize:

- This Chapter provides a kind of introduction to some specific aspects concerning the numerical modeling of BEC and implementing it Monte Carlo event generators, which are useful in presentation of our proposition of modeling BEC provided in the next Chapter V.
- It contains also example of specific application of CAS to model the BEC by means of momenta shifting, in which one makes use of the full information about the cascade hadronization process CAS provides. This shifting is applied now to the intermediate objects rather than to the finally produced particles (what allows to keep intact energy-momentum conservation). In this way one introduces into system strong long-range correlations and gets results similar to observed by UA1 Collaboration experiment [95]. However, one gets also correlations between unlike particles what makes such approach not useful for modeling BEC (at least, not in the simple version discussed here).

# V. Proposition of new method of numerical modeling of BEC

## 1. Introduction

None of generators discussed in Chapter IV (with the exception of the momenta shifting procedure) is giving desired BEC pattern already in a single event. However, in many practical applications, only generator operating on a single event level is useful. This is especially true when one tries to construct the set of reference events for 3 (or more) particle BEC, in which case such set should contain 2 (or more) BEC in a given event. Such generator will be also necessary when attempting (in a near future) to perform analysis on event-by-event basis using high multiplicity data either from RHIC or LHC accelerators.

In this Chapter we shall therefore concentrate on another method of introducing desired bunching of identical particles, which will work already at single event level<sup>33</sup>. For this purpose, we shall extent algorithm presented in [55], which introduces BEC already in a single event and works on the quantum statistical level. It makes direct use of the fact that identical bosonic particles subjected to BEC have, by definition, very strong tendency to bunch themselves in a maximal possible way (restricted only by conservation laws, especially by the energy-momentum conservation) in the same cells in phase-space<sup>34</sup>.

Let us start with short description of method used in [55]. Usually event generator provides us in each event with a number of charged and neutral secondaries (pions) of which we know their energy-momenta and sometimes also spatio-temporal positions of their production points. The weighting procedure discussed in Chapter IV and in [21,87–92] screens therefore all events against the amount of bunching they are already showing and counts them as many times as necessary to get desired pattern of BEC. One can perceive this also as a kind of filtering only events with desired pattern of particle distribution in phase space and enhance them accordingly. Instead of that in [55] the generator providing

---

<sup>33</sup>Shortened version of the material presented here has been published in [23].

<sup>34</sup>In this respect the presented algorithm can be regarded as generalization of the idea of elementary emitting cells introduced in [99] to the case of  $Q > 0$ . In [99] only case of  $[C_2(Q = 0) - 1]$  was considered.

such bunching itself was constructed using the following scheme:

- The available phase space (taken as longitudinal one and represented therefore by rapidity  $Y$ ) has been divided into a fixed number of equal cells (here given by  $\delta y$ ).
- To each  $i$ -th cell a number  $n_i$  of like-charge particles were associated according to Bose-Einstein distribution obtained using maximalization entropy method in information theory approach,

$$P_i^{(n_i)} = \frac{e^{n_i(\mu - \epsilon_i)/T}}{Z_i},$$

where:  $\epsilon_i$  is energy of the  $i$ -th particle,  $Z_i$  the partition function and in this case the "partition temperature"  $T$  and "chemical potential"  $\mu$  are two Lagrange multipliers corresponding to constraints provided by energy and charge conservations, respectively. In this way one encounters already for the fact that produced particles are bosons. Notice that such distribution represents typical example of nonstatistical fluctuations present in the hadronizing source.

After fixing  $T$  and  $\mu$  by means of single particle distribution, the size  $\delta y$  (which was fixed and kept constant) was then the only parameter left and used to obtain desired BEC and intermittency patterns.

In this way the BEC occurs already in a single event on the quantum statistical level. As shown in [55], it turned out to be strictly correlated with the observed intermittency pattern. On the other hand there is no explicit information on the spatio-temporal aspect of the hadronization process in this model<sup>35</sup>.

We propose to extend the above algorithm in such a way as:

- to make it flexible (i.e., not necessarily attached to any particular event generator);
- to make it faster (the most time consuming part of approach [55] is connected with the enforcement of conservation laws in each event, which finally is done only approximately to avoid prohibitively long calculations).

To this aim let us start with the idea of filtering mentioned above in connection with weighting procedure. The ability of performing such filtering already in each event would result in desired BEC pattern preserving at the same time both the energy-momenta and total multiplicity distributions.

What we have in mind here is following observation: among all particles produced by a given event generator one can always find clusters of particles located near each other in phase space in a way resembling BE statistics (at least to a some degree). Such

<sup>35</sup>Therefore such information was in [55] obtained by fitting the resultant  $C_2$  by the same formula we have used in Chapter II.5.

clusters occur because of the nonstatistical fluctuations present in every event generator. We would like now to select, or "filter", them somehow out. This turns out to be possible under the condition that one resigns from some information provided by event generator. The energy-momenta and total charges cannot be changed because they are directly measured. However, the spatio-temporal pattern of event or the charge distribution among particles in event can be altered as being not directly observable. Changes in spatio-temporal pattern correspond, in a sense, to introduction of quantum mechanical element of uncertainty to the otherwise classical event generator and has been discussed to some extend in different context in [87,21,22] and in the Chapter IV before. We shall not pursue it further here. Instead we shall concentrate on charge allocation to the produced particles. In particular, we shall propose to subject all identical particles produced in a given event to a kind of specific charge assignment filter, which either allocates charges to particles, if event generator does not perform this function, or otherwise changes their original charge allocation in an appropriate way. This is quite different approach from that usually used in the context of BEC [17], because instead of symmetrization of appropriate multiparticle wave function one works now in the number of particles basis and implements bosonic character of the produced secondaries by bunching the like-ones in the phase space. In [99] it was done by introducing concept of elementary emitting cell grouping particles of the same charge (*EEC*)<sup>36</sup>, in [55] in the way presented above.

To summarize, our reasoning is following:

- In every event, because of nonstatistical fluctuations existing in a given event generator, one gets groups of particles in phase space resembling groups obtained when using specific event generator [55] providing, by construction, particles satisfying Bose statistics.
- However, in general, particles in such group will have different charges allocated to them by event generator.
- To make such group look like "bosonic particles" (in sense of [55]) one has therefore somehow equalize charges of as many as possible particles in each such group.
- One has to do it without changing neither the initial energy-momentum allocations to particles nor the total multiplicities of particles of given charge.

One can look at the problem also from yet another point of view. Following discussion of the original HBT effect [101] (cf. also [102] and [103]) in order to get  $C_2$  as given by eq.(IV·1) one has to model quantity measuring correlations of fluctuations present in the system and represented by

$$\begin{aligned}\langle n_i n_j \rangle &= \langle n_i \rangle \langle n_j \rangle + \langle (n_i - \langle n_i \rangle)(n_j - \langle n_j \rangle) \rangle \\ &= \langle n_i \rangle \langle n_j \rangle + \rho \sigma(n_i) \sigma(n_j).\end{aligned}\tag{V·1}$$

<sup>36</sup>There are also numerous works concerning effects of such bunching on some characteristics of multiparticle production processes [100].

Here  $n_i \equiv n(p_i)$  denotes the number of particles with momentum  $p_i$ ,  $\sigma(n)$  is the corresponding dispersion of the multiplicity distribution  $P(n)$  and  $\rho$  is the correlation coefficient depending on the type of particles produced:  $\rho = +1, -1, 0$  for bosons, fermions and Boltzmann statistics, respectively. The proposed algorithm should then provide us with the two-particle correlation function  $C_2(Q)$ , which can be written in the form:

$$\begin{aligned} C_2(Q = |p_i - p_j|) &= \frac{\langle n_i n_j \rangle}{\langle n_i \rangle \langle n_j \rangle} \\ &= 1 + \rho \frac{\sigma(n_i)}{\langle n_i \rangle} \cdot \frac{\sigma(n_j)}{\langle n_j \rangle}. \end{aligned} \quad (\text{V.2})$$

To get  $\rho > 0$  (in which we shall be only interested, although the method can be extended to  $\rho < 0$  as well) it is enough to:

- select one of the produced particles,
- allocate to it some charge,
- allocate next (in some prescribed way) the same charge to as many particles located near it in the phase space as possible.

In this way one forms a cell in phase-space occupied by like-charged particles only. This process should be repeated until all particles are used and it should be such that one gets geometrical (Bose-Einstein) distribution of particles in a given cell. Notice that, contrary to all previous methods of modeling BEC, neither the original energy-momentum distributions nor the spatio-temporal pattern provided by our event generator are altered. On the other hand, we change completely the already existing charge pattern but retain both the initial charge of the system and its total multiplicity distribution. Therefore this method works in all cases in which one can resign from controlling the charge flow during hadronization process. The procedure of formation of such cells will be controlled by appropriate weights deciding whether or not a given neighbor of the initially selected particle should be counted as its another member. Using selection procedure which leads to a geometrical particle distribution in cells, one maximizes second term in eq.(V.2) because in this case  $\sigma = \langle n \rangle$ . This is the general idea of what should be done.

## 2. Algorithm

The proposed algorithm, which we shall use in all our calculations performed below, looks then as follows, cf. Fig.V.1. Let in the  $l^{th}$  event ( $l = 1, \dots, N_{event}$ ) our generator provides us with  $n_l = n_l^{(+)} + n_l^{(-)} + n_l^{(0)}$  particles of charges  $\{+\}, \{-\}$  and  $\{0\}$ , respectively. Keeping their energy-momenta  $\{p_j\}$  and spatio-temporal positions  $\{x_i\}$  intact, we allocate to them charges in the following way:

- (1) Choose randomly with weights proportional to

$$\mathcal{P}_l^{(+)} = n_l^{(+)} / n_l, \quad \mathcal{P}_l^{(-)} = n_l^{(-)} / n_l \quad \text{and} \quad \mathcal{P}_l^{(0)} = n_l^{(0)} / n_l \quad (\text{V.3})$$

the  $SIGN (+, 0, -)$ .

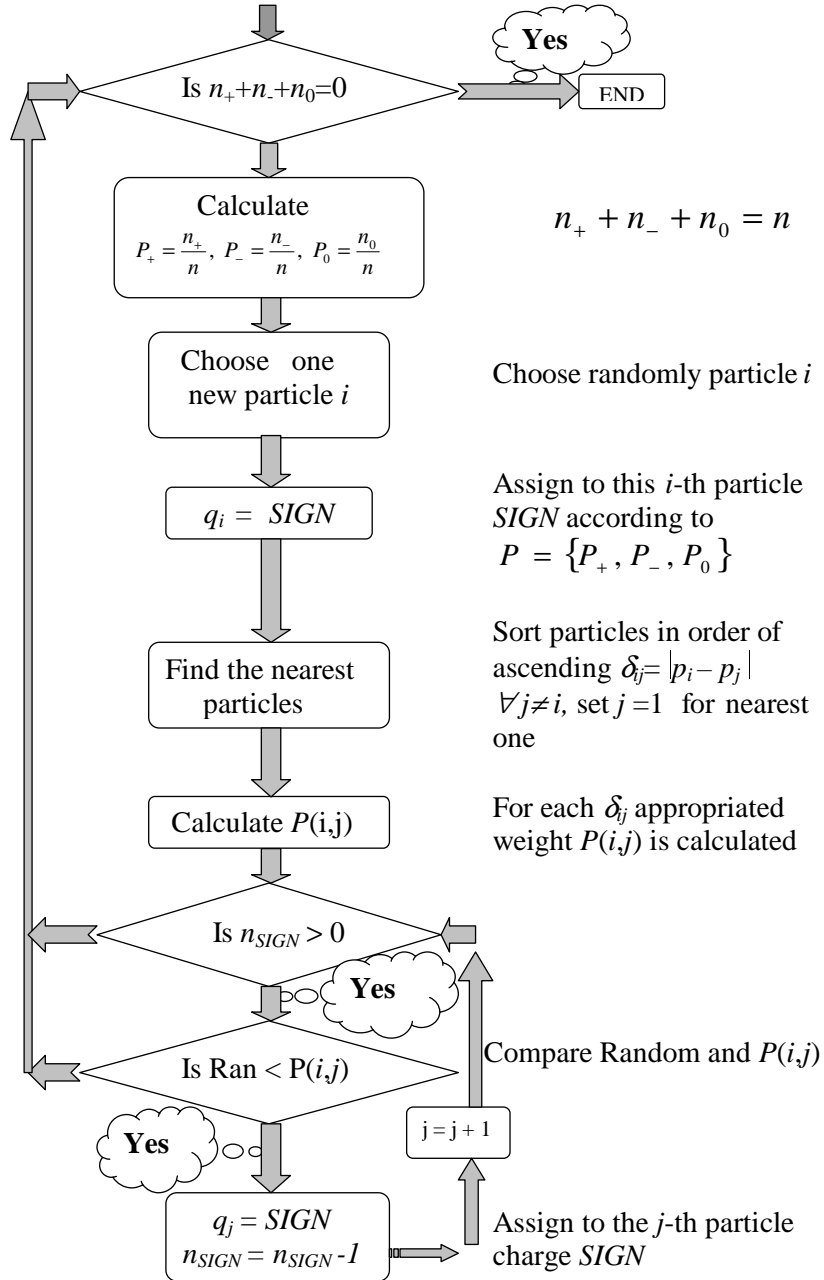


**Fig. V.1.** Chart flow for our algorithm.

- (2) From the particles produced and not yet assigned sign choose randomly single particle (" $i$ ") and assign to it the  $SIGN$  chosen in (1).
- (3) Calculate distances in momenta  $\delta_{ij}(p) = |p_i - p_j|$ , between the chosen particle ( $i$ ) and all other particles ( $j$ ) which are still without signs and arrange them in ascending

order of  $\delta$  with  $j = 1$  denoting the nearest neighbor of chosen  $i^{th}$  particle. To each  $\delta_{ij}$  assign appropriate weight  $P_{ij}$  (the form of which will be discussed below). Set  $j = 1$ .

(4) Choose random number  $r$  from a uniform distribution,  $r \in (0, 1)$ .

(5) If  $n_l^{SIGN} > 0$  then:

- (a) if  $r < P_{ij}$  then charge  $SIGN$  is assigned also to the particle  $(j)$ , the original multiplicity of particles with this  $SIGN$  is reduced by one,  $n_l^{SIGN} = n_l^{SIGN} - 1$ , and one returns to (4) with the next particle selected:  $(j) \Rightarrow (j + 1)$ ;
- (b) if  $r > P_{ij}$  then return to (2) above;

If  $n_l^{SIGN} = 0$  then one returns to point (1) with the updated values of  $\mathcal{P}_l^{(+)}$ ,  $\mathcal{P}_l^{(-)}$  and  $\mathcal{P}_l^{(0)}$ .

(6) If all  $n_l^{(+)} = n_l^{(-)} = n_l^{(0)}$  then stop the procedure for this event.

(7) Repeat all procedure starting from (1) for the next event.

The results of BEC and intermittency obtained using this algorithm are provided in Sections V.3 and V.4 below, respectively. Here we shall discuss in more detail some characteristic features of our algorithm. It is easy to check that for  $P_{ij} = P = const < 1$  this algorithm indeed leads to a pure geometrical (Bose-Einstein) distribution of particles in the phase-space cells formed in this procedure:

$$P_\infty(n_{cell}) = (1 - P)P^{n_{cell}} = \frac{1}{1 + \langle n_{cell} \rangle_\infty} \left( \frac{\langle n_{cell} \rangle_\infty}{1 + \langle n_{cell} \rangle_\infty} \right)^{n_{cell}}, \quad (\text{V.4})$$

with

$$\langle n_{cell} \rangle_\infty = \frac{P}{1 - P} \quad (\text{V.5})$$

in general, i.e., for unlimited number of particles out of which once selects members of a given cell. In reality, however, the pool of available particles is very limited. Denoting their number by  $n_{tot}$  one gets instead of (V.4)

$$P_{n_{tot}}(n_{cell}) = \frac{1 - P}{1 - P^{(n_{tot}+1)}} \cdot P^{n_{cell}} \quad (\text{V.6})$$

and the mean number of particles for such distribution

$$\langle n_{cell} \rangle_{n_{tot}} = \langle n_{cell} \rangle_\infty \cdot \left[ \frac{1 - P^{n_{tot}}}{1 - P^{(n_{tot}+1)}} \right] - n_{tot} \frac{P^{(n_{tot}+1)}}{1 - P^{(n_{tot}+1)}}. \quad (\text{V.7})$$

Because in our algorithm we always choose the first particles and put it to the new cell therefore eq.(V.7) is, in fact, a mean number of particles added to the selected cell. It

means therefore that the true mean number of particles in a cell is given not by eq.(V·5) or eq.(V·7) but by

$$\langle n_{cell} \rangle = 1 + \langle n_{cell} \rangle_{n_{tot}}. \quad (\text{V}\cdot\text{8})$$

The choice of  $P_{ij} = const$  seems therefore to be the most natural one in what concerns the connection of our algorithm with situation encountered in [55]. However, one can also argue that our approach is just a kind of another (albeit more involved) parameterization like, for example, shifting of momenta method [86], in which case limiting ourselves to  $P_{ij} = const$  only is not justifiable. After all, in this case, one neglects completely the whole information provided by event generator in what concerns energy-momenta or space-time positions of produced secondaries. Notice that dynamics is present in our approach in form of nonstatistical fluctuations provided by event generator we are working with. The only additional place where dynamics can enter in our algorithm are weights  $P_{ij}$ . Therefore, in addition to  $P_{ij} = const$  we shall consider also a kind of the "most natural" choices of weights, which use only the available information provided by event generator. We do it for two different hadronization models, CAS and MaxEnt. The comparison between models is done in the following way: to each CAS event characterized by the multiplicity  $n_l$  one builds the corresponding MaxEnt event according to the procedure outlined in Appendix A (cf. eq.(A·14)) (calculating the corresponding Lagrange multiplier  $\beta_l$  or "temperature"  $T_l = 1/\beta_l$ , which describes distribution of particles in phase space). Using now the same multiplicities,  $n_l$ ,  $n_l^{(+)}$ ,  $n_l^{(-)}$  and  $n_l^{(0)}$ , as in CAS, one calculates the corresponding BEC in MaxEnt. The weights we shall use are following:

- for CAS

$$P_{ij} = \exp \left[ -\frac{1}{2} (x_i - x_j)^2 \cdot (p_i - p_j)^2 \right] \quad (\text{V}\cdot\text{9})$$

(dictated by the fact that particles  $(ij)$  described by spatio-temporal wave packets would have widths given by their momentum separation  $\delta_{ij}(p) = |p_i - p_j|$ );

- for MaxEnt

$$P_{ij} = \exp \left[ -\frac{(p_i - p_j)^2}{2\mu_T T_l} \right] \quad (\text{V}\cdot\text{10})$$

( $\mu_T$  is transverse mass put here to be equal  $\mu_T = 0.3$  GeV and the role of spatial dimension is now played by the "temperature"  $T_l$  of the  $l^{th}$  event mentioned above).

The (V·9) and (V·10) seem to be the simplest choices connecting  $P_{ij}$  with details of hadronization process by introducing a kind of overlap between wave packets represented the produced particles, which measure the probability of their bunching in a given emitting cell (the constant in front is set equal to unity, i.e.,  $P_{ij} = 1$  whenever  $x_i = x_j$  or  $p_i = p_j$ ). One should, however, keep in mind that by doing so one is departing from the exact Bose-Einstein character of distribution of particles in a given cell as discussed above, which is *a priori* provided only for  $P_{ij} = const$ . Therefore "most natural" weights  $P_{ij}$  in

(V.9) and (V.10) should be regarded as illustration of effects of such deviation performed in the mentioned above spirit of treating our algorithm as simple parameterization only. Nevertheless, as can be seen below, even for such weights deviations from geometrical shapes are very small.

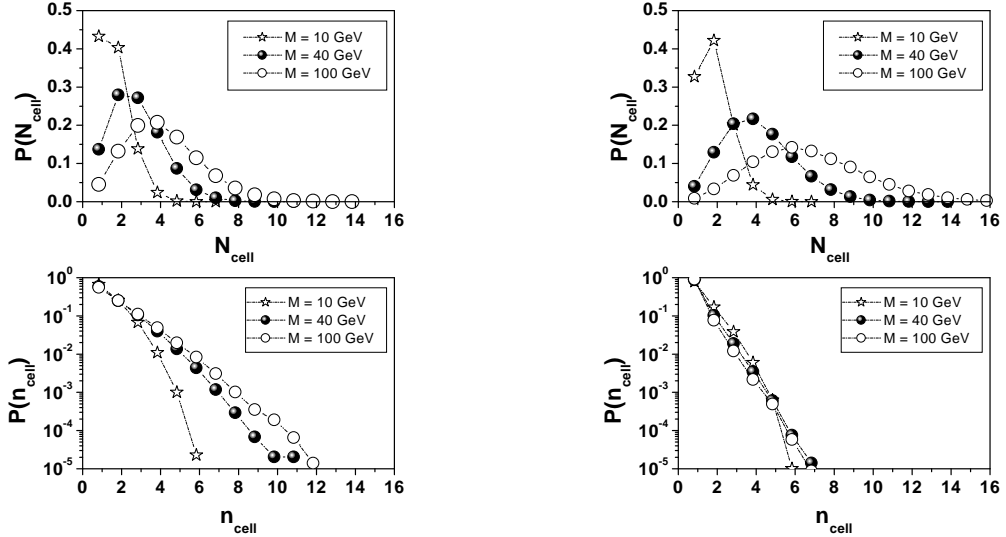


**Fig. V.2.** Number of cells distributions  $P(N_{cell})$  (upper panels) and cell occupation number distributions  $P(n_{cell})$  (multiplicity distributions in the cell, bottom panels) for both  $P_{ij} = 0.5$  (left panels) and  $P_{ij} = \exp [...]$  (cf. eq.(V.9)) (right panels) in the case of CAS hadronization model (for  $D = 1$ ,  $M = 100$  GeV,  $\tau = 0.2$  fm and  $q = 1$ ).

In Fig. V.2 and V.3 and in **Table IV** we show examples of the number of cell distributions  $P(N_{cell})$  and cell occupation number distributions  $P(n_{cell})$  for both types of models, CAS and MaxEnt, and for both types of weights  $P$ . Notice that, because  $n_{tot}$  are never very large in all cases of interest, the  $n_{tot}$  dependence in (V.8) is actually very strong (for example, for  $P_{ij} = 0.75$  and  $n_{tot} = 4$  one gets  $\langle n_{cell} \rangle \simeq 3 \cdot 0.9 - 1.25 = 1.45$  particles only instead of the naively expected 3 particles). This explains results listed in **Table IV** and allows to understand deviations from the straight lines (i.e., from the pure geometrical distributions) seen for small masses in Fig. V.2 and V.3. It should be also noticed that for  $P_{ij} \neq \text{const}$  and given by eqs.(V.9) and (V.10) the occupation number distributions  $P(n_{cell})$  remain very similar to geometrical ones. The only difference is that now  $\langle N_{cell} \rangle$  increases and  $\langle n_{cell} \rangle$  decreases substantially. After application of our algorithm particles show strong tendency to occur in bunches occupying these cell in the phase space (each of such cell is defined, for example, as wave packet in the momentum space centered on the mean momentum of the first selected particle) [99]<sup>37</sup>.

<sup>37</sup>It is interesting to notice that for the case of a constant (preselected) number  $k$  of cells (forming, for example, a single source) producing altogether  $n$  secondaries, our procedure leads to negative binomial

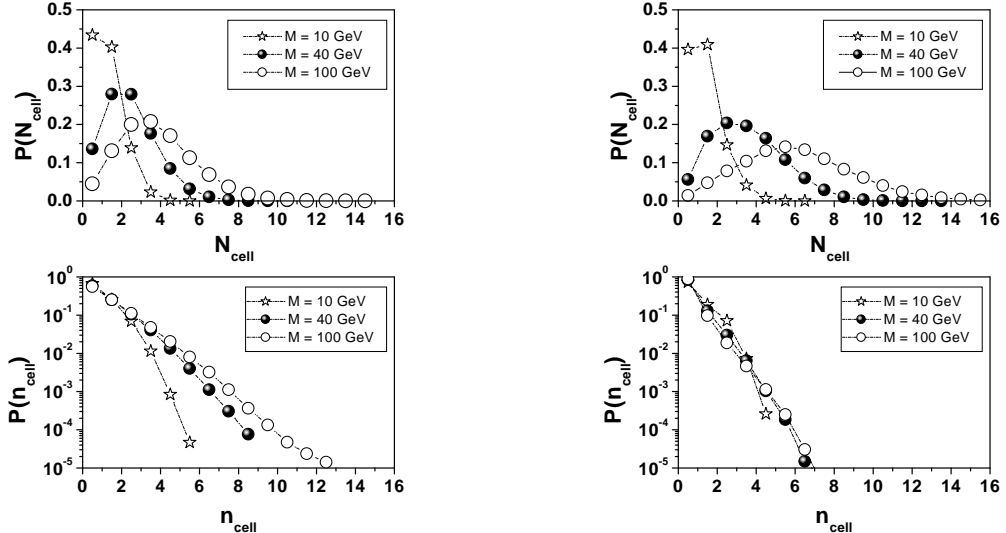


**Fig. V.3.** Number of cells distributions  $P(N_{cell})$  (upper panels) and cell occupation number distributions  $P(n_{cell})$  (multiplicity distribution in the cell, bottom panels) for both  $P_{ij} = 0.5$  (left panel) and  $P_{ij} = \exp [...]$  (cf. eq.(V.10)) (right panel) in the case of MaxEnt hadronization model.

It should be stressed that, although obtained distributions  $P(N_{cell})$  and  $P(n_{cell})$  are very similar and do not depend on the hadronization model we have used in a visible way, there is very strong dependence on the initial mass  $M$ . For bigger masses (i.e., for bigger multiplicities) one can obtain more particles of the same sign in the cell ( $n_{tot}$ ) and, as result, the number of particles in the cell tends to be geometrically distributed as shown above. For small masses there are noticeable deviations for large  $n_{cell}$ , which are caused by very limited number  $n_{tot}$  of particles of given charge to our disposal in such cases. We should stress at this point that we do not have cells void of particles. For small multiplicities the number of cells is simply smaller and their occupation lower. This feature is not shared by model discussed in [55] where in such cases some cells are void of particles (because one always has fixed number of cells for a given mass  $M$  and  $\delta y$  parameter). The (near) geometrical shape of particle distribution in the emitting cell tells us that, indeed, we have accounted (at least in an approximate way) for their bosonic character (Bose-Einstein statistics). That this leads to  $C_2(Q) > 1$  for  $Q \rightarrow 0$  was already demonstrated in [55]. However, notice that in contrast to [55] case we are now working with particles provided us by some quite general event generator and both the sizes of phase-space cells and their number are varying from event to event and within given event

distribution [99]:

$$P(n; k) = \sum_{n_1, n_2, \dots, n_k} \prod_i \left[ \frac{\left(\frac{\langle n \rangle}{k}\right)^{n_i}}{\left(1 + \frac{\langle n \rangle}{k}\right)^{n_i+1}} \right] = \binom{n+k-1}{n} \frac{\left(\frac{\langle n \rangle}{k}\right)^n}{\left(1 + \frac{\langle n \rangle}{k}\right)^{n+k}}, \quad (\text{V.11})$$

which, for large values of  $k$ , goes to Poisson distribution:  $P(n; k) \xrightarrow{k \rightarrow \infty} P(n) = \frac{\langle n \rangle^n}{n!} e^{-\langle n \rangle}$ .

depending on the values of weights  $P_{ij}$ . It is important to realize that, because we do not restrict *a priori* the number of particles which can be put in a given cell, we are automatically getting BEC of *all orders*<sup>38</sup>. It means therefore that  $C_2(Q=0)$  calculated in such environment of multiparticle BEC can exceed 2 (cf., [91]) (and, indeed, such tendency is clearly observed in Fig.V.8 below).

		$M$		10 GeV		40 GeV		100 GeV	
		Model used:		CAS	MaxEnt	CAS	MaxEnt	CAS	MaxEnt
$P_{ij} = 0.75$	$\langle N_{cell} \rangle$	1.38	1.38	1.97	1.97	2.65	2.66		
	$\sigma_N$	0.59	0.59	0.98	0.98	1.33	1.33		
	$\langle n_{cell} \rangle$	1.82	1.82	2.49	2.49	2.88	2.86		
	$\sigma_n$	0.90	0.90	1.57	1.58	2.06	2.04		
	$3 \langle N_{cell} \rangle \cdot \langle n_{cell} \rangle$	7.53	7.53	14.71	14.71	22.90	22.82		
$P_{ij} = 0.5$	$\langle N_{cell} \rangle$	1.76	1.76	2.96	2.95	4.31	4.32		
	$\sigma_N$	0.79	0.79	1.37	1.37	1.95	1.95		
	$\langle n_{cell} \rangle$	1.43	1.43	1.67	1.67	1.77	1.77		
	$\sigma_n$	0.68	0.68	0.99	0.98	1.13	1.13		
	$3 \langle N_{cell} \rangle \cdot \langle n_{cell} \rangle$	7.55	7.55	14.82	14.77	22.89	22.94		
$P_{ij} = P_{ij}(p, x)$	$\langle N_{cell} \rangle$	1.94	1.85	4.21	4.04	6.87	6.61		
	$\sigma_N$	0.87	0.87	1.83	1.85	2.88	2.87		
	$\langle n_{cell} \rangle$	1.29	1.36	1.17	1.21	1.11	1.15		
	$\sigma_n$	0.59	0.65	0.47	0.53	0.38	0.46		
	$3 \langle N_{cell} \rangle \cdot \langle n_{cell} \rangle$	7.51	7.55	14.78	14.67	22.67	22.80		

**Table IV.** List of the mean values and the dispersions of the distributions of cells and their occupancies depicted in Figs.V.2 and V.3. The results for case of  $P_{ij} = 0.75$  are also listed for comparison. The values of  $3 \langle N_{cell} \rangle \cdot \langle n_{cell} \rangle$  should reproduce the total multiplicities obtained for CAS (those for MaxEnt are the same by assumption). This is, indeed, the case as can be seen comparing them with total multiplicities given in **Table I** (the differences are  $\leq 0.5$  particle and are due to the different averaging procedures used in both cases). Notice that for  $P_{ij} = \text{const}$  the results for CAS and MaxEnt are practically identical. Differences occur only for the "most natural" weights  $P_{ij} = P_{ij}(p, x)$  as given by eqs.(V.9) and (V.10) below.

---

<sup>38</sup>The highest order of BEC will be limited by the multiplicity one can reach in a single cell in a given event. The other point, not discussed here, is that by limiting *a priori* the maximal number of particles, which can be allocated to a given cell one can, in principle, model not only Bose statistics, but also, the so called interpolating  $q$  statistics (or parastatistics) [104], including (perhaps) also Fermi statistics. This point will not be pursued here. However, it must be stressed that, from what was said above concerning the role of limited  $n_{tot}$  in changing  $\langle n_{cell} \rangle$ , the expected effects will probably be very small.

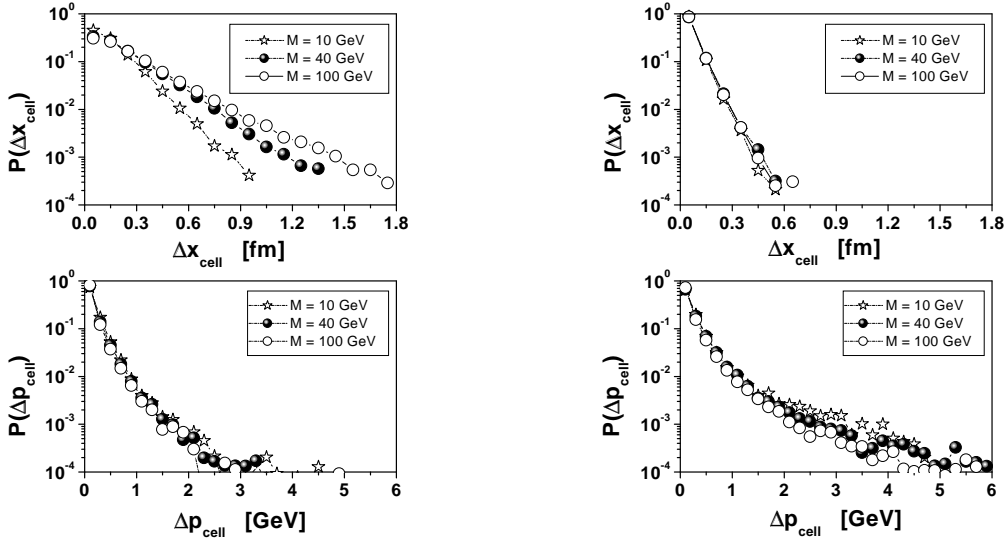


**Fig. V.4.** Distribution of mean quadratic sizes of cell in both the configuration space (upper panels) and in the phase space (bottom panels) calculated in CAS for "slow" cascade ( $\tau = 0.2$  fm, left panels) and for "fast" cascade ( $\tau = \frac{0.2}{M}$  fm, right panels). In both cases  $q = 1$ . The weights  $P_{ij} = \exp[\dots]$  (cf. eq.(V.9) and eq.(V.10)) were used.

	$M$	10 GeV	40 GeV	100 GeV
$\tau = 0.2$ fm	$\langle \Delta x_{cell} \rangle$	0.15	0.21	0.24
	$\sigma_x$	0.12	0.19	0.23
	$\langle \Delta p_{cell} \rangle$	0.19	0.18	0.16
	$\sigma_p$	0.23	0.22	0.19
$\tau = \frac{0.2}{M}$ fm	$\langle \Delta x_{cell} \rangle$	0.07	0.07	0.07
	$\sigma_x$	0.04	0.05	0.05
	$\langle \Delta p_{cell} \rangle$	0.28	0.27	0.23
	$\sigma_p$	0.44	0.50	0.41

**Table VI.** List of the mean cell sizes in configuration space ( $\langle \Delta x_{cell} \rangle$  in [ $fm$ ]) and momentum space ( $\langle \Delta p_{cell} \rangle$  in [ $GeV$ ]) together with their respective dispersions ( $\sigma_{x,p}$ ) obtained from Fig.V.4

Finally, let us discuss the sizes of elementary emitting cells in phase space and configuration space for the most "natural choice" of weight,  $P_{ij} = \exp[-\frac{1}{2}(x_i - x_j)^2 \cdot (p_i - p_j)^2]$  (cf. discussion following eqs.(V.9) and (V.10) below)). Because of the fact that our cascade for  $\tau = 0.2$  fm is becoming more diluted in configuration space with increasing energy, as it was pointed out in Chapter II (i.e.  $|x_i - x_j|$  gets bigger), the corresponding sizes of the cells in phase space (i.e.,  $|p_i - p_j|$ ) are decreasing (to keep  $(x_i - x_j)(p_i - p_j)$  in the weight  $P_{ij}$  the same). The reverse situation is encountered for the other choice of decay parameter, i.e., for  $\tau \sim 1/M$  (cf. Fig.V.4). This is because in this case we are getting higher density of the produced particles when energy  $M$  increases. In Fig.V.4 we provide distributions of the cell sizes both in the configuration space and the phase space. The resulting mean quadratic sizes and their dispersions are presented in **Table VI**.

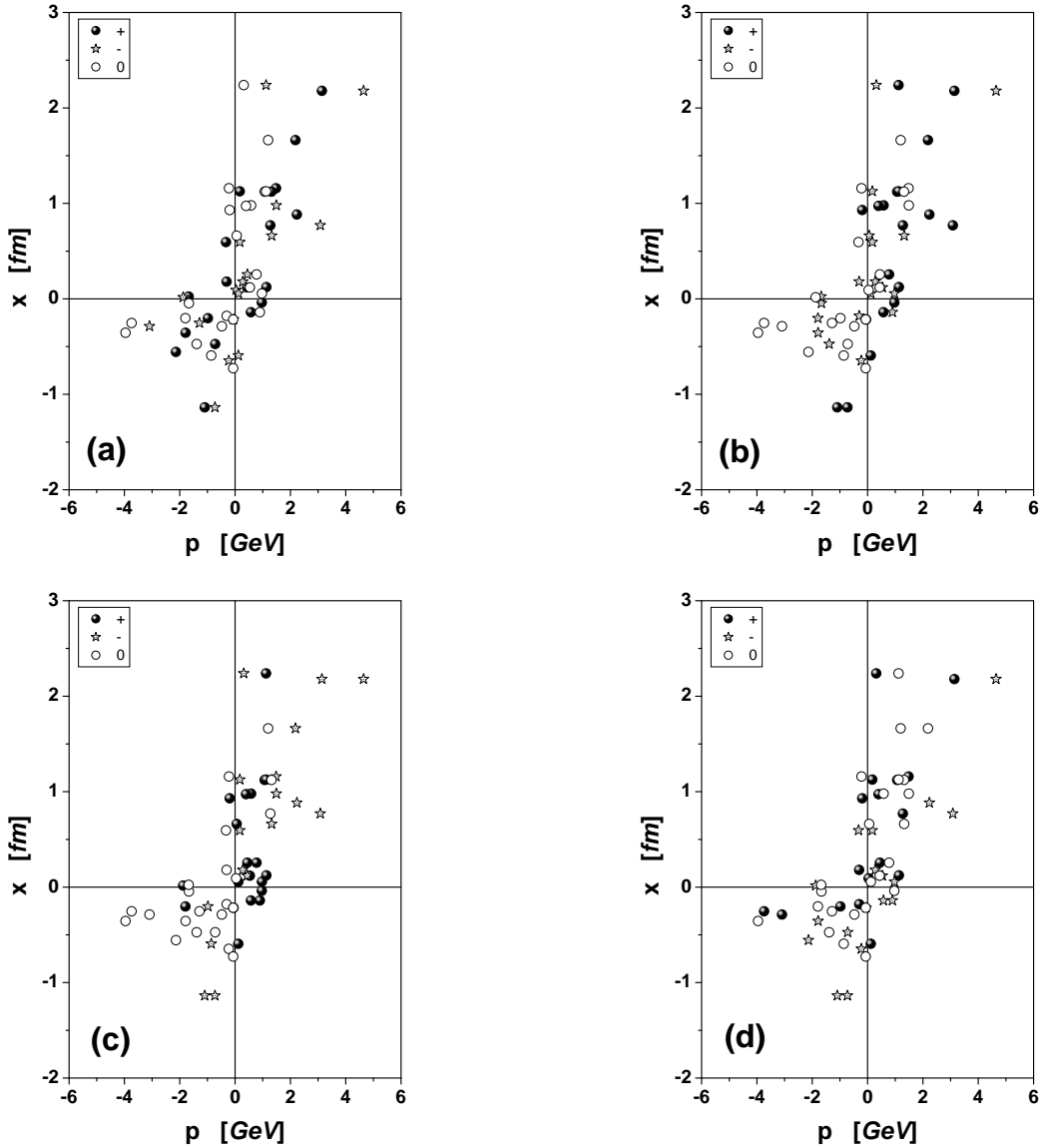


**Fig. V.5.**  $x - p$  scatter plots for event with  $N_{tot} = 62$  ( $N_+ = N_- = 19$  and  $N_0 = 24$ ) particles produced by CAS for  $M = 100$  GeV and the same parameters as in Fig.V.8 (left bottom panel): (a) original charge distribution provided by CAS, (b) charge distribution resulting from our algorithm with  $P_{ij} = 0.5$ , (c) the same with  $P_{ij} = 0.75$  and (d) with  $P_{ij}$  given by eq.(V·9). Actually, for the  $x - p$  range shown here one has only  $N_+ = 19$ ,  $N_- = 17$  and  $N_0 = 23$ , in total  $N = 59$  particles displayed.

To summarize and conclude discussion of emitting cells:

- our algorithm divides particles into a number of cells containing like-charge particles only distributed following essentially geometrical distribution (i.e., satisfying Bose-Einstein statistics in the way discussed in [55]);
- the cells are of varying sizes, both in momenta (for  $P_{ij} = const$ ) and in space (for  $P_{ij}$  given by eqs.(V·9) and (V·10)); there are also cells containing single particle only;

- our cells can partially overlap in momentum (and/or space for  $P_{ij} \neq \text{const}$ ), a situation which does not exist in [55]<sup>39</sup>.

The action of our algorithm is summarized on  $x - p$  scatter plot presented in Fig.V.5 where one event out of those composing bottom-left panel of Fig.V.8 below is displayed in detail.

Let us now demonstrate, using CAS model as example, what changes in the original physical picture our algorithm leads to. As we already mentioned, we do not change neither the initial energy-momentum nor spatio-temporal flows, however, we do profoundly change the charge flow provided by event generator. It is best seen when comparing Figs.V.6 and V.7. Whereas former shows typical charge flow existing in the CAS model (with only single-charged decay vertices), later exhibits the charge flow necessary to get new assignment of charges ( keeping all charged and neutral multiplicities the same as given originally in Fig.V.6). It was obtained by working the cascade tree "backward" after application of our charge reassignment. The characteristic feature of Fig. V.7 is the appearance of multi-like-charged decay vertices (with charges as high as  $\{4^+\}$  or  $\{4^-\}$  in the case considered here). The total charge is, however, still conserved as are the charges in decaying vertices (i.e., no spurious charge is being produced because of our algorithm, only decays of the type  $\{-\} \rightarrow \{4^-\} + \{3^+\}$  etc, show now up).

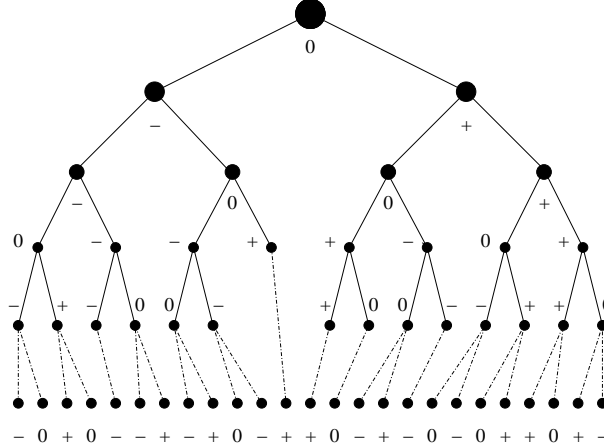


**Fig. V.6.** Example of the charge flow obtained with the simplest charge conservation pattern in vertices:  $\{0\} \rightarrow \{+\}\{-\}$ ,  $\{+\} \rightarrow \{+\}\{0\}$  and  $\{-\} \rightarrow \{-\}\{0\}$ . Notice that charge in each vertex does not exceed unity.

---

<sup>39</sup>It can be observed, for example, by comparing  $3\langle N_{cell} \rangle \langle \Delta x_{cell} \rangle$  from **Tables IV and VI** with the corresponding "Sizes A" in **Table II**. Considering case of  $M = 100$  GeV cascade one has  $3 \cdot 0.24 \cdot 6.61 \sim 4.76$  fm for  $\tau = 0.2$  fm and  $3 \cdot 0.07 \cdot 6.87 \sim 1.44$  fm for  $\tau = 0.2/M$  fm, to be compared with  $2 \cdot 1.82 = 3.6$  fm and  $2 \cdot 0.59 = 1.18$  fm, respectively.

The above picture suggest therefore a possible general approach to a possible numerical modeling of BEC. Namely, to get BEC in an event generator it is enough to allow for accumulation of charges of the same sign at some point of hadronization procedure modeled by this generator. This is, however, very difficult (if not impossible) task because it leads to insurmountable problems with their subsequent proper deexcitation to single charged final particles<sup>40</sup>. Our algorithm seems to provide the possible shortcut by reassigning anew already existing charges and resigning from the full information of what it amounts to in the intermediate steps of hadronization. However, it can happen that the nonstatistical fluctuations present already in a given algorithm are too weak to lead to desired BEC pattern. In that case Fig.V.7 and discussion connected with it suggest the possible (albeit very difficult) solution.

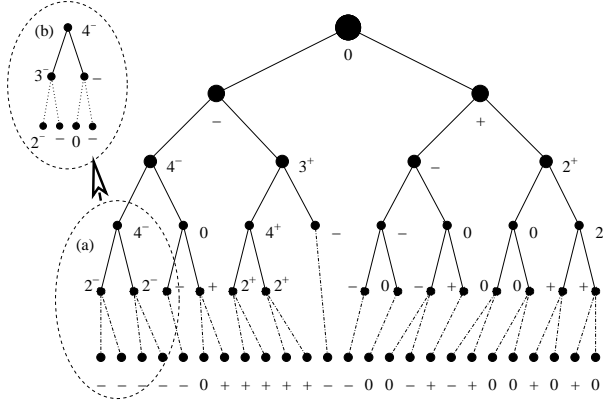


**Fig. V.7.** The same cascade as in Fig.V.6 in what concerns phase-space topology but with different assignment of final charges (preserving, however, the total numbers of neutral, positive and negative charges presented in Fig.V.6). To obtain such final assignment one has to allow for multiparticle charged vertices. Inlet shows different possible assignment with  $2^-$  being either a resonance or state, which will further decay into two  $1^-$  particles.

---

<sup>40</sup>For example, at  $l^{th}$  level of cascade one can encounter situation when object of mass slightly bigger than two masses of final particles,  $2\mu$ , wants to decay into two pions but at the same time it will posses charge greater than total charge of two pions, say  $3^-$  (cf. Fig.V.7). To treat such multicharged object as resonances or clusters as proposed in [105] could perhaps be (at least partial) solution provided one would be able to spot them easily enough in the cascades and force then to decay immediately into final pions of the same charge. There remains open problem of possible modeling such effect in other event generators, not considered here. So far we can only say that in the LUND [9] (or other string models) one can imagine that it could proceed through the formation of charged (instead of neutral) dipoles from the initial colour string, i.e., by allowing formation of (multi)like charged systems of opposite signs out of vacuum when breaking the string.

### 3. Numerical simulations of BEC

Let us now proceed to numerical simulations using our algorithm and let us start with BEC. Two cases will be considered: the single and multiple sources discussed in turn.

**Single source.** To demonstrate the abilities of our algorithm we show in Fig.V.8 results for two different models of hadronization of mass  $M$ : CAS and MaxEnt (limited for simplicity to one-dimensional cases only).

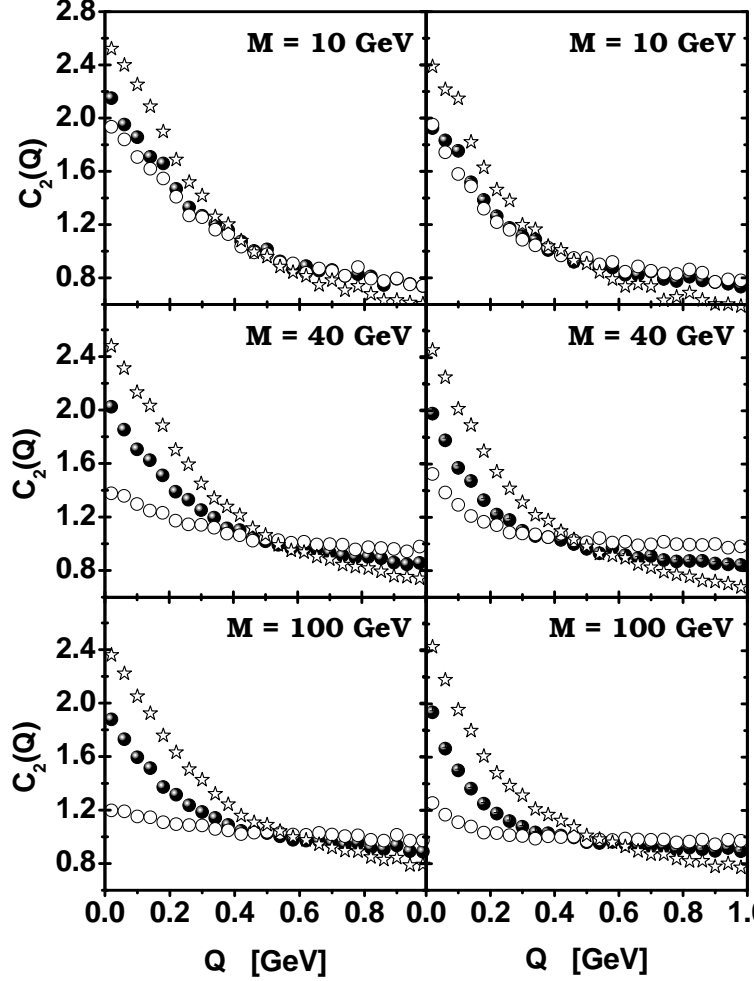


**Fig. V.8.** Comparison of BEC obtained using our algorithm for CAS (with  $\tau = 0.2$  fm and  $q = 1$ ) (left panels) and MaxEnt (right panels) types of the emitting one-dimensional sources of different masses  $M$ . Black symbols are for  $P_{ij} = 0.5$ , open stars are for  $P_{ij} = 0.75$  and open symbols for the "most natural" choices of  $P_{ij}$  discussed in text (eqs.(V.9) and (V.10)).

CAS is based on the phase-space and space-time cascade model discussed in Section II. MaxEnt is simple statistical model based on information theory concepts presented in Appendix A providing us only with the momenta distributions and used already before

in Chapter II.2. None of them shows BEC. As can be seen in Fig.V.8, application of our algorithm results in a clear BEC type behaviour of correlation functions  $C_2(Q)$  (which come out to be of exponential shape). They apparently do not depend much on the type of hadronization used. The comparison between models is done in the same way as mentioned already before when discussing the cell number distribution (cf. Fig.V.2).

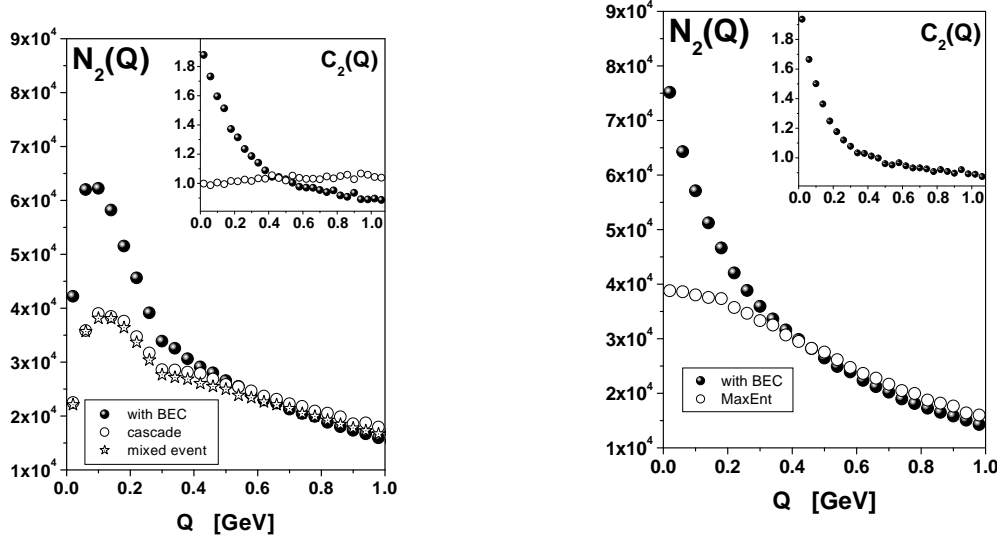


**Fig. V.9.** Comparison of the number of pairs distributions in the case of the CAS hadronization model (for  $M = 100$  GeV,  $\tau = 0.2$  fm and  $q = 1$ ) (left panel) and the MaxEnt one (right panel) with the constant weights,  $P_{ij} = 0.5$ . Insets show the corresponding  $C_2(Q)$  functions.

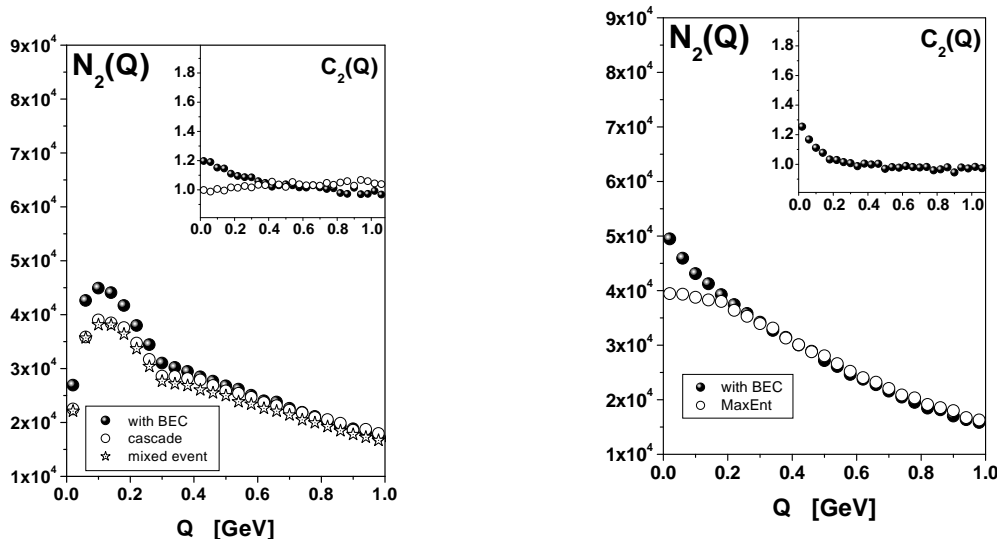


**Fig. V.10.** Comparison of the number of pairs distribution for the cases presented in Fig.V.9 with the weights  $P_{ij}$  calculated according to eq.(V.9) and eq.(V.10), respectively.

Although the BEC pattern presented in Fig.V.8 is similar in both the CAS and MaxEnt cases, the original pairs distributions and V.10) obtained in both models differ substantially (cf. Figs.V.9. On the left panels of Fig.V.9 and V.10 one can find comparison of the pairs distribution as given by the cascade simulation process with what is obtained after applying our algorithm and with what one obtains using the mixing of events procedure used to obtain reference distribution (cf. Appendix C, eq.(C.11)). As one can see application of mixing of events brings points with BEC back to those obtained from the pure cascade. Because of this we shall use in what follows as reference event needed to calculate the correlation function (cf. eq.(C.11)) just the output distribution of our cascade. On the right panels the same results (except of mixed events) are presented for MaxEnt model. In this case the same reference events used as for CAS.

	$M$	10 GeV		40 GeV		100 GeV	
Model used:		CAS	MaxEnt	CAS	MaxEnt	CAS	MaxEnt
$P_{ij} = 0.75$	$\gamma$	0.45	0.52	0.60	0.63	0.71	0.76
	$\lambda$	5.16	4.02	3.38	3.12	2.55	2.36
	$R$	0.59	0.70	0.58	0.69	0.62	0.79
$P_{ij} = 0.5$	$\gamma$	0.68	0.73	0.82	0.86	0.89	0.92
	$\lambda$	2.37	1.88	1.59	1.42	1.21	1.23
	$R$	0.66	0.83	0.74	1.03	0.87	1.32
$P_{ij} = P_{ij}(p, x)$	$\gamma$	0.75	0.80	0.95	1.00	0.97	0.98
	$\lambda$	1.52	1.56	0.40	0.59	0.21	0.33
	$R$	0.64	0.94	0.59	1.34	0.44	1.67

**Table V.** List of parameters  $\gamma$ ,  $\lambda$  and  $R$  (in fm) in formula (V.12) fitting data shown in Figs.V.8.

To recollect: the similarity of BEC patterns in both CAS and MaxEnt types of models originates in the fact that BEC effect is in our case given entirely by the number of particles of the same charge in a phase-space cell and number of such cells. This depends on  $P_{ij}$ , the bigger  $P_{ij}$  the more particles and bigger  $C_2(Q = 0)$ ; smaller  $P_{ij}$  leads to the increasing number of cells, which, in turn, results in decreasing  $C_2(Q = 0)$ , as already noticed in [99]. Only after connecting  $P_{ij}$  with details of hadronization process, some differences between models start to be visible. They originate entirely in differences in the number of elementary cells and number of particles located in them. Therefore the "sizes"  $R$  obtained from the exponential fits to results in Fig.V.8,

$$C_2(Q) = \gamma [1 + \lambda \cdot \exp(-Q \cdot R)], \quad (\text{V.12})$$

where  $\lambda$  is usually called chaoticity parameter [17], correspond to the sizes of respective elementary cells rather than to sizes of the hadronizing sources itself. In this way the size of the elementary cells plays the same role as the correlation length occurring in the weight method (see Chapter IV.3).

For  $P_{ij} = 0.5$  the "size"  $R$  varies weakly between 0.66 to 0.87 fm when going from  $M = 10$  to 100 GeV for CAS and between 0.83 and 1.32 fm for MaxEnt whereas for other

weights discussed above it varies, respectively, from 0.64 to 0.44 fm for CAS and from 0.94 to 1.67 fm MaxEnt (cf. **Table V**). This should be contrasted with the real sizes of CAS sources changing from 0.43 fm for  $M = 10$  GeV to 1.82 fm for  $M = 100$  GeV deduced in Chapter II (cf. **Table II**).

**Multiple sources.** So far we were considering only simple sources. It is interesting to investigate the correlation function behaviour in the case when our source consist in reality with a number of subsources. In general such possibility would allow for completely new extension of CAS model. We shall, however, limit ourselves here to the most simple case only<sup>41</sup>. Let us suppose therefore that our mass  $M$  consists of a number  $2^k$  of subsources hadronizing independently and located at the same place, both in configuration space and in phase space. It turns out that in this case the resulting  $C_2$ 's are sensitive to whether:

- one applies our algorithm of assigning charges to all particles from subsources taken together or
- one applies it to each of the subsource independently.

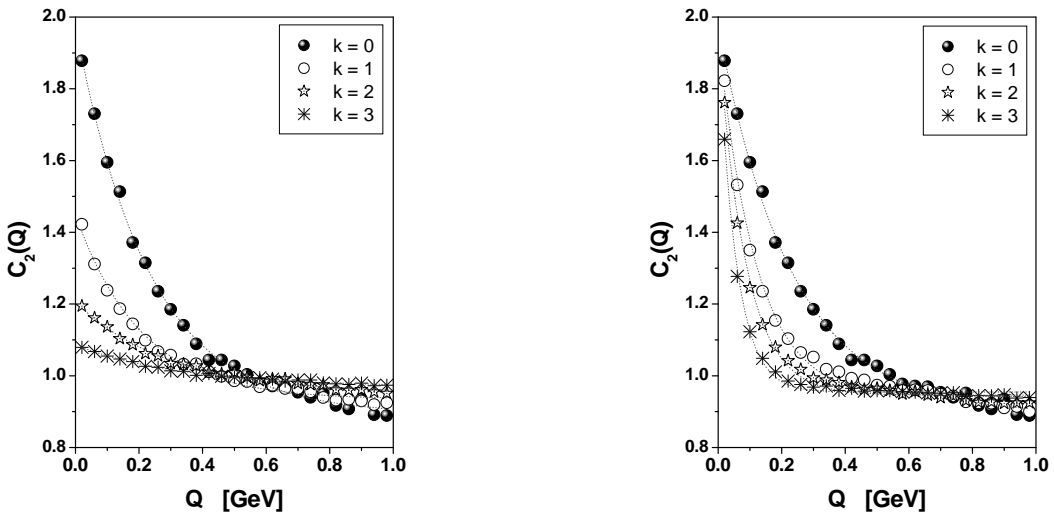


**Fig. V.11.** Dependence of BEC calculated using our algorithm (with  $P_{ij} = 0.5$ ) for the CAS type of the hadronic source (for  $\tau = 0.2$  fm,  $q = 1$ ) on the actual number of sources emitting particles: the original mass  $M = 100$  GeV ( $k = 0$ ) is divided into  $2^k$  sources with  $k = 1, 2, 3$ , respectively, positioned in the same place. Left panel is for the case when all subsources are treated independently ("Indep" in Table VII) whereas the right one is for the case when all particles from subsources are taken together when applying our algorithm ("Split" in Table VII).

Whereas the total multiplicity in both cases is the same (higher than for single source), the results are completely different:

---

<sup>41</sup>In other approaches the case of two sources separated in the configuration space was investigated in [106] whereas many sources effect in general was discussed in [107].

- in the former case one has roughly the same  $\lambda$  but the "size" of the whole source  $R$  is now increasing,
- in the later case "sizes"  $R$  (defined as before) are decreasing with  $\lambda = C_2(Q=0) - 1$  falling dramatically with increasing  $k$  (roughly like  $2^{-k}$ ).

The results for both cases (calculated for the constant weights  $P_{ij} = 0.5$ ) are shown in Fig.V.11 with the corresponding values of  $R$  and  $\lambda$  presented in **Table VII**.

	M	100 GeV	$2 \times 50$ GeV	$4 \times 25$ GeV	$8 \times 12.5$ GeV
Indep	$\lambda$	1.08	0.51	0.25	0.12
	$R$	0.87	0.96	0.68	0.59
	$\langle N_{cell} \rangle$	4.14	3.16	2.36	1.78
	$\langle n_{cell} \rangle$	1.60	1.53	1.44	1.32
Split	$\lambda$	1.08	1.01	1.00	0.99
	$R$	0.87	1.68	2.29	3.53
	$\langle N_{cell} \rangle$	4.14	5.97	8.43	11.85
	$\langle n_{cell} \rangle$	1.60	1.67	1.72	1.75

**Table VII.** List of parameters  $\lambda$  and  $R$  (in fm) fitting data shown in Figs.V.11 by the following formula:  $C_2(Q) = 1 + \lambda \exp(-R \cdot Q)$  ("Indep" is for left panel in Fig.V.11 and "Split" for right panel).

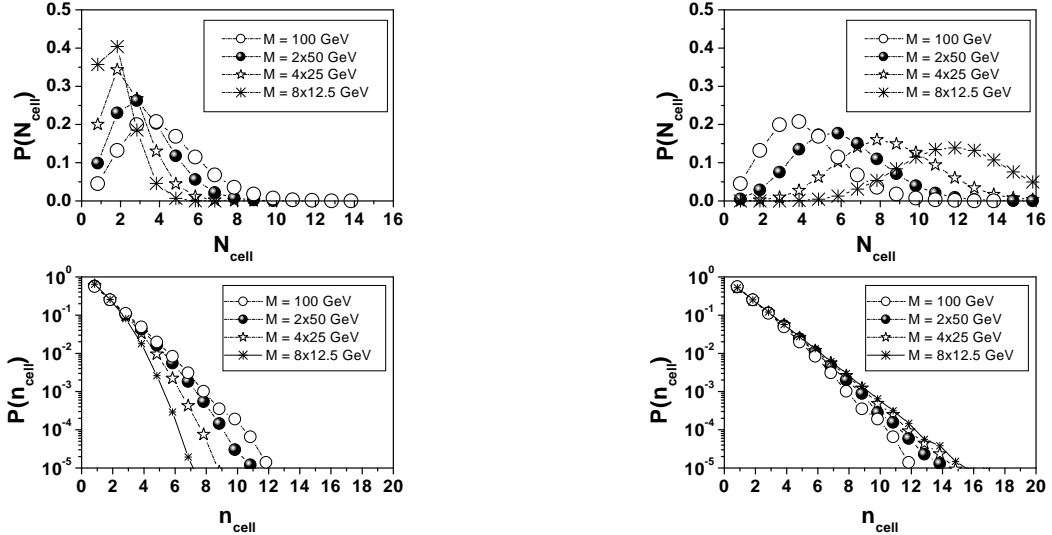


**Fig. V.12.** Number of cells distributions  $P(N_{cell})$  and cell occupation number distributions  $P(n_{cell})$  for the cascade presented at Figs.V.11 (left panels are for "Indep" and right for "Split" sources). Notice that for "Indep" sources  $P(N_{cell})$  show number of cells in a single independent subsource.

The increase of  $R$  for the "Split" type of sources is to be correlated with higher density of particles in the cell,  $P(n_{cell})$ , achieved in this case (cf. Fig.V.12). This results in smaller average distance  $Q$  between particles in phase space, which in turn leads to higher  $R$ . On the contrary, if subsources are of the "Indep" type, i.e., they are totally independent, the density of particles in subsources with smaller mass is smaller and  $R$  is decreasing with  $k$  (in similar manner as it is decreasing with  $M$  for  $P_{ij} = 0.5$  in **Table V** above). Also

$\lambda$  is decreasing in this case, as pointed above (cf. also [99]). The results for MaxEnt, not shown here, are very similar.

#### 4. BEC and intermittency

Let us now demonstrate how our new way of introduction BEC influence the observed intermittency pattern. It is known that, from the point of view of intermittency, models belong either to category, which can reproduce it easily (like  $\alpha$ -model [54], geometrical branching model [108] or one-dimensional special model of intermittency by Dias de Deus [109]) but otherwise are not complete or particularly predictive, or to category of models aimed to reproduce everything, which hardly show any intermittency (like, for example, DPM [5], Lund [9] and the like). Actually, even our CAS model produces (for the value of parameters leading to realistic energy dependence of multiplicity of produced secondaries and for  $D = 1$  case) very weak intermittency signal, as discussed in Chapter II (see Fig.V.13), mainly due to the finiteness of the cascades and the fact that it proceeds in the invariant mass  $M$  rather than in rapidity for which all factorial moments are calculated.

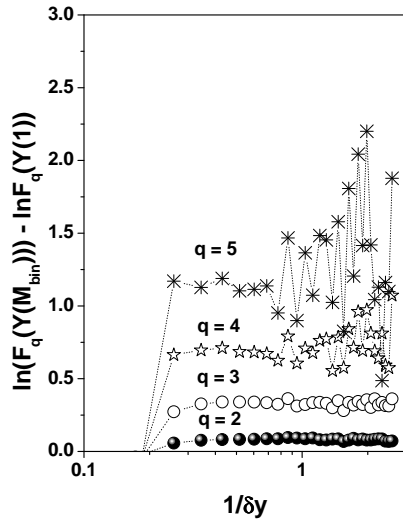


**Fig. V.13.** Example of scaled "horizontal" factorial moments  $F_q(M)$  of multiplicity of negatively charged particles as function of the reverse width of the bin in rapidity space,  $1/\delta y$ , for the one-dimensional cascade (with  $M = 100$  GeV,  $\tau = 0.2$  fm and  $q = 1$ ) presented in Chapter II.4.

The natural question arises: is our new implementation of BEC influencing intermittency pattern of a given event? The answer is positive and corresponding results are shown in Fig.V.13-V.15. One gets strong intermittency signal after application of charge assignment procedure, both for CAS and MaxEnt hadronization models. It follows the BEC pattern shown in Fig.V.8, i.e., intermittency is stronger when the BEC effect is stronger. It means therefore, that, as long as our reassignment of charges can be identified with incorporation of BEC into hadronization process, intermittency we are obtaining this way

is intimately connected with BEC, as was already anticipated in [18,31,91,29] and seen experimentally in [95].

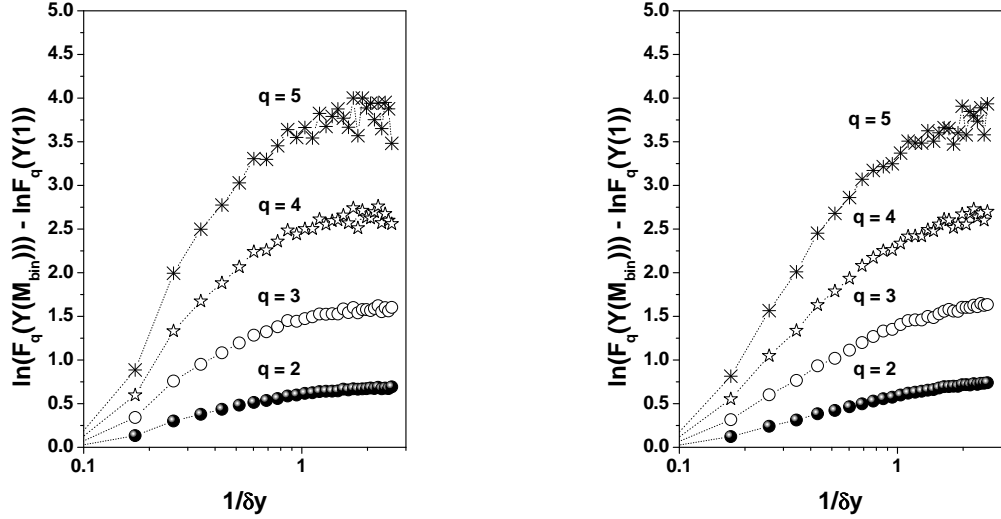


**Fig. V.14.** Examples of scaled "horizontal" factorial moments  $F_q(M)$  after application charge reassignment procedure with  $P_{ij} = 0.5$ . Left panel present results for CAS hadronization model with the same set of parameters as in Fig.V.13, right panel corresponds to MaxEnt hadronization model with  $M = 100$  GeV.

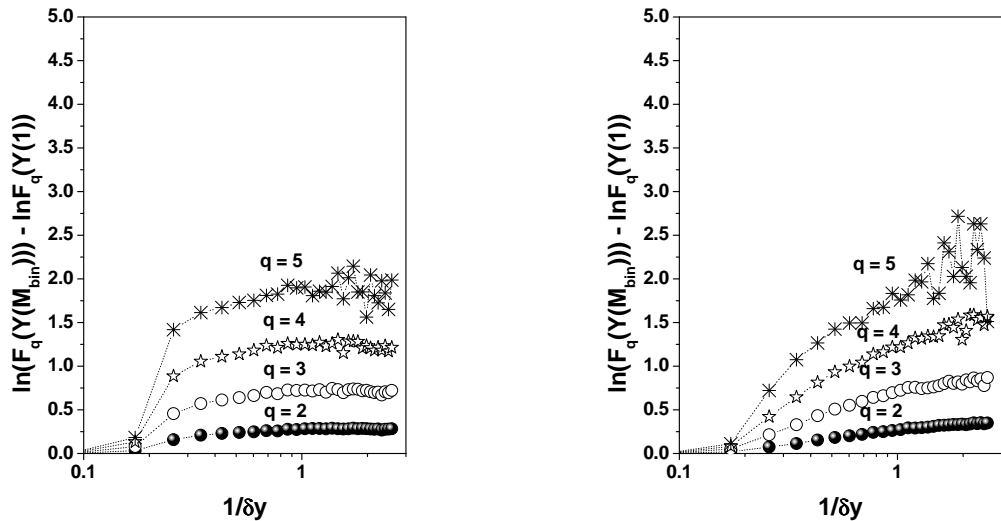


**Fig. V.15.** Examples of scaled "horizontal" factorial moments  $F_q(M)$  after application charge reassignment procedure with  $P_{ij}$  defined by eqs.(V.9)-(V.10). Left panel present results for CAS hadronization model with the same set of parameters as in Fig.V.13, right panel corresponds to MaxEnt hadronization model with  $M = 100$  GeV.

It is interesting to note differences in the shape of scaled factorial moments resulted from BEC and presented in Figs.V.14-V.15. The factorial moments corresponding to MaxEnt hadronization model look more power-law like than moments for CAS model. This is especially visible for the case of "most natural" choice of weight  $P_{ij}$ .

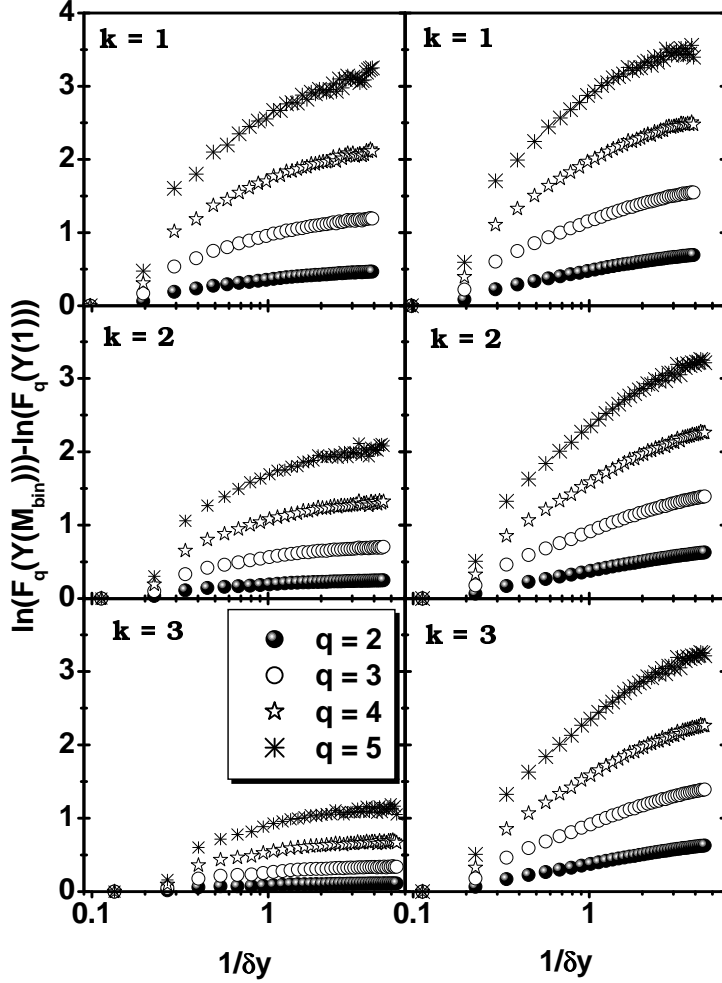


**Fig. V.16.** Dependence of factorial moments  $F_q$  calculated using our algorithm (with  $P_{ij} = 0.5$ ) for the same type of the CAS hadronic source as in Fig.V.11 on the actual number of sources emitting particles: the original mass  $M = 100$  GeV is divided into  $2^k$  sources with  $k = 1, 2, 3$ , respectively, positioned in the same place. Left panel is for the case when all subsources are treated independently ("Indep") whereas the right one is for the case when all particles from subsources are taken together ("Split") when applying our algorithm.

So far we have presented results for intermittency resulting from a simple source only. In Fig.V.16 we provide the intermittency patterns for the case of multiple sources. It extends therefore analysis of the multiple sources case presented in Fig.V.12 for BEC to the case of fluctuations as represented by the factorial moments  $F_q$ . Notice the strong

correlation between the observed behaviour of factorial moments and the type of source considered. The weaker BEC in Fig.V.12, the smaller values of  $F_q$  is observed<sup>42</sup>.

### 5. Example of confrontation with data for $e^+e^-$ annihilation into hadrons

Finally, let us address the most important question. Can one attempt to fit some experimental data (on BEC and/or on intermittency) using such approach? Surprisingly (considering the simplicity of the CAS model used for this purpose) the answer is positive and illustrative results are presented in Fig.V.17. Because we are, so far, by definition avoiding problems of multiple sources of varying masses and their distribution, we have to use for this purpose the simplest case of  $e^+e^-$  annihilation. For this purpose we have chosen data obtained by DELPHI Collaboration [110,111], Fig.V.17. As can be seen they can be fitted fairly well already with  $P_{ij} = \text{const}$ , but only for the case of two "Split" type sources (i.e., our source consists of 2 subsources but we do not distinguish which particle emerges from which subsource). We have used the CAS model with the same parameters as in Fig.V.11. In this case the charge multiplicities for our CAS and  $e^+e^-$  data are the same ( $N_{ch} \sim 21$ ). However, it seems that within the present CAS model, we are unable to fit simultaneously both the BEC and intermittency seen in data. The latter need much higher value of the  $P_{ij}$  parameter. But even then it turns out that we can not obtain agreement with experimental data for all moments. With  $P_{ij} = 0.5$  we fit only  $F_2$  and for  $P_{ij} = 0.75$  only  $F_5$  (cf. Figs.V.17 and V.18). From the point of view of our algorithm it looks like data would indicate the existence of stronger fluctuations as seen by  $F_q$  than those leading to BEC pattern. Obviously our CAS model lack this additional fluctuation component.

Nevertheless, remembering the crudeness of the CAS model used here, these results reassure us that our method of modeling BEC can be useful in practical applications. So far our calculations are for direct pions only, i.e., we have not considered production of resonances (for which selection of charges should be done independently). We shall not cover this subject here, nor shall we include final state interactions. We expect, however, that they would most probably, influence mostly the final  $P_{ij}$  needed to fit data. Therefore the  $P_{ij} \neq \text{const}$  choice of probabilities tells us, in a sense, what should be expected. One can also think of other way of accounting for resonances. Namely, one can not subject them to charge assignment procedure at all, reserving it only for direct pions. However, after performing assignment of charges to direct pions, one could decay our resonances and calculate BEC pattern for the whole set of particles. As above, we expect that it will substantially influence  $P_{ij}$  needed to fit data and can be accounted for by a suitable choice of weights. Let us remark only that, in general, resonances lead to decrease of

<sup>42</sup>Actually, any procedure shifting momenta of particles, and ours in a sense can be regarded as belonging to this category, will introduce intermittency. This is of course also true for the momenta shifting method presented in [11,86].

$C_2(Q = 0) - 1$  (i.e., to decrease of parameter  $\lambda$ ) whereas final state interaction, should decrease  $\lambda$  when introduced to CAS, and will increase it when included into data. One should also be aware of the fact that the region influenced by both these effects is limited to very small  $Q$  and therefore is hardly visible in data. In what concerns factorial moments  $F_q$  it is hard to estimate the way in which both effects can influence them.

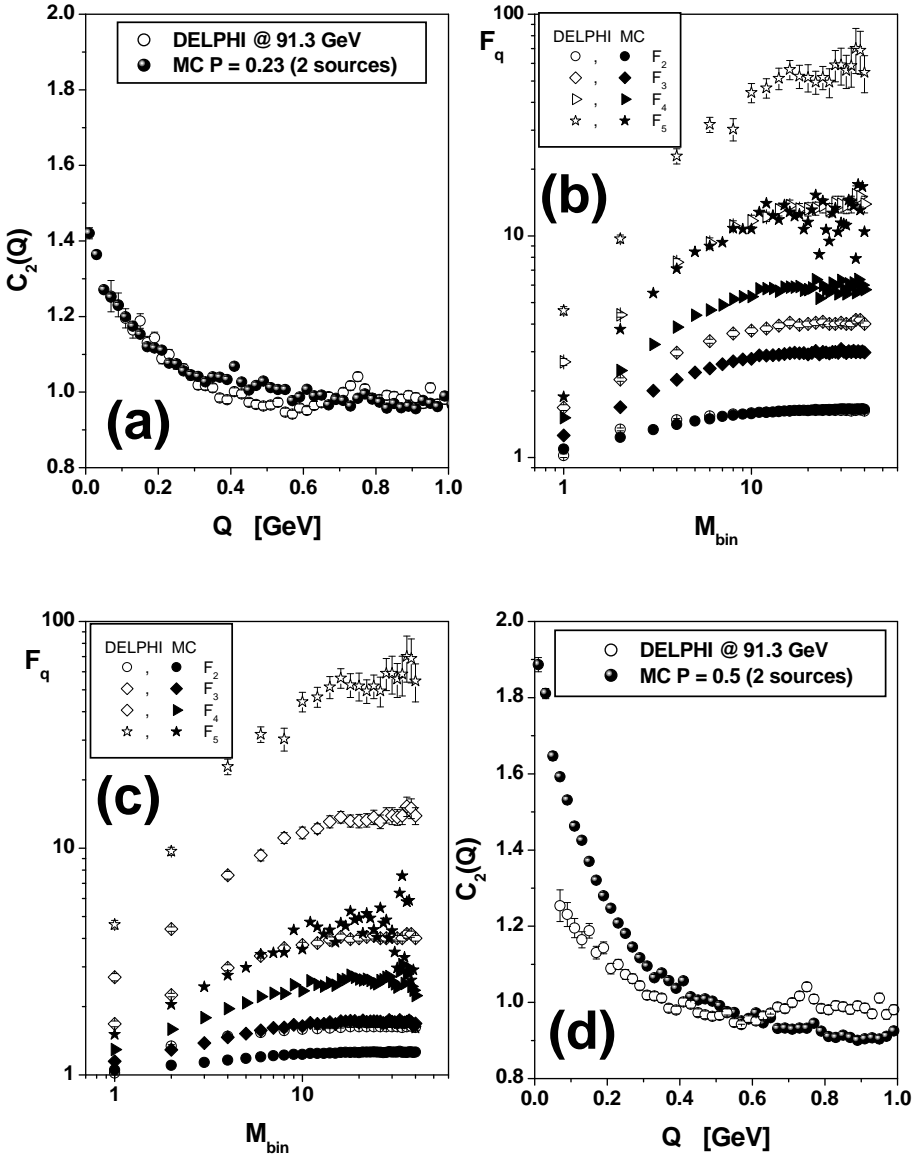


**Fig. V.17.** The examples of the best fits to the  $e^+e^-$  annihilation data by DELPHI on BEC [110] in (a) and, independently, on factorial moments [111]  $F_q$  in (b) using CAS model with 2 subsources. In (c) are shown the respective factorial moments for parameters used in (a) (when fitting BEC) whereas in (d) the respective BEC patterns for parameters used in (b) (when fitting factorial moments). Notice that left panels ((a) and (c)) are obtained for  $P_{ij} = 0.23$  whereas right panels ((b) and (d)) for  $P_{ij} = 0.5$ .

Notice that the best results for both BEC and factorial moments are obtained using multiple sources, i.e., when enriching the original simple minded structure of CAS by element, which can be connected with mass distribution  $M$ . Only in its "Split" version one gets possibility of obtaining different "sizes"  $R$ , a fact which allows to fit  $e^+e^-$  annihilation data. This feature of our model allows also to understand the increase of such "size"  $R$  with atomic number  $A$  in nuclear collisions. That is because with increasing  $A$  the number of collided nucleons, which somehow must correspond to the number of sources in our case, also increases. If the corresponding sources turn out to be of the "split" type, the increase of  $R$  follows then naturally.

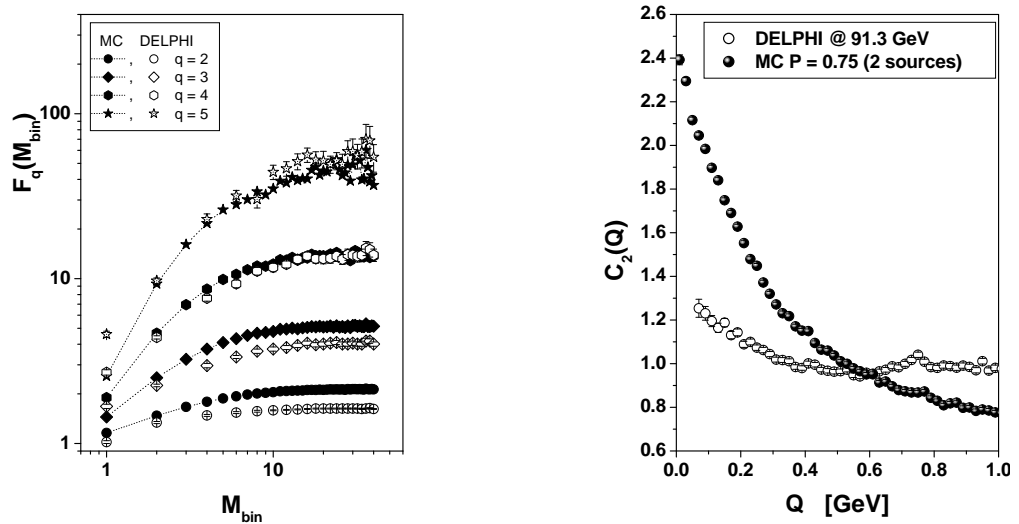


**Fig. V.18.** The examples of the best fits on  $e^+e^-$  annihilation by DELPHI on factorial moments [111]  $F_q$  in (left panel) and on BEC [110] in (right panel) using the CAS model with  $P_{ij} = 0.75$  and for 2 sources as in Fig.V.17. Now  $F_5$  is fitted fairly well whereas  $F_2$  is slightly overshooted.

On the other hand, the fact that "Indep" version of such approach leads to strong decrease of the parameter  $\lambda$  (i.e., the value of intercept  $C_2(Q = 0) - 1$ ) allows us to interpret the recently established weak BEC signal in the so called inter- $W$  BEC (i.e., BEC between pions each originating from a different  $W$  in fully hadronic  $W^+W^-$  final states [112]) as indication that produced  $W$  should be treated as independent sources ("Indep" type in Fig.V.11 above). This must be also regarded as prediction of our approach. To be even more speculative one can claim that taking a suitable combination of both types of sources one could fit data on  $WW$  (there would remain, however, problem of physical justification of such procedure - we shall not discuss it further).

## 6. Summary

To summarize:

- We propose a new and fast method of modeling BEC, which does it by making use of the fact that BEC phenomenon exist for identical bosonic particles, i.e., for particles satisfying Bose-Einstein statistics, which in the operational terms means that identical partials are bunched in cells in phase space according to geometrical (Bose-Einstein) distribution.
- Our proposition differs from the method proposed previously in [55] in that our algorithm is not limited to any special kind of Monte Carlo event generator (for example, to the one based on statistical model, as used in [55]) but can be applied as an independent additional routine to (probably) most generators existing at present. It does not change neither the spatio-temporal nor energy-momentum patterns of the event provided by event generator. Instead it attempts to find groups of particles located nearby in phase-space in a manner resembling Bose statistics and endows them with the like charges (keeping, however, intact the original number of positive, negative and neutral particles). All this is done for a single event whereas most of other methods mentioned in this work lead to BEC only for all events.
- The price which must be paid is that the original charge assignment provided by a given event generator is now neglected and all charges are assigned anew according to the principle mentioned above. In physical terms it means that the original event generator is effectively modified in such a way as to allow for multicharged intermediate states (clusters, strings, fireballs, etc.) to occur. The ability to do so is therefore the criterion whether given algorithm is suitable or not to be endowed with our procedure of modeling BEC. Actually, if such modification could be introduced directly to event generator one would get equivalent of [55]. This is, however, extremely difficult task and in this respect, our algorithm presents a kind of a short-cut realization of such idea.
- The parameter used in our case is the probability  $P_{ij}$  (constant or depending on the output of generator) that given particle likes to enter the cell formed already by other particles of the same charge. The size of such cell (which is free parameter in [55]) varies now depending on external conditions (like total number of particles and weights  $P_{ij}$ ). Both the number of such cells and multiplicity in them are varying from event to event. It should be noted that:
  - ♣ What we are doing could be perceived as another kind of shifting of momenta method proposed in [11,86]. However, we do not violate energy-momenta and there is physical picture (multicharged objects) behind our method (notwithstanding approximate Bose-Einstein statistics we are achieving in our cells), therefore such naive opinion is not valid.
  - ♣ Our parameter  $P_{ij}$  leads to a "size" parameters  $R$  which are quite different from the actual "sizes" expected from the measurement of BEC. However, the same is true for the weight method where  $R_{input}$  in eq.(IV.21) are completely different

from the "size"  $R$  emerging from fits to  $C_2(Q)$ . This is because  $R_{input}$  are essentially representing a kind of correlation length, which would be regarded as equivalent (in a loose sense) to the size of our cells.

- The CAS model used here to confront our results with experimental data is so far very crude. However, even at present stage it can fit some data for BEC and for intermittency (with only direct pions used, so far), albeit not simultaneously.

We conclude that our method of modeling BEC (perhaps with resonances and final state interactions included) can be now used together with other event generators describing successfully all aspects of multiparticle production processes (excluding BEC). To this end we have to our disposal:

- weights  $P_{ij}$ ;
- the number of subsources composing our hadronization source;
- their types: "Indep" or "Split."

They all are fixing the basic quantities in our algorithm, namely the number of elementary cells and the number of particles (of the same charges) in any of such cells. They in turn directly influence the "chaoticity" parameter  $\lambda$  and the "size"  $R$  used in fitting experimental data.

## VI. Summary and conclusions

The main subject of this work was the role played by fluctuations, correlations (in the form of BEC) and non-extensivity in hadronic processes. In particular we were interested in the following three topics:

- (i) interrelations between the space-time fluctuations of the hadronic source and the expected BEC pattern;
- (ii) the intrinsic fluctuations leading to non-extensivity;
- (iii) the new numerical modeling of BEC and fluctuation pattern (intermittency) it leads to.

Our results can be summarized as follows:

- In what concerns interrelation between the space-time fluctuations present in the hadronic source and the observed pattern of BEC we have found that obtained results depend crucially on the way the BEC are incorporated in the event. Using "afterburner" method, as in Chapter II.5, one is sensitive only to the intrinsic intermittency pattern of CAS, which, as has been demonstrated in Chapter II.4, is very weak. The reason is mainly due to the fact that our hadronization cascade proceeds in the invariant masses of the consecutive (sub)systems. The (multi)fractal structure present in this case in masses is not visible in other variables, like rapidities or spatial positions of production points. The hadronizing source  $\rho(r)$  has therefore never the simple power like structure as expected (or assumed) in [18,19,31] but instead shows a much more complicated form. As result one is not fully reproducing analytical expectations of [18,19,31] concerning BEC and intermittency (in rapidity space). The shape of  $C_2$  is only partially power-like, in a very limited range of  $Q$ . On the other hand, it is neither purely exponential (although very similar to it for one dimensional  $D = 1$  cascades) nor purely gaussian (resembling it to some extent for  $D = 3$  cascades).
- The situation changes, however, dramatically after using our new method of producing Bose-Einstein correlations, which is supposed to extend and replace the one proposed sometime ago in [55]. The method we propose makes use of the fact that because of non-statistical fluctuations present in the event generator there are, in each event, configurations of particles in phase space resembling configuration typical for bosonic particles. The only obstacle is that such configuration (bunches

of particles) contain particles of different charges. What we have proposed is to make them composed of mostly like-charged particles (to the extend limited only by action of conservation laws). Our method allows to introduce correlations essentially to any hadronization scheme already on a single event level and, in addition, it results also in strong signal of intermittency. It confirms therefore that, at least very substantial part of the intermittency phenomenon is closely connected with the bunching of particles provided by BEC. As Figs.V.6 and V.7 clearly show, the possible physical origin of such effect is production of multivalued charged clusters in the course of hadronization process. The first attempts to fit experimental data on  $e^+e^-$  annihilation using this method, although not totally satisfactory, are in principle positive and promising. We regard this as most important result of our work. The true experimental applications would have to include the proper treatment of resonances and final state interactions and is outside the scope of this work. It is clear that one should use for such purpose more sophisticated event generator than our CAS model and to endow it with our scheme of introducing BEC.

- In what concerns examples of non-extensivity, two of them illustrate the recently discovered fact [49,50] (cf. also [51]) that it occurs not only as results of some memory effects or long-range correlations present in the system (or because of its (multi)fractal structure) but also as a result of some intrinsic dynamical fluctuations it exhibits. The most important result is the possible connection between such fluctuations of the temperature  $T$  of the hadronic system and the  $p_T$  distributions pattern observed experimentally. This is because, it allows in principle to obtain information on the total heat capacity of the system considered, which is very important parameter when considering problem of QGP production in heavy ion collisions. Unfortunately, as we have demonstrated, it will be very difficult to extract this information from experimental data (perhaps the use of  $\Phi$  measure instead, as recently proposed in [78], would be more profitable in this respect). If successful, it would, however, provide the most valuable information on the possible phase transitions to QGP phase. The other result provides justification (if not derivation) of the widely used formula (III.4) describing the particle spectra in cosmic ray physics and is also worth to be stressed. Because the resultant  $q$  is smaller than unity in this case, the character of fluctuations (caused by joint action of the inelasticity and multiplicity distributions) existing here is, as discussed in [50], quite different than that encountered when discussing fluctuation of temperature (for which  $q > 1$ ). Finally, we have demonstrated that  $\Phi$  measure of fluctuations (as introduced in [72], notwithstanding all its limitations discussed by us in [74]) is very sensitive to the deviations from  $q = 1$  (cf. Chapter III.3). The  $|q - 1|$  can then describe in a phenomenological way all possible deviations from Boltzmann-Gibbs statistics not accounted for in explicit calculations based on normal statistical model approach.

We conclude that our model investigation clearly shows that nonstatistical fluctuations present in hadronic systems can be behind many features observed experimentally. To mention only two examples considered in details here:

- (1) they can allow to model BEC in a new way

(2) and they also lead, at some circumstances, to apparently non-extensive behaviour of some observables.

They should therefore be seriously considered as being a permanent feature of any event generator aimed to describe multiparticle production data. The way it will be implemented is an open question. The CAS model used here is just an illustration of how it can be done in case of BEC (in fact, in many event generators some features illustrated by CAS are already present). The non-extensivity (intrinsic fluctuations) will have to be added in some more general way, however, perhaps by changing statistics used in a given approach.

# Appendices

## A. Hadronization based on application of information theory approach (MaxEnt)<sup>43</sup>

It is rather common situation in description of multiparticle production data (most of which are just single particle distribution of different sorts) that many different (i.e., based on completely different theoretical assumptions) models lead to very similar results. This leads to suspicion that data from inclusive experiments contain only very limited amount of dynamical *information* and that most of it reflects some physically important constraints, which must always be accounted for as the basic assumptions of the model. Indeed, there exist a number of studies showing that already the pure phase-space calculations using transverse momentum cut-off can satisfactorily explain many of the observed phenomena in single particle inclusive experiments [113].

It is therefore important to separate phase-space effects from dynamical ones in order to extract non-trivial dynamical information from the observations of various phenomena in inclusive reactions. Only then one will be able to properly evaluate theoretical models, i.e. to establish their proper and important dynamical ingredients and to distinguish them from trivial ones.

The question therefore arises how to define and to measure the triviality (or trivial information). The most natural approach is to say that triviality means the lack of information, i.e., the less informative the more trivial. One is then led to information theory for definition of the measure of triviality. It is worth to mention at this point that applications of information theory in high energy physics has already long history [114,115] (cf. [30] for further references).

Following the line of discussion presented in [114] one connects then triviality with the information entropy and the whole problem reduces to maximalization the information entropy under some imposed constraints, which, in our case, are the assumptions of a theoretical model or the already established empirical facts. The estimate of a distribution function obtained in this way is most trivial and maximally model independent and

---

<sup>43</sup>The material of this Section is essentially collected from Ref. [30].

only it can be compared with the experimental data. The agreement with data means that there is no more information left in them, otherwise there is still some additional information different from that used in the input and it allows to modify the model.

To obtain the most probable distribution  $\rho$  one has to maximize information entropy introduced by Shannon [116]

$$S_1^{(I)}[\rho(x)] = - \int_{\Gamma} \rho(x) \ln[\mathcal{W}\rho(x)] dx \quad (\text{A.1})$$

where the subscript 1 means that we are dealing with *extensive* case here (i.e.,  $q = 1$  cf. Appendix B for its extension to the non-extensive,  $q \neq 1$  one) and  $\mathcal{W}$  denotes size of a elementary cell in phase space  $\Gamma$ . The next step is to specify constraints distribution  $\rho$  has to satisfy. These constraints must reflect our knowledge we have about  $\rho$ . The first and most obvious one is the fact that  $\rho(x)$  being a probability distribution must be non-negative and normalized, i.e., that

$$\int_{\Gamma} dx \rho(x) = 1. \quad (\text{A.2})$$

The rest of the remain known information can be expressed in the form of expectation values of  $k$  dynamical quantities  $\langle F_k \rangle_1 = f_k, k = 1, \dots, m < n$ :

$$\langle F_k \rangle_1 = \int_{\Gamma} dx F_k(x) \rho(x). \quad (\text{A.3})$$

Proceeding now in the usual way [114], i.e., varying  $S_I$  with respect to  $\rho$  with Lagrange multipliers  $-(1 + \Omega)$  and  $\lambda_i, i = 1, \dots, m$ , one gets that

$$\rho(x) = \exp(\Omega - \sum_{k=1}^m \lambda_k \cdot F_k(x)). \quad (\text{A.4})$$

It means that our distribution  $\rho$  is given in terms of Lagrange multipliers  $(\Omega, \lambda_i)$ , which must be determined from the constraint equations (A.2), (A.3):

$$\Omega = -\ln \int_{\Gamma} dx \exp \left[ - \sum_{k=1}^m \lambda_k \cdot F_k(x) \right] \equiv -\ln Z, \quad (\text{A.5})$$

$$f_k = \langle F_k \rangle_1 = \frac{1}{Z} \int_{\Gamma} dx F_k(x) \cdot \exp \left[ - \sum_{k=1}^m \lambda_k \cdot F_k(x) \right] = \frac{\partial \Omega(\lambda_1, \dots, \lambda_m)}{\partial \lambda_k}. \quad (\text{A.6})$$

It allows to write out the desired distribution  $\rho(x)$  in the following final form

$$\rho(x) = \frac{1}{Z} \exp \left[ - \sum_{k=1}^m \lambda_k \cdot F_k(x) \right]. \quad (\text{A.7})$$

For example, the knowledge of only the mean multiplicity  $\langle n \rangle$  results in the geometrical (or Bose-Einstein) multiparticle distribution  $P(n)$ <sup>44</sup>:

$$P(n) = \frac{1}{1 + \langle n \rangle} \cdot \left( \frac{\langle n \rangle}{1 + \langle n \rangle} \right)^n, \quad (\text{A.8})$$

as the most probable one. Allowing additionally for  $k$  independent, equally emitting sources leads immediately to the so-called negative-binomial form of  $P(n)$  [117]:

$$P(n) = \frac{\Gamma(k+n)}{\Gamma(k) \cdot \Gamma(n+1)} \cdot \frac{k^k \cdot \langle n \rangle^n}{(k + \langle n \rangle)^{k+n}}. \quad (\text{A.9})$$

It arises from the fact that now our  $\mathcal{W}$ , which was independent on  $n$  and which assumes equal probability for each cell of phase space, must be changed accordingly, namely  $\mathcal{W} \rightarrow \frac{\Gamma(k+n)}{\Gamma(k) \cdot \Gamma(n+1)} \mathcal{W}$ . Finally, adding to the knowledge of  $\langle n \rangle$  in (A.8) additional information that particles are *indistinguishable* one gets immediately (due to the necessary in this case replacement  $\mathcal{W} \rightarrow n! \mathcal{W}$  in eq.(A.1)) Poisson rather than geometrical distribution  $P(n)$ :

$$P(n) = \frac{\langle n \rangle^n}{n!} \cdot e^{-\langle n \rangle}. \quad (\text{A.10})$$

The MaxEnt model used in this work originated from applying this procedure to obtain the most probable single-particle inclusive distribution [30]. Let us define the semi-inclusive normalized rapidity distribution,

$$f_N(y) = \frac{1}{N} \frac{dN}{dy} = \frac{1}{\sigma_N \cdot N} \int d^2 p_T \left[ \frac{Ed\sigma}{d^3 p} \right]_{y \text{fixed}}, \quad (\text{A.11})$$

for an event in which a fireball of mass  $M$  decays (in its rest frame) into exactly  $N$  secondaries with strongly damped transverse momenta  $p_T$  (which are represented by fixed average transverse mass  $\mu_T = \sqrt{\mu^2 + \langle p_T \rangle^2}$ ). The mass spectrum  $\tau(M)$  and multiplicity distribution  $P(N)$  are assumed to be known from elsewhere and only one kind of produced hadrons (namely, pions of mass  $\mu$  and mean transverse momentum  $\langle p_T \rangle$ ) will be considered in what follows. It means that we are dealing with a one-dimensional decay represented by distribution  $f_N(y) = f_N(y; M, \mu_T)$  which is nothing else but probability density to find a single particle at rapidity  $y$ . To find it, we are looking according to the procedure outlined above, for  $f_N(y)$  which maximizes the information entropy  $S_1^{(I)}$  defined as

$$S_1^{(I)}(y) = - \int_{-Y_M}^{Y_M} dy f_N(y) \ln[f_N(y)] \quad (\text{A.12})$$

and subjected to constraints of normalization and energy conservation:

$$\begin{aligned} \int_{-Y_M}^{Y_M} dy f_N(y) &= 1, \\ N \cdot \int_{-Y_M}^{Y_M} dy \mu_T \cdot \cosh(y) f_N(y) &= M. \end{aligned} \quad (\text{A.13})$$

<sup>44</sup>The more usual form of the geometrical distribution  $P(n)$ , i.e.,  $P(n) = \frac{1}{\langle n \rangle} e^{-\frac{n}{\langle n \rangle}}$ , can be derived by the replacement:  $\frac{\langle n \rangle}{1 + \langle n \rangle} \rightarrow \exp(-\frac{1}{\langle n \rangle})$ , in the case when  $\langle n \rangle \gg 1$ .

Because in the rest frame of the fireball  $M$  our distribution is symmetric function, i.e.,  $f_N(-y) = f_N(y)$ , therefore the momentum-conservation constraint is satisfied automatically and Lagrange multiplier corresponding to it is zero. Notice that constraints (A·13) represent only conservation laws, not dynamics. The latter is supposed to enter through the mass spectrum  $\tau(M)$  of the produced of our fireballs and through their decay pattern as given by the multiplicity distribution  $P(N; M)$  for a given mass  $M$ .

As result one gets the following most probable distribution:

$$f_N(y) = \frac{1}{Z(M, N, \mu_T)} \exp[-\beta \mu_T \cosh(y)], \quad (\text{A}\cdot14)$$

where

$$Z = Z(M, N, \mu_T) = \int_{-Y_M}^{Y_M} dy \exp(-\beta \mu_T \cosh(y)) \quad (\text{A}\cdot15)$$

is the normalization constant and  $\beta = \beta(M, N, \mu_T)$  is the Lagrange multiplier, which must be calculated from the energy conservation conditions (A·13) with

$$Y_M = Y_M(M, N, \mu_T) = \ln \left\{ \frac{M'}{2\mu_T} \left[ 1 + \left[ 1 - \frac{4\mu_T^2}{M'^2} \right]^{1/2} \right] \right\}, \quad M' = M - (N - 2) \cdot \mu_T. \quad (\text{A}\cdot16)$$

being the maximal rapidity available. Notice that for  $M' \gg 2\mu_T$  it is equal to  $Y_M \simeq \ln(M/\mu_T) = \ln(N_{max})$ , i.e., is given by the maximal possible multiplicity  $N_{max}$ . For  $N \ll N_{max} = M/\mu_T$ , which is usually the case,  $Y_M$  essentially does not depend on  $N$ .

The main features of our final distribution  $f_N(y) \simeq f_N(y; \mu_T, M, N)$  are:

- (i) Lagrange multiplier  $\beta > 0$  (i.e., "temperature"  $T = 1/\beta$  is positive) only for multiplicities limited to

$$\begin{aligned} N > N_0 = N_0(M, N, \mu_T) &= \frac{MY_M}{\mu_T \sinh Y_M} \xrightarrow[\text{large } N_{max}]{} 2 \ln \frac{M}{\mu_T} \\ &= 2 \ln (N_{max}) \end{aligned} \quad (\text{A}\cdot17)$$

- (ii) It means that for  $N = N_0$  we have  $\beta = 0$ , i.e.,  $f(y)$  is in this case *strictly flat*. It means that *exact* Feynmann scaling (or plateau in the rapidity distribution) is realized *only* if the mean multiplicity of the reaction  $N = \bar{N}(M)$  follows the rule (A·17) (i.e.,  $N = N_0(M)$ ) as a function of the energy  $M$ .

- (iii) Notice that  $f(y)$  can be written in the following form:

$$f(y) = \frac{1}{Z} \exp \left[ -\bar{\beta} \cdot \frac{\mu_T \cosh y}{\langle E \rangle} \right], \quad (\text{A}\cdot18)$$

where  $\langle E \rangle = M/N$  is the mean energy available to the particle in a given event and  $\bar{\beta} = \beta \cdot M/N$ . It means that it shows a kind of scaling. For large enough masses  $M$  (i.e., for large enough  $N_{max} = M/\mu_T$ , cf. Fig.A.1) in the usually explored range of multiplicities  $N = N_{\pm} = \bar{N}(M) \pm \sigma$ , the resulting  $\bar{\beta}$  is almost constant as a function of  $\langle E \rangle$  (i.e.,  $\beta \propto N/M$ ) which means a kind of approximate scaling in the variable  $z = E/\langle E \rangle$ ,  $E = \mu_T \cosh y$ , in this region.

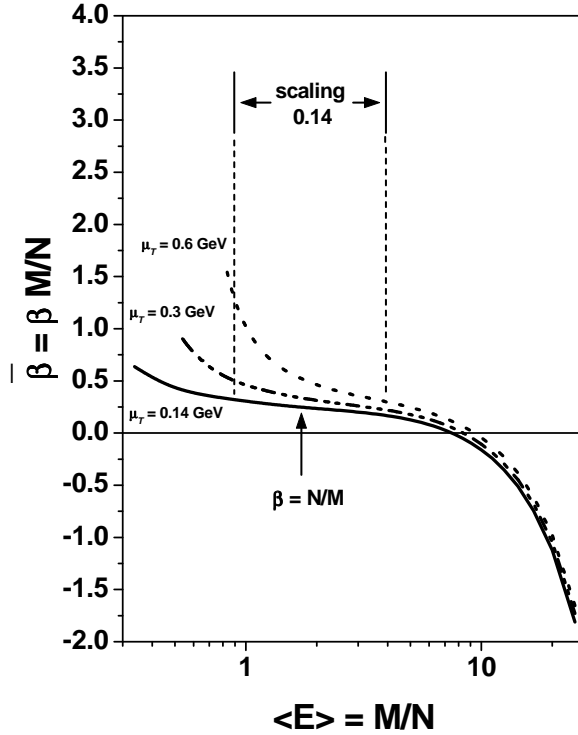


**Fig. A.1.** Example of sensitivity of  $\bar{\beta}$  on different choices of  $\mu_T$ . Notice the occurrence of  $\bar{\beta} \simeq \text{const}$  (scaling region) for diminishing  $\mu_T$ .

- (iv) For  $N < N_0$ ,  $\beta$  is negative,  $\beta < 0$ . In fact for  $\beta \xrightarrow[N \rightarrow 2]{} -\infty$   $f(y)$  takes a double  $\delta$ -function shape:

$$f(y; N = 2) = \frac{1}{2} [\delta(y - y_M) + \delta(y + y_M)]. \quad (\text{A.19})$$

Notice that apparently totally disparate theoretical models can successfully describe the same experimental data in all cases in which they share the same set of basic relevant assumptions. Their apparent theoretical differences correspond therefore to spurious information, which could be removed from the model without spoiling comparison with data<sup>45</sup>.

<sup>45</sup>Very good, albeit totally forgotten, example of such situation encountered in early years at multi-particle production has been provided in [114]. It is demonstrated there that all, apparently completely disparate, theoretical models describing the ISR data at that time, can do this only because they contain, either explicitly or implicitly, the same two features: that transverse momenta of secondaries are limited (longitudinal phase space dominance) and that only part of the available initial energy  $\sqrt{s}$ , equal to  $K\sqrt{s}$ , is used for production (existence of the inelasticity  $K$ ,  $K \in (0, 1)$ ). All other features of these models

Another important point is that although our formula (A.14) is identical to those used in thermal models [119] (with  $\beta = \frac{1}{T}$ , i.e., inverse temperature), parameter  $\beta$  being a Lagrange multiplier can take any (positive and negative) values, depending on the circumstances. It is therefore worth to remind at this point [120,121] that exponential form encountered here originates probably from the fact that the actual measurements extend only to a part of the total system. In this case the unmeasured part (which has to be averaged over) represents a kind of thermal bath with temperature  $T = \frac{1}{\beta}$ . This is good place to mention that in the case of finiteness of such thermal bath a power-like non-extensive behaviour replaces previous exponential one, cf. [122], and in addition to the temperature  $T$ , a parameter  $q \neq 1$  occurs in a natural way (for  $q \rightarrow 1$  this power-like distribution goes over to the previous exponential one). This parameter can be then associated [122] with the non-extensivity index of Tsallis statistics [24], see Appendix B.

## B. Some basic notions on non-extensive statistics

Long time ago, several new developments in statistical mechanics took place. In particular, it was shown that in the presence of long-range forces and/or in irreversible processes related to the microscopic long-time memory effects, the *extensive* thermodynamics is no longer correct and, consequently, the shapes of the equilibrium particle distribution functions can differ from the conventional well-known distributions corresponding to Boltzmann-Gibbs statistics. Standard sums, or integrals, which appear in the calculations of thermodynamical quantities, like partition function, entropy, internal energy, etc., can diverge in these situations. A number of ways of possible generalization of statistical mechanic for these cases was proposed. Among them the most interesting for us is the generalization of the conventional Boltzmann-Gibbs statistics (A.1) proposed by Tsallis [24]. This generalization has proved to be able to overcome difficulties the conventional statistical mechanics is faced with in many physical problems, where the presence of long-range interactions, long-range microscopic memory, fractal space-time structure or intrinsic fluctuations are encountered.

The Tsallis generalized thermostatistics is based on the following one parameter generalization of the Shannon-Boltzmann-Gibbs entropy [24]<sup>46</sup>:

$$S_q^{(I)}(\rho) = -\frac{1}{1-q} \left( 1 - \int_{\Gamma} d(x/\mathcal{W}) [\mathcal{W}\rho(x)]^q \right) \quad (q \in \mathbb{R}). \quad (\text{B.1})$$

The new entropy has the usual properties of positivity, equiprobability, concavity and irreversibility, preserves the whole mathematical structure of thermodynamics (Legendre

(responsible for their apparent differences) turned out to be simply *irrelevant*.

It is also interesting to mention at this point that first paper on information theory and multiparticle production has been published already at 1963, at the very dawn of multiparticle physics [118].

<sup>46</sup>Actually, this form of entropy has been originally introduced already by J.H.Havrda and F.Charvat in [123] and sometimes is referred to as THC entropy, see [124].

transformations) and reduces to the conventional Boltzmann-Gibbs entropy (A·1) in the limit  $q \rightarrow 1$ . However, it is not additive for the independent subsystems (hence the name 'non-extensive' given to the resulting statistical mechanics). The deformation parameter (known also as entropic index)  $q$  measures the degree of non-extensivity of the theory. In fact, if we have two independent subsystems  $A$  and  $B$ , such that the probability of  $A + B$  can be factorized into  $\rho_{A \cup B}(\Gamma_A, \Gamma_B) = \rho_A(\Gamma_A) \cdot \rho_B(\Gamma_B)$ , the global entropy is not simply the sum of their respective entropies but instead

$$S_q^{(I)}(A \cup B) = S_q^{(I)}(A) + S_q^{(I)}(B) + (1 - q)S_q^{(I)}(A) \cdot S_q^{(I)}(B) \quad (\text{B}\cdot2)$$

We immediately see that, since in all cases  $S_q^{(I)} \geq 0$ , it means that  $q < 1$ ,  $q = 1$  and  $q > 1$  corresponding, respectively, to *superadditivity*, *additivity* and *subadditivity*.

Using the procedure of maximalization of information entropy outlined in Appendix A, we get immediately the most plausible probability distribution of some events  $x$  subjected to the set of constraints provided in the form of unnormalized  $q$ -generalized expectation values (replacing those given by eq.(A·3)),

$$\langle F_k \rangle_q = \int_{\Gamma} dx F_k(x) [\rho(x)]^q, \quad (\text{B}\cdot3)$$

which is given in the following form:

$$\rho_q(x) = \frac{1}{Z_q} \left[ 1 - (1 - q) \sum_{k=1}^m \lambda_k \cdot F_k(x) \right]^{\frac{1}{1-q}} \xrightarrow{q \rightarrow 1} \rho(x) = \frac{1}{Z} \exp \left[ - \sum_{k=1}^m \lambda_k \cdot F_k(x) \right] \quad (\text{B}\cdot4)$$

As before, also here Lagrange multipliers  $\lambda_k$  can be expressed in terms of  $\langle F_k \rangle_q$  representing imposed constraints and  $Z_q$  arising from the normalization condition. Notice that whereas in the extensive, i.e.,  $q = 1$  case, all values of  $x \in (0; \infty)$  are admissible, for non-extensive case of  $q \neq 1$  we have restrictions on  $x$  to only such values that

$$1 - (1 - q) \sum_{k=1}^m \lambda_k \cdot F_k(x) > 0. \quad (\text{B}\cdot5)$$

There exists formalism, which expresses both Tsallis entropy and the expectation value using the so-called escort probability distributions [125,126],

$$P_i = \frac{p_i^q}{\sum_i p_i^q}. \quad (\text{B}\cdot6)$$

However, it is known [127] that such approach is different from the normal non-extensive formalism because Tsallis entropy expressed in terms of the escort probability distributions has difficulty with the property of concavity. From our limited point of view, it seems that there is no problem in what concerns practical, phenomenological applications of non-extensivity as discussed in our paper. Namely, using (B·6) one gets distribution of the type

$$c \left[ 1 - (1 - q) \frac{x}{l} \right]^{\frac{q}{1-q}} \quad (\text{B}\cdot7)$$

which is, in fact, *formally identical* with that in (B·4)

$$c \left[ 1 - (1 - Q) \frac{x}{L} \right]^{\frac{1}{1-Q}}, \quad (\text{B}\cdot\text{8})$$

provided we identify  $Q = 1 + \frac{q-1}{q}$ ,  $L = l/q$  and  $c = \frac{2-Q}{L} = \frac{1}{l}$ . The mean value is now  $\langle x \rangle = \frac{L}{3-2Q} = \frac{l}{2-q}$  and  $0 < Q < 1.5$  (or  $0.5 < q < 2$ ). Both distributions are identical and problem, which of them better describes data is artificial. Therefore in what follows we shall use throughout this paper the old approach leading to (B·4).

One of the most interesting example where non-extensivity appears in natural way is the *anomalous* diffusion [128]. By this we mean any transport mechanism, which like diffusion, behaves at mesoscopic level as an isotropic random process, but which violates the well-known Einstein relation [129]:

$$\langle x^2 \rangle = 2Dt. \quad (\text{B}\cdot\text{9})$$

Most of the literature on anomalous diffusion has been devoted to processes in which the mean square displacement  $\langle x^2 \rangle$  varies with time as

$$\langle x^2 \rangle \propto t^{2/z}, \quad (\text{B}\cdot\text{10})$$

where  $z (\neq 2)$  is dynamic exponent (or random walk fractal dimension) of the transport process under consideration. In this notation normal diffusion corresponds to  $z = 2$ . For  $z > 2$  the growth rate of the mean square displacement is smaller than in normal diffusion, and transport is consequently said to be *subdiffusive*. On the other hand, for  $z < 2$  the mean square displacement grows relatively faster and transport is *superdiffusive*. We shall concentrate in what follows on this latter case because it is directly connected to derivation of Lévy distributions [130] using Tsallis statistics.

The class of Lévy distributions is defined through their characteristic function  $C(u)$ , which in its most general form may be written as:

$$C(k) = \exp(-c | k |^\gamma \cdot (1 + i\beta\omega(\gamma, k))) \quad (\text{B}\cdot\text{11})$$

where  $c$  is the scale factor, the characteristic index (or Lévy exponent)  $0 < \gamma < 2$  governs the form of the tail of the distribution, the index  $-1 \leq \beta \leq 1$  determines the symmetry properties of the distribution, and  $\omega(\gamma, k) = \text{sgn}(k) \cdot \tan(\gamma\pi/2)$  if  $\gamma \neq 1$  and  $(2/\pi) \cdot \ln | k |$  if  $\gamma = 1$ . The corresponding probability distribution is obtained through Fourier inversion of  $C(k)$ :

$$L_\gamma(x) = \frac{1}{2\pi} \int_{\Gamma} C(k) \exp(ikx) dk. \quad (\text{B}\cdot\text{12})$$

The full probability distribution function for the Lévy distribution is known analytically only when  $\gamma = 1$  (Cauchy distribution) and  $\gamma = 2$  (Gaussian distribution). However, both the value of the Lévy distribution at the origin,

$$L_\gamma(x=0) = \frac{\Gamma(1/\gamma)}{\pi\gamma(c)^{1/\gamma}}, \quad (\text{B}\cdot\text{13})$$

and in the tails (for  $\gamma < 2$ )

$$L_\gamma \rightarrow \frac{c\Gamma(1+\gamma) \sin(\pi\gamma/2)}{\pi |x|^{\gamma+1}}, \quad x \rightarrow \infty. \quad (\text{B.14})$$

are known analytically.

The main interest of Lévy functions in the mathematical theory of distributions comes from the fact that they are stable by what we understand that these distributions are invariant under convolution with themselves. This can be readily proven in the Fourier representation, where the convolution transforms into ordinary product (for the simplicity, let us take the symmetric Lévy distribution with  $\beta = 0$ ):

$$\underbrace{L_\gamma(x) * \dots * L_\gamma(x)}_N \rightarrow \prod_{i=1}^N \exp(-c_i |k|^\gamma) = \exp\left(-\sum_{i=1}^N c_i |k|^\gamma\right) = \tilde{L}_\gamma(x). \quad (\text{B.15})$$

This illustrates the fact that if the distribution of a physical property is stable, the statistics of that property will be persistent. Another important property of Lévy distributions, which is reflected in its power-law large- $x$  asymptotic behavior ,

$$L_\gamma(x) \sim \frac{1}{x^{1+\gamma}} \quad (\text{B.16})$$

is the absence of characteristic length scales. In other words, Lévy distributions obeys the scaling law

$$L_\gamma(x; N) = \frac{1}{N^{1/\gamma}} \cdot L_\gamma\left(\frac{x}{N^{1/\gamma}}\right), \quad (\text{B.17})$$

which means that probability  $L_\gamma(x; N)$  for a sum of  $N$  random variables is, up to a certain scale factor, identical to that of the individual variables. This is typical signature of fractal (self-similar) behavior: *The whole looks like its part*. In particular, it can be shown that the set of points visited by this kind of random walk is fractal of dimension  $\gamma$  [131].

One of the most elegant manners of obtaining Lévy-like distribution function is to use maximum entropy formalism. In the traditional frame of Boltzmann-Gibbs statistics, the application of the maximum entropy formalism to fractal random walks would require forcing the jump probability to satisfy rather artificial or unconventional constraints. It seems therefore reasonable to use the Tsallis formalism since this formalism was specially designed to include self-similar systems, which are (multi-)fractals and systems with long-range interactions.

Applying procedure of maximalization of information entropy to the case of Tsallis statistics and imposing the constraint that

$$\langle x^2 \rangle_q = \int_{\Gamma} x^2 [\rho(x)]^q dx, \quad (\text{B.18})$$

we obtain distribution that develops power-law tail depending on the value of the parameter  $q$ :

$$\rho(x) = \frac{1}{Z_q} [1 - (1 - q)\beta \cdot x^2]^{\frac{1}{1-q}}, \quad (\text{B.19})$$

where

$$Z_q = \int_{\Gamma} [1 - (1 - q)\beta \cdot x^2]^{\frac{1}{1-q}} dx. \quad (\text{B.20})$$

It turns out from eq.(B.19) that the normalization of  $\rho(x)$  is guaranteed for  $q < 3$  only. The Tsallis exponent for random walks is therefore restricted to the interval  $q \in (-\infty, 3)$ . For  $-\infty \leq q < 1$  we obtain [24]

$$\rho_q(x) = \beta \left[ \frac{1 - q}{\pi(3 - q)} \right]^{1/2} \frac{\Gamma(\frac{5-3q}{2(1-q)})}{\Gamma(\frac{2-q}{1-q})} \left[ 1 - \frac{1 - q}{3 - q} \beta x^2 \right]^{1/(1-q)}. \quad (\text{B.21})$$

Restricting itself to  $1 < q < 3$  one gets the following distribution

$$\rho_q(x) = \beta \left[ \frac{q - 1}{\pi(3 - q)} \right]^{1/2} \frac{\Gamma(\frac{1}{q-1})}{\Gamma(\frac{3-q}{2(q-1)})} \frac{1}{\left[ 1 + \frac{q-1}{3-q} \beta x^2 \right]^{1/(q-1)}}, \quad (\text{B.22})$$

which in the limit  $|x| \rightarrow \infty$  behaves as

$$\rho_q(x) \propto (x/\sqrt{\beta})^{-2/(q-1)}, \quad (\text{B.23})$$

i.e., it is Lévy distribution with

$$\gamma = \frac{3 - q}{q - 1} \quad (5/3 < q < 3). \quad (\text{B.24})$$

The value of  $q$  fixes then the generalized statistics compatible with the fractal of dimension  $\gamma$ . In order to have a well-defined self-similar structure, this fractal dimension must be smaller than the spatial dimension,  $\gamma < d$ .

The first obvious application of Tsallis statistics useful for us here is extension of eq.(A.14) to  $q \neq 1$  case. Proceeding as in Appendix A but instead of BG entropy

$$S^{(I)} = - \int dy f(y) \ln f(y) \quad (\text{B.25})$$

the Tsallis  $q$ -entropy [24] (which in the limit  $q \rightarrow 1$ , goes into (B.25)),

$$S_q^{(I)} = - \frac{1 - \int dy [f(y)]^q}{1 - q} \quad (\text{B.26})$$

together with the modified energy conservation constraint (A.13)

$$\int dy \mu_T \cosh y [f(y)]^q = \frac{M}{N}, \quad (\text{B.27})$$

one gets instead eq.(A·14) the following distribution:

$$f_q(y) = \frac{1}{Z_q(M, N, \mu_T)} [1 - (1 - q)\beta_q(M, N) \cdot \mu_T \cosh y]^{\frac{1}{1-q}} \quad (\text{B} \cdot 28)$$

In the non-extensive case  $\beta_q(M, N) = 0$ , i.e.,  $f_q(y) = \text{const}$ , for

$$N = (N_q)_0 \simeq 2 \left( \ln \frac{M}{\mu_T} \right)^q = 2 (\ln N_{max})^q. \quad (\text{B} \cdot 29)$$

It means that by varying the value of the parameter  $q$  one is able to find such value of  $q$  for a given  $N = N_q$  for which the Feynmann scaling, i.e., flat rapidity distribution, can be restored. The differences between both approaches (i.e.,  $q = 1$  and  $q \neq 1$ ) is best seen in Fig.B.1.

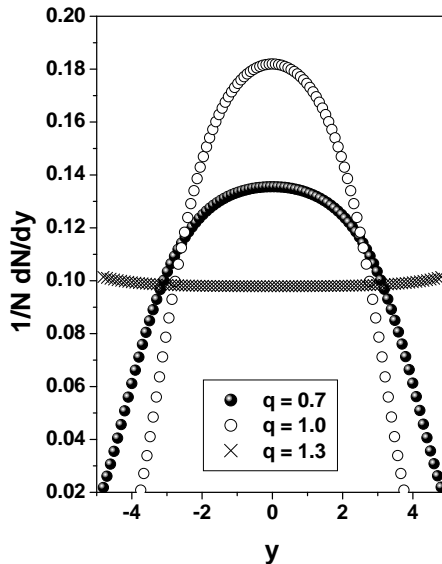


**Fig. B.1.** The examples of the most probable rapidity distributions obtained by extending analysis of (eq.(A·14)) to the nonexponential ( $q \neq 1$ ) distributions given by eq.(B·28)

Another example where Tsallis statistics can be applied is the formula for mean occupation numbers generalizing the Bose-Einstein or Fermi-Dirac ones to a  $q \neq 1$  case. The single particle distribution function can be obtained through the procedure of maximizing the Tsallis entropy outlined before in this section for discrete case under the constraints of keeping constant the average internal energy

$$U_q = \langle E \rangle_q = \sum_m p_m^q E_m, \quad (\text{B} \cdot 30)$$

and the average number of particles

$$N_q = \langle N \rangle_q = \sum_m p_m^q N_m. \quad (\text{B} \cdot 31)$$

For a dilute gas of particles and/or for  $q \approx 1$  values, the average occupational number can be written in a simple analytical form [132]<sup>47</sup>

$$\langle n_i \rangle_q = \frac{1}{[1 - (1 - q)\beta(\epsilon_i - \mu)]^{1/(q-1)} \pm 1}, \quad (\text{B}\cdot\text{32})$$

where the + sign is for fermions, the – for bosons and  $\beta$  is usual Lagrange multiplier. In the limit  $q \rightarrow 1$  (extensive statistics), one recovers the conventional Fermi-Dirac and Bose-Einstein distributions

$$\langle n_i \rangle = \frac{1}{\exp[\beta(\epsilon_i - \mu)] \pm 1}. \quad (\text{B}\cdot\text{33})$$

It is worth to note that Tsallis generalized statistics does not entail a violation of the Pauli exclusion principle and does not modify the inclusive behavior of the bosons, but it modifies the extensive nature of the standard statistics. Moreover, when the entropic  $q$  parameter is smaller than 1, the distributions (B·32) have a natural high-energy cut-off, provided by condition that (cf. also (B·5))

$$1 - (1 - q)\beta(\epsilon_i - \mu) > 0, \quad (\text{B}\cdot\text{34})$$

which implies that the energy tail is depleted; when  $q$  is greater than 1, cut-off is absent and the energy tail of particle distribution is enhanced.

Let us finally recollect also the recent conjecture [49–51] that, in addition to what was already mentioned at the beginning of this Appendix. The non-extensivity (in the sense that parameter  $q \neq 1$  occurs and exponential distributions became power-like) can occur because of fluctuations. In this case  $|1 - q|$  will be a measure of such fluctuations. This conjecture is based on simple fact that according to representation of the Euler gamma function one has for  $q > 1$

$$\left(1 + \frac{x}{\lambda_0} \frac{1}{\alpha}\right)^{-\alpha} = \frac{1}{\Gamma(\alpha)} \int_0^\infty d\eta \eta^{\alpha-1} \exp\left[-\eta \left(1 + \frac{x}{\lambda_0} \frac{1}{\alpha}\right)\right] \quad (\text{B}\cdot\text{35})$$

where  $\alpha = \frac{1}{q-1}$ . Changing now variables to  $\eta = \alpha \left(\frac{\lambda_0}{\lambda}\right)$  one gets from (B·35) that ( $C_q$  is the normalization constant)

$$C_q \left(1 + \frac{x}{\lambda_0} \frac{1}{\alpha}\right)^{-\alpha} = C_q \int_0^\infty d\left(\frac{1}{\lambda}\right) f\left(\frac{1}{\lambda}\right) e^{-x/\lambda}, \quad (\text{B}\cdot\text{36})$$

where ( $\mu = \alpha \lambda_0$ )

$$f\left(\frac{1}{\lambda}\right) = \frac{\mu}{\Gamma(\alpha)} \left(\frac{\mu}{\lambda}\right)^{\alpha-1} e^{-\frac{\mu}{\lambda}}. \quad (\text{B}\cdot\text{37})$$

---

<sup>47</sup>Another kind of the generalized mean occupation number derivation was recently proposed by C.Bech in [133].

It is our basic formula used in eqs.(III·1) and (III·22). Notice that

$$\left\langle \frac{1}{\lambda} \right\rangle \quad \text{and} \quad \left\langle \left( \frac{1}{\lambda} \right)^2 \right\rangle - \left\langle \frac{1}{\lambda} \right\rangle^2 = \frac{1}{\alpha \lambda_0^2}, \quad (\text{B} \cdot 38)$$

what leads to normalized variance

$$\omega = \frac{\left\langle \left( \frac{1}{\lambda} \right)^2 \right\rangle - \left\langle \frac{1}{\lambda} \right\rangle^2}{\left\langle \frac{1}{\lambda} \right\rangle^2} = \frac{1}{\alpha} = q - 1. \quad (\text{B} \cdot 39)$$

For the case of  $q < 1$  one has account for the fact that now  $x \in [0, \frac{\lambda_0}{1-q}]$  only. In this case the corresponding representation of the Euler gamma function is (now  $\alpha' = -\alpha = \frac{1}{1-q}$ )

$$\left( 1 - \frac{x}{\lambda_0} \frac{1}{\alpha'} \right)^{-\alpha'} = \frac{1}{\Gamma(\alpha')} \int_0^\infty d\eta \eta^{\alpha'-1} \exp \left[ -\eta \left( 1 + \frac{x}{\lambda_0 \alpha' - x} \right) \right]. \quad (\text{B} \cdot 40)$$

Changing now variables to  $\eta = \frac{\lambda_0 \alpha' - x}{\lambda}$  one gets again eq.(B·35) but  $\alpha \rightarrow \alpha'$  and with  $f_{q<1}(\frac{1}{\lambda})$  given by eq.(B·37) but with  $\alpha \rightarrow \alpha'$  and  $\mu \rightarrow \mu(x) = \lambda_0 \alpha' - x$ . Although in this case fluctuations depend on the variable in question, i.e.,

$$\left\langle \frac{1}{\lambda} \right\rangle = \frac{1}{\lambda_0 - \frac{x}{\alpha'}} \quad \text{and} \quad \left\langle \left( \frac{1}{\lambda} \right)^2 \right\rangle - \left\langle \frac{1}{\lambda} \right\rangle^2 = \frac{1}{\alpha'} \frac{1}{\left( \lambda_0 - \frac{x}{\alpha'} \right)^2}. \quad (\text{B} \cdot 41)$$

The relative variance is independent on  $x$  and again given only by  $q$ :

$$\omega = \frac{1}{\alpha'} = 1 - q. \quad (\text{B} \cdot 42)$$

In examples discussed in Chapter III both  $q < 1$  and  $q > 1$  cases are considered<sup>48</sup>.

There is, in addition to what was explicitly presented in Chapter III and explicitly discussed above, already a number of known applications of Tsallis statistics to multiparticle physics [50]. It is worth to mention that they are all rather recent (what means that this field of research is still in its infancy). We shall list them here shortly for completeness:

<sup>48</sup>It is probably a right place to mention here very interesting observation concerning the possible role of fluctuations in high energy production processes. Namely, in [134] it was shown that gaussian fluctuations introduced to Schwinger formula for particle creation from vacuum, which is the basis of all string models of hadronization, changes the original gaussian shape of distributions in transverse mass variable (not observed experimentally) into exponential one (observer in experiment). The resulting inverse slope of this exponential distribution, which is expected to be the measure of "temperature"  $T$  of reaction,

$$T = \sqrt{\frac{\langle \kappa^2 \rangle}{2\pi}}, \quad (\text{B} \cdot 43)$$

is given by parameter  $\langle \kappa^2 \rangle$ , which characterizes width of gaussian fluctuations imposed on the string tension parameter  $\kappa$  (i.e., on the amount of vacuum energy stored in length of 1 fm).

- In [135] non-extensive statistics has been used to explain the phenomenon of *long-flying component* observed in some cosmic rays experiments.
- In [85] an interesting attempt was presented to fit the energy spectra in both the longitudinal and transverse momenta of particles produced in the  $e^+e^-$  annihilation processes at high energies using  $q$ -statistical model. In this way, one has energy independent temperature  $T \sim 110\text{MeV}$  and non-extensivity parameter  $q$  rising with energy from  $q = 1.1$  to  $q = 1.2$  and reflecting long range correlations in the phase space arising in the hadronization process in which quarks and gluons combine together forming hadrons. In similar way in [133] the possible generalization of the so-called Hagedorn model of multiparticle production [136] to  $q$ -statistics was presented.
- In [137] the nuclear multifragmentation was discussed in the canonical formalism of the non-extensive statistics.
- The non-extensivity in hadronic quantum scattering systems has been extensively investigated in [138].
- In [139] the widely known phenomenon of the non-exponential decays has been linked to the possible fluctuations in the system and to resulting from it non-extensivity.
- Ref. [140] provides analysis of the equilibrium distribution of heavy quarks in Fokker-Planck dynamics. It was demonstrated that thermalization of charmed quarks in QGP, proceeding via collisions with light quarks and gluons, results in a spectral shape, which can be described only by the Tsallis distribution with  $q = 1.114$  and  $T = 135\text{ MeV}$ .
- To the extend to which self-organized criticality (SOC) is connected with non-extensivity [24] one should also mention here a very innovative (from the point of view of high energy collisions) application of the concept of SOC to such processes [141]. Similar SOC behaviour of cascade processes encountered in cosmic ray experiments have been also analyzed from the  $q$ -statistics point of view in [142]. In [143] it was demonstrated that the some concept can be also used to explain results of [141].
- To the extent to which deformation parameter of quantum groups is connected with the non-extensivity parameter of Tsallis statistics [144] one should mention here the recently proposed [145] use of quantum groups to describe Bose-Einstein correlations.
- The works on intermittency using properties of the so called Lévy stable distributions (for example [146]) should be also listed here.

### C. Some basic notions on Bose-Einstein correlations

The study of Bose-Einstein correlations (BEC) has already long history [101,147] (cf. also [17]). It is best illustrated by experimental fact (cf. for example, [95,110,111] and reference therein) that particles of the same charge (mostly pions), which are produced in high energy reactions are bunched in momentum space, as seen in Fig.C.1 showing, as an illustration, results from OPAL experiment at LEP [148]. We shall collect here some introductory concepts and formulas concerning BEC used in this work. These correlations are consequence of quantum mechanical interference of the second kind in the corresponding symmetrical  $n$ -particle wave function. They contain a large amount of information about statistical properties of the momentum- *and* configuration space distribution of the system, and thus can be used (at least in principle) to reconstruct the geometry of the source producing hadrons [149]. In contrast to the situation found in astronomy, where Hanbury Brown and Twiss first measured the radii of stars by analyzing the correlation functions of photons [101], the correlation function measurements in heavy ion collisions are substantially complicated by

- the time-dependence and short life-time of the particle emitting source,
- the position-momentum correlations in the source resulting from the strong dynamical expansion of the collision region,
- other dynamical origin of particle momentum correlations (i.e., effects of resonances and final state interaction including Coulomb interactions).

They have to be subtracted properly to make a space-time interpretation of the measured correlation data possible.

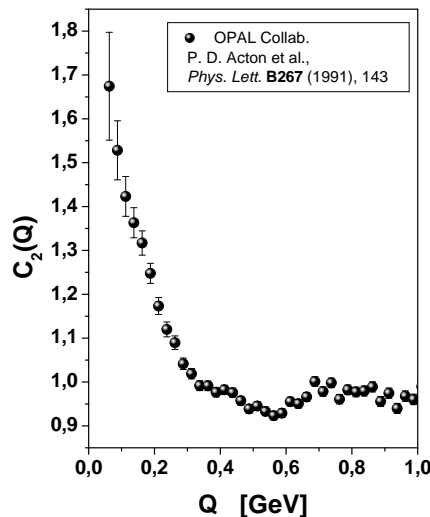


**Fig. C.1.** Examples of Bose-Einstein correlations between  $\pi$  in the reaction of  $e^+e^-$  annihilation observed in experiment OPAL [148] ( $Q = |p_1 - p_2|$ ).

We shall recollect now, for the purpose of our dissertation only, some aspects of the classical picture of BEC in multiparticle processes (for the case of 2-particle correlations only). Let us first consider production and detection of one single particle, cf. Fig.C.2. Suppose it is produced at point  $X$  and detected at point  $x$ . The amplitude  $A$  for its is in the plane wave approximation, given by production amplitude  $g(p, X)$  and by phase  $\phi(X)$ :

$$A = g(p, X) \cdot \exp(ip(X - x)) \cdot \exp(i\phi(X)). \quad (\text{C.1})$$

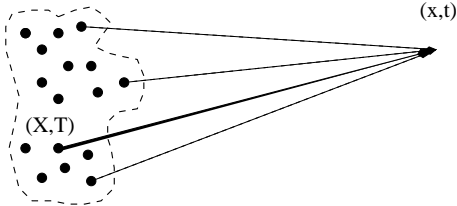


**Fig. C.2.**

Consider now the case when production points  $X$  of the detected particle are distributed according to some distribution function  $\rho(x)$ . The total amplitude of detected wavefunction is now expressed by

$$\Psi(p, x) = \int dX \rho(X) \cdot g(p, X) \cdot \exp(i\phi(X)) \cdot \exp(ip(X - x)). \quad (\text{C.2})$$

Therefore corresponding probability of detecting such single particle at point  $x$  is expressed in terms of single-particle distribution function  $P(p)$  defined as the square of total probability amplitude

$$P(p) \equiv | \Psi(p, x) |^2 = \int dX \rho(X) \cdot | g(p, X) |^2. \quad (\text{C.3})$$

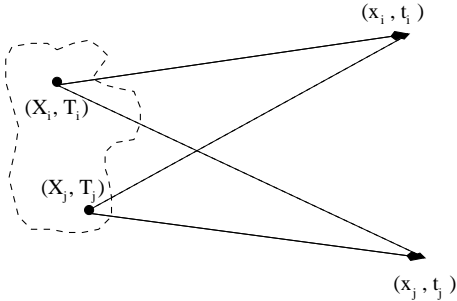


**Fig. C.3.**

In similar way one derives two-particle probability function, cf. Fig.C.3. Assuming that particles are identical pions originating from the production points  $X_i$  and  $X_j$ , the usual

for bosons symmetrization of the corresponding two-particle amplitude results in the following two-particle amplitude:

$$\Psi_{ij}(x_i, x_j) = \frac{1}{\sqrt{2}} \{ \Psi(p_i, x_i) \cdot \Psi(p_j, x_j) + \Psi(p_j, x_i) \cdot \Psi(p_i, x_j) \}. \quad (\text{C.4})$$

The measurement of two pions emerging from a *chaotic*<sup>49</sup> source leads to summation over all possible production points. Using density distribution and relation derived for the single-particle probability (i.e., assuming factorization of the two particle density into product of single particle ones) the corresponding two-particle probability function  $P(p_i, p_j)$  is given by

$$P(p_i, p_j) = P(p_i) \cdot P(p_j) + \\ | \int dX \rho(X) \cdot [g(p_i, X)]^* \cdot g(p_j, X) \cdot \exp(i(p_i - p_j)X) |^2. \quad (\text{C.5})$$

We can now define the following two-particle correlation function<sup>50</sup>

$$C_2(p_i, p_j) \equiv \frac{P(p_i, p_j)}{P(p_i) \cdot P(p_j)} \quad (\text{C.6})$$

given in terms of ratio of the corresponding two- and single particle probabilities. Introducing the notion of the effective source density function  $\rho_{eff}(X)$  defined by

$$\rho_{eff}(X) = \rho(X) \cdot \frac{g(p_i, X) \cdot g(p_j, X)}{\sqrt{P(p_i)} \cdot \sqrt{P(p_j)}} \quad (\text{C.7})$$

eq.(C.6) can be rewritten as

$$C_2(p_i, p_j) = 1 + | \int dX \rho_{eff}(X) \cdot \exp(i \cdot q \cdot X) |^2 = 1 + | \tilde{\rho}_{eff}(q) |^2, \quad (\text{C.8})$$

where  $\tilde{\rho}_{eff}(q)$  is the Fourier transform of the effective source density distribution  $\rho(X)$  and  $q = |p_i - p_j|$  is the relative momentum difference.

The emitting source will be now characterized by its density distribution  $\rho(x)$ , for which different choices can be made. The most popular is the Gaussian one<sup>51</sup>

$$\rho(X) \sim e^{-X^2/R^2}. \quad (\text{C.9})$$

<sup>49</sup>The word *chaotic* means that for such source  $\int dX e^{i \cdot \phi(X)} = 0$ .

<sup>50</sup>More general expression for the correlation function  $C_2(q)$  can be written in the following form  $C_2(p_i, p_j) \equiv \mathcal{N} \cdot \frac{P(p_i, p_j)}{P(p_i) \cdot P(p_j)}$ , where  $\mathcal{N}$  is the normalization coefficient, which can be taken as either  $\mathcal{N} = 1$  or  $\mathcal{N} = \frac{\langle N \rangle^2}{\langle N(N-1) \rangle}$ .

<sup>51</sup>For the whole list of possible analytical form of distribution  $\rho(x)$  see, for example, [56] (cf. also [149]).

The correlation function can be rewritten in this case as

$$C_2(p_i, p_j) \sim 1 + e^{-q^2 \cdot R^2}. \quad (\text{C.10})$$

In the experiment  $C_2(q)$  is usually determined by dividing the differential cross section for pairs of like-charge pions by that for the pairs in the *reference sample*, which should be free of Bose-Einstein correlations

$$C_2(q) = \frac{N_{\text{pairs}}^{++,--}(q)}{N_{\text{pairs}}^{\text{ref}}(q)}, \quad (\text{C.11})$$

where  $N_{\text{pairs}}^{\text{ref}}(q)$  is number of pairs in the reference sample. One such reference sample consists of pairs of unlike-charged pions. Another method of obtaining a reference sample uses the technique of event mixing. Usually the normalization to the analogous Monte Carlo function without BEC is performed as well.

## References

- [1] E.Shuryak, *Phys. Rep.* **61** (1980) 71.
- [2] Cf., for example, H.Satz, *Ann. Rev. Nucl. Part. Sci.* **35** (1985) 245 and *Color Deconfinement in Nuclear Collisions*, hep-ph/0007069, to appear in *Rep. Prog. Phys.* (2001), and references therein.
- [3] Cf. any of the *Quark Matter* series of proceedings, for example, *QM'97 Nucl. Phys.* **A638** (1998), *QM'99, Nucl. Phys.* **A661** (1999) or the recent *QM'01, Nucl. Phys.* **A** (2001), in press.
- [4] E.Laermann, *Nucl. Phys.* **A610** (1996) 1c.
- [5] A.Capella, A.Kaidalov and J.Tran Thanh Van, *Heavy Ion Phys.* **9** (1999) 169 (hep-ph/9903244); A. Capella et al., *Phys. Rep.* **236** (1994) 225.
- [6] K.Werner, *Phys. Rep.* **232** (1993) 87.
- [7] N.S.Amelin, M.A.Braun and C.Pajares, *Phys. Lett.* **B306** (1993) 312; *Z. Phys.* **C63** (1994) 507
- [8] K.Geiger and B.Müller, *Nucl. Phys.* **B369** (1992) 600;  
K.Geiger, *Phys. Rep.* **258** (1995) 237.
- [9] B.Andersson et al., *Phys. Rep.* **97** (1987) 31,  
B.Andersson, G.Gustafson and B.Nilson-Almquist, *Nucl. Phys.* **B281** (1987) 289,  
T.Sjöstrand and M.van Zijl, *Phys. Rev.* **D36** (1987) 2019; T.Sjöstrand, *Comp. Phys. Comm.* **1994** 74.
- [10] H.Sorge, H.Stöcker, and W.Greiner, *Ann. Phys.* **192** (1989) 266.
- [11] L.Lönnblad and T.Sjöstrand, *Phys. Lett.* **B351** (1995) 293.
- [12] K.Werner, *Tools for RHIC: Review of Models*, *J. Phys.* **G27** (2001) 625 and references therein.
- [13] D.E.Kahama and S.H.Kahama, *Phys. Rev.* **C58** (1998) 3574; *Phys. Rev.* **C59** (1999) 1651.
- [14] H.Müller, *Eur. Phys. J.* **C18** (2001) 563.
- [15] R.C.Hwa and Y.Wu, *Phys. Rev.* **D60** (1999) 097501;  
Zhen Cao and R.C.Hwa, *Phys. Rev.* **D59** (1999) 114023.

- [16] K.J.Escola, *On predictions of the first results from RHIC*, plenary talk at QM2001, *Nucl. Phys.* **A698** (2001) 78;  
Cf. also S.A.Bass et al., *Prog. Part. Nucl. Phys.* **41** (1998) 225.
- [17] Cf. for example, the most recent reviews and references therein: R.Weiner, *Bose-Einstein Correlations in Particle and Nuclear Physics.*, A Collection of Reprints, John Wiley&Sons, 1997; *Phys. Rep.* **327** (2000) 249 and *Introduction to Bose-Einstein Correlations and Subatomic Interferometry*, John Wiley&Sons, 2000;  
U.A.Wiedemann and U.Heinz, *Phys. Rep.* **319** (1999) 145;  
T.Csörgő, in *Particle Production Spanning MeV and TeV Energies*, eds. W.Kittel et al., NATO Science Series C, vol. 554, Kluwer Acad. Pub. (2000), p.203;  
G.Baym, *Acta Phys. Pol.* **B29** (1998) 1839.
- [18] A.Białas, *Acta Phys. Pol.* **B23** (1992) 561 and *Nucl. Phys.* **A545** (1992) 285c;  
cf. also in *Proc. of the XXVII Int. Conf. on High Energy Phys.*, Glasgow, UK, 1994, ed.P.J.Bursey et al., Bristol, UK 1994, Vol.III, p. 128.  
For the most recent summary of the problem, see A.Białas, in *Proc. of the XXVII ISMD*, Delphi, Greece, 1998 (hep-ph/9812457) and references therein.
- [19] J.Pišút, N.Pišútová and B.Tomášik, *Acta Phys. Slov.* **46** (1996) 517 and  
*Phys. Lett.* **B368** (1996) 179.
- [20] O.V.Utyuzh, G.Wilk and Z.Włodarczyk, *Phys. Rev.* **D61** (2000) 034007 and *Czech J. Phys.* **50/S2** (2000) 132 (hep-ph/9910355).
- [21] J.P.Sullivan et al., *Phys. Rev. Lett.* **70** (1993) 3000.
- [22] K.Geiger, J.Ellis, U.Heinz and U.A.Wiedemann, *Phys. Rev.* **D61** (2000) 054002.
- [23] O.V.Utyuzh, G.Wilk and Z.Włodarczyk, *Bose-Einstein correlations in cascade processes and non-extensive statistics.*, hep-ph/0101161, Proc. of the XXXth ISMD, Tihany, October 9-15, 2000, Hungary, eds. T.Csörgő et al., World Scientific (2001), pp.373-378 and *Numerical modeling of correlations*, presented at XXXIth ISMD, Datong, 1-7 September 2001, to be published in proceedings (e-Conf Proceedings and WS). See also *Numerical modeling of Bose-Einstein correlations*, hep-ph/0110353, accepted in *Phys. Lett.* **B**.
- [24] C.Tsallis, *J. Stat. Phys.* **52** (1988) 479.  
For updated bibliography on this subject cf. <http://tsallis.cat.cbpf.br/biblio.htm>. Recent summary is provided in the special issue of *Braz. J. Phys.* **29** (No 1) (1999) (available also at [http://sbf.if.usp.br/WWW\\_pages/Journals/BJP/Vol29/Num1/index.thm](http://sbf.if.usp.br/WWW_pages/Journals/BJP/Vol29/Num1/index.thm)). Cf. also: *Non-extensive Statistical Mechanics and Its Applications*, Eds. S.Abe and Y.Okamoto, LPN560, Springer 2001.
- [25] F.S.Navarra, O.V.Utyuzh, G.Wilk and Z. Włodarczyk, "Violation of the Feynmann scaling law as a manifestation of non-extensivity", hep-ph/0009165, to be published in *Nuovo Cim.* **C24** (2001), July-September issue.
- [26] O.V.Utyuzh, G.Wilk and Z.Włodarczyk, *J. Phys.* **G26** (2000) L39.

- [27] O.V.Utyuzh, G.Wilk and Z.Włodarczyk, *How to observe fluctuating temperature?*, hep-ph/0103273.
- [28] E.A.De Wolf, I.M.Dremin and W.Kittel, *Phys. Rep.* **270** (1996) 1;  
P.Bożek, M.Płoszajczak and Botet, *Phys. Rep.* **252** (1995) 101;  
I.V.Andreev, I.M.Dremin,M.Biyajima and N.Suzuki, *Int. J. Mod. Phys.* **A10** (1995) 3951.
- [29] P.Carruthers, E.M.Friedlander, C.C.Shin and R.M.Weiner, *Phys. Lett.* **B222** (1989) 487.
- [30] G.Wilk and Z.Włodarczyk, *Phys. Rev.* **D43** (1991) 794.
- [31] B.Ziaja, *Z. Phys.* **C71** (1996) 639;  
A.Bialas and B.Ziaja, *Acta Phys. Pol.* **B24** (1993) 1509.
- [32] I.Sarcevic and H.Satz, *Phys. Lett.* **B233** (1989) 251.
- [33] B.Iványi, Zs.Schram, K.Sailer and W.Greiner, *Heavy Ion Phys.* **3** (1996) 5.
- [34] Z.Cao and R.C.Hwa, *Phys. Rev. Lett.* **75** (1995) 1268; *Phys. Rev.* **D53** (1996) 6608; **D54** (1996) 6674;  
See also R.C.Hwa and Y.Wu, *Phys. Rev.* **C60** (1999) 054904, and references therein;  
M.V.Tokarev et al., *Int. J. Mod. Phys.* **A16** (2001) 1281 and references therein.
- [35] I.Zborovsky, *Z-scaling, fractality, and principles of relativity in the interactions of hadrons and nuclei at high energies*. hep-ph/0101018 or I.Zborovsky et al., *Z-scaling, fractality, and principles of relativity in the interactions of hadrons and nuclei at high energies*, JINR preprint E2-2001-14, presented at QM2001, Jan. 15-21, 2001, StonyBrook, USA.
- [36] I.M.Dremin and B.B.Levchenko, *Phys. Lett.* **B292** (1992) 155.
- [37] A.Białas and K.Zalewski, *Phys. Lett.* **B238** (1990) 413;  
A.Białas, A.Szczerba and K.Zalewski, *Z. Phys.* **C46** (1990) 163;  
J.M.Alberty and A.Białas, *Z. Phys.* **C50** (1991) 315;  
A.Białas and J.Czyżewski, *Phys. Lett.* **B463** (1999) 303.
- [38] P.Carruthers, *Int. J. Mod. Phys.* **A4** (1989) 5589.
- [39] J.M.Dremin, *Pisma Zh. Eksp. Teor. Fiz.* **45** (1987) 505 [*JETP Lett.* **45** (1987) 643].
- [40] L.D.Landau and Bilenkij, *Nuovo. Cimento Suppl.* **3** (1956) 15; R.B.Clare and D.Strottmann, *Phys. Rep.* **141** (1986) 177; E.V.Shuryak, *Jad. Fiz.* **16** (1972) 395. For the most recent applications of such approach see F.Becattini and G.Passaleva, *Statistical hadronization model and transverse momentum spectra of hadrons in high energy collisions*, hep-ph/0110312 and K.Redlich et al., *Conservation laws and particle production in heavy ion collisions*, hep-ph/0110337 and references therein.
- [41] M.Chaichan and H.Satz, *Phys. Lett.* **B50** (1974) 362.
- [42] F.Grassi, Y.Hama, S.S.Padula and O.Socolowski, *Phys. Rev.* **C62** (2000) 044904.

- [43] T.Kanki, K.Kinoshita, H.Sumiyoshi and F.Takagi, *Prog. Theor. Phys.* **97** (Suppl. A) (1988) 1.
- [44] W. Braunschweig et al., (TASSO Collab.), *Z. Phys.* **C45** (1989) 193;  
P.Abreu et al., (DELPHI Collab.), *Z. Phys.* **C52** (1991) 271.
- [45] A.Wróblewski, *Acta Phys. Pol.* **B4** (1973) 857.
- [46] Z.Koba, H.B.Nielsen and P.Olesen, *Nucl. Phys.* **B40** (1972) 317.
- [47] S.Hegyi, *Nucl. Phys.* **B92** (Proc. Suppl.) (2001) 122 and references therein.
- [48] J.Masarik, A.Nogová, J.Pišút, and N.Pišútová, *Z. Phys.* **C75** (1997) 95; *Acta Phys. Slov.* **47** (1997) 63. See also M.Šíket, J.Masarik, A.Nogová, J.Pišút, and N.Pišútová, *ibid.* **48** (1998) 563.
- [49] G.Wilk and Z.Włodarczyk, *Phys. Rev. Lett.* **89** (2000) 2770.
- [50] G.Wilk and Z.Włodarczyk, *Chaos, Solutions and Fractals* **13** (2002) 581 (hep-ph/0004250) and *Imprints of non-extensivity in multiparticle production*, to be published in the Proc. of 6<sup>th</sup> Int. Workshop on Rel. Aspects of Nucl. Phys. (RAPN2001), Caraguatuba, Tabatinga Beach, São Paulo, Brazil, October 17-20, 2000, World Scientific (2001), in press (hep-ph/0011189).
- [51] C.Beck, *Non-additivity of Tsallis entropies and fluctuations*, cond-mat/0105371 and *Dynamical foundations of non-extensive statistical mechanics*, cond-mat/0105374; Cf. also L.S.F.Olavo, *Phys. Rev.* **E64** (2001) 036125.
- [52] W.Ochs, *Z. Phys.* **C15** (1982) 227 and **C29** (1984) 131.
- [53] B.Dubrulle and J.-Ph. Laval, *Eur. Phys. J.* **B4** (1998) 143.
- [54] A.Bialas and R.Peschanski, *Nucl. Phys.* **B273** (1986) 703; **B306** (1988) 857.
- [55] T.Osada, M.Maruyama and F.Takagi, *Phys. Rev.* **D59** (1999) 014024.
- [56] R.Shimoda, M.Biyajima and N.Suzuki, *Prog. Theor. Phys.* **89** (1993) 697;  
T.Mizoguchi, M.Biyajima and T.Kagea, *ibid.* (1994) 905.
- [57] H.Paul, *Rev. Mod. Phys.* **54** (1982) 1061;  
M.C.Teich and B.E.A.Saleh, *Prog. in Optics* **26**, edited by E.Wolf (North-Holland, Amsterdam, 1988), ch. 1, pp. 1-104.
- [58] F.Becattini and U.Heinz, *Z. Phys.* **C76** (1997) 269; F.Becattini, *Z. Phys.* **C69** (1996) 485.
- [59] W.M.Alberico, A.Lavango and P.Quarati, *Eur. J. Phys.* **C12** (2000) 499.
- [60] S.Gavin, *Nucl. Phys.* **B351** (1991) 561;  
H.Heiselberg and X.N.Wang, *Phys. Rev.* **C53** (1996) 1892;  
T.S.Biró and C.Greiner, *Phys. Rev. Lett.* **79** (1997) 3138;  
J.Rau, *Phys. Rev.* **D50** (1994) 6911;

- S.Schmidt et al., *Int, J. Mod. Phys.* **E7** (1998) 709 and *Phys. Rev.* **D59** (1999) 094005;  
Cs. Anderlik et al., *Phys. Rev.* **C59** (1999) 388 and 3309;  
V.K. Magas et al., *Phys. Lett.* **459** (1999) 33;  
J.Hormuzdiar et al., *Particle Multiplicities and Thermalization in High Energy Collisions*, nucl-th/0001044; cf. also [40].
- [61] R.P.Feynman, *Phys. Rev. Lett.* **23** (1969) 1414.
- [62] A.Ohsawa, *Prog. Theor. Phys.* **92** (1994) 1005. For most recent analysis of this type see A.Ohsawa, E.H.Shibuya and M.Tamada, *Phys. Rev* **D64** (2001) 054004.
- [63] J.Wdowczyk and A.W.Wolfendale, *J. Phys. G* **10** (1984) 257; and *J. Phys. G* **13** (1987) 411.
- [64] R.M.Baltrusaitis et al., (UA5 Collab.) *Phys. Rev. Lett.* **52** (1993) 1380.
- [65] R.Harr et al., (P238 Collab.) *Phys. Lett.* **B401** (1997) 176.
- [66] E.Pare et al., (UA7 Collab.) *Phys. Lett.* **B242** (1990) 531.
- [67] L.A.Anchrdoqui, M.T.Dova, L.N.Epele and S.J.Sciuto, *Phys. Rev.* **D59** (1999) 094003 and references therein.
- [68] Z.Włodarczyk, *J. Phys. G* **21** (1995) 281;  
cf. also: F.O.Durães, F.S.Navarra and G.Wilk, *Phys. Rev.* **D50** (1994) 6804.
- [69] Cf., for example, S.Hegyi, *Phys. Lett.* **B466** (1999) 380; and *Phys. Lett.* **B467** (1999) 126.
- [70] L.Stodolsky, *Phys. Rev. Lett.* **75** (1995) 1044;  
S.Mrówczyński, *Phys. Lett.* **B430** (1998) 9;  
E.V.Shuryak, *Phys. Lett.* **B423** (1998) 9.
- [71] M.Stephanov, K.Rajagopal and E.Shuryak, *Phys. Rev. Lett.* **81** (1998) 4816; *Phys. Rev.* **D60** (1999) 114028.
- [72] M.Gaździcki and S.Mrówczyński, *Z.Phys.* **C54** (1992) 127.
- [73] G.Odyniec, *Acta Phys. Polon.* **B30** (1999) 385;  
K.Fiałkowski and R.Wit, *Acta Phys. Pol.* **B30** (1999) 2759 (hep-ph/9905270);  
S.A.Voloshin, V.Koch and H.G.Ritter, *Event-by-event fluctuations in collective quantities*, LBNL-42992A (March 1999) preprint, nucl-th/9903060;  
G.Baym and H.Heiselberg, *Phys. Lett.* **B469** (1999) 11;  
R.Korus and S.Mrówczyński, *Phys. Rev.* **C64** (2001) 054906.
- [74] O.Utyuzh, G.Wilk and Z.Włodarczyk, *Phys. Rev.* **C64** (2001) 027901.
- [75] M.Gaździcki, *Eur. Phys. J.* **C8** (1999) 131.
- [76] S.V.Afanasiev et al. (NA49 Collab.), *Phys. Rev. Lett.* **86** (2001) 1965.
- [77] S.Mrówczyński, *Phys. Lett.* **B459** (1999) 13.

- [78] R.Korus, S.Mrówczyński, M.Rybczyński, and Z.Włodarczyk, *Phys. Rev.* **C64** (2001) 054908.
- [79] F.Büyükkiliç, D.Demirhan and A.Güleç, *Phys. Lett.* **A197** (1995) 209; U.Tirnakli, F.Büyükkiliç, D.Demirhan, *Physica* **A240** (1997) 657.
- [80] T.Alber et al. (NA35 Collab.), *Eur. Phys. J.* **C2** (1998) 643.
- [81] S.Mrówczyński, *Phys. Rev.* **C57** (1998) 1518.
- [82] T.C.P.Chui, D.R.Swanson, M.J.Adriaans, J.A.Nissen and J.A.Lipa, *Phys. Rev. Lett.* **69** (1992) 3005;  
C.Kittel, *Physics Today* **5** (1988) 93; B.B.Mandelbrot, *Physics Today* **1** (1989) 71;  
L.D.Landau, I.M.Lifschitz, *Course of Theoretical Physics: Statistical Physics*, Pergmon Press, New York 1958;  
H.B.Prosper, *Am. J. Phys.* **61** (1993) 54;  
G.D.J.Phillies, *Am. J. Phys.* **52** (1984) 629.
- [83] K.Kadaja and M.Martinis, *Z. Phys.* **C56** (1992) 437.
- [84] M.Gaździcki and M.I.Gorenstein, *Phys. Lett.* **B517** (2001) 250.
- [85] I.Bediaga, E.M.F.Curado and J.M.de Miranda, *Physica* **A286** (2000) 156.
- [86] L.Lönnblad and T.Sjöstrand, *Eur. Phys. J.* **C2** (1998) 165.
- [87] A.Białas and A.Krzywicki, *Phys. Lett.* **B354** (1995) 134;  
cf. also: H.Merlitz and D.Pelte, *Z. Phys.* **A351** (1995) 187 and *Z. Phys.* **A357** (1997) 175;  
U.A.Wiedemann et al., *Phys. Rev.* **C56** (1997) R614; T.Csörgő and J.Zimányi, *Phys. Rev. Lett.* **80** (1998) 916 and *Heavy Ion Phys.* **9** (1999) 241.
- [88] K.Fiałkowski and R.Wit, *Eur. Phys. J.* **C2** (1998) 691 and **C13** (2000) 133.
- [89] K.Fiałkowski and R.Wit, *Z. Phys.* **C74** (1997) 145.
- [90] K.Fiałkowski, R. Wit and J.Wosiek, *Phys. Rev.* **D57** (1998) 094013.
- [91] T.Wibig, *Phys. Rev.* **D53** (1996) 3586.
- [92] B.Andersson and M.Ringnér, *Nucl. Phys.* **B513** (1998) 627 and *Phys. Lett.* **B241** (1998) 288;  
B.Andersson and W.Hofmann, *Phys. Lett.* **169B** (1986) 364;  
B.Andersson, *Acta Phys. Pol.* **B29** (1998) 1885.
- [93] K.Binder, *Monte-Carlo Meth. in Stat. Phys.*, Springer-Verlag (Berlin, Heidelberg, New York) 1979;  
N.Metropolis et al., *J. Chem. Phys.* **21** (1953) 1087;  
H.Gould and J.Tobochnik, *Computer Simulation Methods*, part 2, Addison-Wealey, New York 1988.

- [94] W.Zajc, *Phys. Rev.* **D35** (1987) 3396;  
R.L.Ray, *Phys. Rev.* **C57** (1998) 2532;  
J.G.Cramer, "Event Simulation of High-Order Bose-Einstein and Coulomb Correlations", University of Washington preprint (1996), unpublished.
- [95] B.Buschbeck and N.Neumeister (UA1-Minimum-Bias Collab.) in: XXII Intern. Symp. om Multiparticle Dynamics, ed. C.Pajares (World Scientific, Singapore, 1993) p. 246;  
UA1-MINIMUM BIAS-Collaboration, *Z. Phys.* **C60** (1993) 633.
- [96] I.V.Andreev, M.Plümer, B.R.Schlei and R.M.Weiner, *Phys. Lett.* **B321** (1994) 277.
- [97] K.Zalewski, *Acta Phys. Pol.* **B28** (1997) 1131;  
J.Wosiek, *Phys. Lett.* **B399** (1997) 130.
- [98] T.A.Trainor, *Nucl. Phys. (Proc. Suppl.)* **B92** (2001) 16.
- [99] M.Biyajima, N.Suzuki, G.Wilk and Z.Włodarczyk, *Phys. Lett.* **B386** (1996) 297.
- [100] W.J.Knox, *Phys. Rev.* **D10** (1974) 65;  
E.H.De Groot and H.Satz, *Nucl. Phys.* **B130** (1977) 257;  
J.Kriptganz, *Acta Phys. Polon.* **B8** (1977) 945;  
A.M.Cooper, O.Miyamuro, A.Suzuki and K.Takakeshi, *Phys. Lett.* **B87** (1979) 393;  
F.Takagi, *Prog. Theor. Phys. Suppl.* **120** (1995) 201.
- [101] R.Hanbury Brown and R.Q.Twiss, *Proc. Roy. Soc. (London)* **A243** (1957) 291.
- [102] K.Fiałkowski, in Proc. of the XXX ISDM, Tihany, Hungary, 9-13 October 2000, Eds., T.Csörgő et al, Wordl Scientific 2001, p.357.
- [103] M.Stepanov, *Thermal fluctuations in the interacting pion gas*, hep-ph/0110077.
- [104] Cf. for example, R.Ramanathan, *Phys. Rev.* **D45** (1992) 4706;  
S.Chaturvedi, *Phys. Rev.* **E54** (1996) 1378;  
S.Chaturvedi and V.Srinivasan, *Physica* **A246** (1997) 576;  
G.Kaniadakis, A.Lavango and P.Quarati, *Mod. Phys. Lett.* **B10** (1996) 497 and references therein.
- [105] B.Buschbeck and H.C.Eggers, *Nucl. Phys. B (Proc. Suppl.)* **92** (2001) 235.
- [106] T.Csörgő, *Nucl. Phys.* **B92** (Proc. Suppl.) (2001) 223.
- [107] G.Alexander and E.K.G.Sarkasisyan, *Nucl. Phys.* **B92** (Proc. Suppl.) (2001) 211, and *Phys. Lett.* **B487** (2000) 215.
- [108] R.Hwa and J.C.Pan, *Phys. Rev.* **D45** (1992) 106.
- [109] J.Dias de Deus, *Phys. Lett.* **194** (1987) 297.
- [110] P. Abreu et al., (DELPHI Collab.) *Phys. Lett.* **B286** (1992) 201.
- [111] P.Abreu et al., (DELPHI Collab.) *Phys. Lett.* **B247** (1990) 137.

- [112] Cf. Š. Todorova-Nová, "Inter-W Bose-Einstein correlation ... or not?", hep-exp/0101057; (Also in Proc. on the XXXth ISMD, Tihany, October 9-15, 2000, Hungary, eds. T.Csörgő et al., World Scientific (2001), p. 343) and *Acta Phys. Pol. B* **32** (2001) 3973.
- [113] E.H.Groot and Th.W.Ruijgrok, *Nucl. Phys.* **B27**, (1971) 45 and the references therein.
- [114] Y.-A. Chao, *Nucl. Phys.* **B40** (1972) 475.
- [115] P.Rotelli, *Phys. Rev.* **182** (1969) 1622.
- [116] C.E.Shannon, *Bell System Tech. J.* **27** (1948) 379; **27** (1948) 623.
- [117] M.I.Gorenstein, *Yad. Fiz.* **31** (1980) 1630 [*Sov. J. Nucl. Phys.* **31** (1980) 845]; B.Carazza and Gandolfi, *Lett. Nuovo Cim.* **15** (1976) 553.
- [118] Q.A.M.M.Yahaya, *Nuovo Cim.* **30** (1963) 143.
- [119] Cf. for example, *proc. of Quark Matter'99*, *Nucl. Phys.* **A525** (1999) and relevant references therein.
- [120] E.T.Jaynes, *Phys. Rev.* **106** (1957) 620 and **108** (1957) 171.
- [121] L.Van Hove, *Z.Phys.* **C21** (1983) 93 and **C27** (1985) 135.
- [122] A.R.Plastino and A.Plastino, *Phys. Lett.* **A193** (1994) 251 and *Braz. J. Phys.* **29** (1999) 50.
- [123] J.H.Havrda and F.Chavrat, *Kybernetica* **3** (1967) 30.
- [124] P.Jizba and T.Arimitsu, *The world according to Rényi: thermodynamics of fractal systems*, cond-mat/0108184.
- [125] C.Beck and F.Schlögl, *Thermodynamics of chaotic systems*, Cambridge Univ. Press, Cambridge, 1993.
- [126] C.Tsallis, R.S.Mendes and A.R.Plastino, *Physica* **A261** (1998) 534.
- [127] S.Abe, *Phys. Lett.* **A275** (2000) 250.
- [128] J.-P. Bouchaud and A.Georges, *Phys. Rep.* **195** (1990) 127; J.Bernasconi, H.Beyelev, S.Straessler and S.Alexander, *Phys. Rev. Lett.* **42** (1979) 819; J.Machta, *J. Phys.* **A18** (1985) L531.
- [129] A. Einstein, *Ann. Phys.* **17** (1905) 549.
- [130] P. Lévy, *Théorie de l'addition des variables aléatoires* (Gauthier-Villars, Paris, 1937).
- [131] B.D.Hughes, M.F.Shlesinger, and E.W.Montroll, *Proc. Acad. Sci. USA* **78** (1981) 3287.
- [132] U.Tirnakli, F.Büyükkiliç, D.Demirhan, *Phys. Lett. A* **245** (1998) 62; D.F.Torres and U.Tirnakli, *Phys. A* **261** (1998) 499.

- [133] C.Beck, *Physica* **A286** (2000) 164;
- [134] A.Białas, *Phys. Lett.* **B466** (1999) 301.
- [135] G.Wilk and Z.Włodarczyk, *Nucl. Phys. B (Proc. Suppl.)* **A75** (1999) 191.
- [136] R.Hagedorn, *Nuovo Cim. Suppl.* **3** (1965) 147;  
 R.Hagedorn and J.Rafelski, *Phys. Lett.* **B97** (1980) 136.  
 For more recent application of this approach see F.Schnedermann, J.Solfrank and U.Heinz,  
*Phys. Rev.* **C48** (1993) 2462 and L.P.Csernai, *Introduction to Heavy Ion Collisions*, Wiley,  
 New York, 1994.
- [137] K.K.Gudima, A.S.Parvan, M.Ploszajczak and V.D.Toneev, *Phys. Rev. Lett.* **85** (2000)  
 4651. Cf. also K.K.Gudima, Ploszajczak and V.D.Toneev, *Fragile signs of criticality in the  
 nuclear multifragmentation*, nucl-th/0106018, and references therein.
- [138] D.B.Ion and M.L.D.Ion, *Phys. Lett.* **B503** (2001) 263 and references therein.
- [139] G.Wilk and Z.Włodarczyk, *Phys. Lett.* **A290** (2001) 55.
- [140] D.B.Walton and J.Rafelski, *Phys. Rev. Lett.* **84** (2000) 31.
- [141] Meng Ta-chung, R.Rittel and Z.Yang, *Phys. Rev. Lett.* **82** (1999) 2044;  
 C.Boros, Meng Ta-chung, R.Rittel, K.Tabelow and Z.Yang, *Phys. Rev.* **D61** (2000) 094010;  
 Jing-hua Fu, Meng Ta-chung, R.Rittel and K.Tabelow, *Phys. Rev. Lett.* **86** (2001) 1961.
- [142] M.Rybczyński, Z.Włodarczyk and G.Wilk, *Nucl. Phys. B (Proc. Suppl.)* **97** (2001) 81.
- [143] G.Wilk and Z.Włodarczyk, "Application of non-extensive statistics to particle and nuclear  
 physics", hep-ph/0108215; to be published in Proc. of the Int. School and Conference  
 on "Non Extensive Thermodynamics and Physical Applications", Villasimius-Capo Boi  
 (Cagliari), Italy 23-30 May, 2001, *Physica* **A** (2002).
- [144] C.Tsallis, *Phys. Lett.* **A195** (1994) 329;  
 A.Lavango, P.Narayana Swamy, *Phys. Rev.* **E61** (2000) 1218.
- [145] D.V.Anchishkin, A.M.Gavrilik and N.Z.Igorov, *Eur. Phys. J.* **A7** (2000) 229 and *Mod.  
 Phys. Lett.* **A15** (2000) 1637. Cf. also A.M.Gavrilik, *Nucl. Phys. B (Proc. Suppl.)* **102**  
 (2001) 298 and references therein.
- [146] R.Peschanski, *Nucl. Phys.* **B253** (1991) 225 or S.Hegyi, *Phys. Lett.* **B387** (1996) 642 (and  
 references therein).
- [147] G.Goldhaber *et al.*, *Phys. Rev.* **120** (1960) 300.
- [148] P.D.Acton *et al.*, (OPAL Collab.), *Phys. Lett.* **B267** (1991) 143.
- [149] T.Csörgő and S.Hegyi, *Phys. Lett.* **B489** (2000) 15;  
 D.A.Brown and P.Danielewicz, *Phys. Rev.* **C64** (2001) 014902 and references therein.

## Acknowledgments

I would like to recall here all those who helped me in any way during my PhD studies in Warsaw.

First of all, I would like to thank The Andrzej Soltan Institute for Nuclear Studies (SINS) for warm hospitality extended to me during my PhD studies there. My special thanks go to the director of SINS, Prof. Z.Sujkowski, and to the leader of PhD studies at SINS, Prof. L.Lukaszuk, for the opportunity they offered me by accepting to the PhD studies.

I am also very grateful to Doc. Grzegorz Wilk, my thesis advisor, for all help, support and knowledge I have received from him. It has been for me a real pleasure to work with him and to learn from his experience.

My very sincere gratitude goes to Prof. Z. Włodarczyk for his help and encouragement during the course of preparing my thesis.

A lot of my friends were very helpful to me during my PhD studies. I am especially indebted to Oleg and Inna Mazonka, Andrzej and Miroslava Pasternak, Boris Sidorenko, Alexander Undynko and Igor Muntyan.

My special thanks goes to my parents and to my family. I own a lot to my wife for her patience, love, support and friendship. My warm gratitude goes also to my brother Vyacheslav for his encouragement, his support and lot of valuable discussions.

The partial support of Polish Committee for Scientific Research (grant 5 P03B 091 21) is gratefully acknowledged.